Differentiation of Mouse Embryonic Stem Cells Using PEG-Fibrinogen Hydrogel Microspheres

by

Samuel Shing-I Chang

A thesis submitted to the Graduate Faculty of
Auburn University
in partial fulfillment of the
requirements for the Degree of
Master of Science

Auburn, Alabama
August 4, 2012

Keywords: cardiac, engineering, hydrogel, stem cell

Approved by

Elizabeth Lipke, Chair, Assistant Professor of Chemical Engineering
Mark Byrne, Daniel F. & Josephine Breeden Associate Professor of Chemical Engineering
Christopher Easley, Assistant Professor of Chemistry

Abstract

Cardiac disease is the leading cause of death worldwide, and current treatments are either ineffective at significantly prolonging lifespan or are unavailable to the majority of patients in need due to a lack of supply. Application of engineered heart tissue is a promising method to repair damaged hearts, but there are many challenges to generate functional cardiac tissue which can integrate with damaged myocardium. We have developed a highly scalable method for producing cardiac tissue from mouse embryonic stem cells (mESCs) using poly(ethylene glycol)-diacrylate (PEGDA) based hydrogels with a conjugated fibrinogen protein functional motif. Hydrogels consisted of dispersed microsphere cell-carriers to be utilized as *in vitro* differentiation systems or as a possible injectable delivery vehicle. Cells were encapsulated within the hydrogel polymer precursor and microspheres were generated via water-in-oil emulsification. The generation of microspheres with reproducible diameter distributions within the range of roughly 70-200 μm was demonstrated. The microspheres acted as differentiation vehicles; as the cells proliferated and remodeled the surrounding matrix, they formed embryoid bodies which exhibited spontaneous contraction as early as 10 days into differentiation. Cell activity within the microsphere was primarily characterized by phase-contrast microscopy. Differentiation of encapsulated cells was verified using qPCR and immunohistochemical techniques. This method is the first to describe the proliferation and differentiation of encapsulated mouse pluripotent stem cells using a PEG-based hydrogel.

Acknowledgments

I would first like to thank all of the members, past and present, of the Lipke lab, because my work would not have been possible without their contributions. Specifically I would like to thank Alex Hodge and Aaron Seeto for all of their help; we have worked together on many different things from stem cell expansion and differentiation to setting-up and testing several different cameras for the inverted microscope. I could not have asked for a more enriching experience of setting up and developing the Lipke lab without you two; thank you! I would also like to acknowledge the invaluable help of Stephen Hicks for being such a dedicated worker with such a skilled eye for technical details and fixing anything! For my other undergraduates whom I have mentored: Samantha Scott for helping with microsphere diameter measurements and Bianca Williams, it has been a pleasure mentoring you and I know you will go far! Thank you Dr. Dunn and Wes Grove for bringing so much energy and enthusiasm into our lab. Finally, I would like to thank Dr. Lipke for being patient with me and being an ever constant wealth of knowledge and wisdom for overseeing my project. Non-members of our lab from around Auburn University have also contributed to various methods for me to generate results; I'd like to thank Dr. Mike Miller, Dr. Michael Meadows, Dr. Raj Amin, and Dr. Frank Bartol's lab group. Finally I would like to thank Dr. Dror Seliktar and his lab group for their generous donation of a batch of PEG-fibrinogen which was instrumental in generating some of my finest results. It has been quite a journey!

Table of Contents

List of Tables

List of Figures

List of Abbreviations

PEGDA	Poly(ethylene glycol) diacrylate
mESC	Mouse embryonic stem cell
PF	PEG-fibrinogen
EHT	Engineered heart tissue
EB	Embryoid body
hMSC	Human mesenchymal stem cell
EPC	Endothelial progenitor cell
LIF	Leukemia inhibitory factor
iPSC	Induced pluripotent stem cell
PVA	Poly(vinyl alcohol)
HA	Hyaluronic acid
ECM	Extracellular matrix
MMP	Matrix metalloproteinase
BMP	Bone morphogenic protein
TGF	Transforming growth factor
PLGA	Poly(lactic-*co*-glycolic acid)
MEF	Mouse embryonic fibroblast
NVP	*N*-Vinylpyrrolidone
PBS	Phophate buffered saline

TEA	Triethanol amine
DMEM	Dulbecco’s modified eagle medium
GAPDH	Glyceraldehyde 3-phosphate dehydrogenase
FBS	Fetal bovine serum

I. Background

1.1 *Cardiac diseases and regeneration of specialized tissue*

Cardiac diseases are the number one cause of death in industrialized nations[1,2,3] and 11.8% of non-institutionalized adults in the United States have been diagnosed with heart disease[4]. Heart disease includes coronary heart disease, ischemic heart disease, hypertensive heart disease, valvular heart disease, and myocardial disease. Such diseases can lead to episodes of acute myocardial infarction (commonly known as a heart attack) and can result in congestive heart failure, in which the heart can no longer pump enough blood to meet the metabolic needs of the body. Patients who suffer from advanced stages of heart failure have a poor prognosis for survival, and the large disparity between numbers of donors and recipients leaves few viable treatments. It is estimated that 50,000 people worldwide are candidates for transplantation, with only about one tenth of that number of transplants being performed on an annual basis[5]. Artificial prosthetic hearts and heart assist devices have demonstrated some success in prolonging the lives of patients receiving treatment[6], but their development is slow and clinical trials have seen limited success. Due to the nature of heart transplants and the stigma surrounding artificial hearts and organs, engineered heart tissue may provide an encompassing treatment for heart failure.

The heart's unique electromechanical characteristics and the myocardium's extremely high metabolic demands make heart tissue an advanced tissue. Because of this, adult heart tissue possesses extremely low cell turnover rates and regenerative capability, as is also the case for other advanced tissues within the body. The lack of widely available and effective treatments for heart disease and other types of organ failure has resulted in widespread research efforts in the field of tissue engineering to develop advanced tissues *in vitro* to replace damaged and diseased

ones. Advanced tissues are characterized by having highly specialized functions within the body and include cardiac, lung, liver, neural, and pancreatic tissues. Such tissues are difficult to culture for two underlying reasons. The first reason is that these specialized tissues do not naturally renew and repair themselves in an adult, thus making it difficult for the body to compensate for the lost function of the tissue when the tissue experiences significant acute or cumulative damage. Mature cardiomyocytes have exited the cell replication cycle and do not regenerate[7]; this characteristic also carries over to the *in vitro* environment and thus limits *in vitro* expansion capabilities of cardiomyocytes. The second challenge involved in culturing and studying specialized tissues *in vitro* is that the specialized phenotype and function of these tissues are difficult to maintain once removed from the host tissue. These specialized tissues are prone to de-differentiation due to their endogenous occupation of a specific cell niche that is complex and very sensitive to external factors. Cardiomyocytes possess exceptionally high metabolic demand, thus necessitating sufficient vascularization of their tissue to enable their proper function. Cardiomyocytes behave differently or may simply become apoptotic once removed from their natural niche or following an ischemic event, where the natural environment of cardiomyocytes is altered[8]. Thus conventional tissue engineering methods using expanded adult cells have been largely unsuccessful in generating appropriate quantities of cardiac tissues, leading scientists to examine regeneration in other animal species or by studying tissue development.

The regenerative capacity of cardiomyocytes in mammals is insufficient to recover from an ischemic episode, but this is not true for all vertebrates. In some organisms such as zebrafish, and newts, satellite heart cells are capable of regenerating and repairing major damage[9]. In newts, cardiomyocytes are capable of sensing cardiac damage and re-entering the cell cycle to

generate more cardiomyocytes[10]. The mechanism for this has been shown to involve the dedifferentiation of cardiomyocytes to allow for the proliferation of predecessor cells, where these progenitor cells down-regulate the expression of contractile proteins such as α-myosin heavy chain[10]. Cardiac regeneration in zebrafish has been shown to initiate the proliferation of resident cardiac progenitor cells[11]. Mammalian cardiac regeneration cannot sufficiently compensate for ischemic tissue by natural mechanisms, but regeneration has been demonstrated to be possible by transgenically altering mice[12]. By observing the mechanisms of regeneration in other organisms, it is clear that a stem cell population is the best source for derivation of cardiomyocytes. There are many types of stem cells, however, and their propensity to differentiate into cardiomyocytes has been shown to affect the success of cardiac derivation.

1.2 *Stem cells as a cell therapy source*

A number of types of stem cell have been studied for their potential as cardiac cell precursors, including skeletal myoblasts, bone-marrow derived hematopoietic cells, embryonic and mesenchymal stem cells, and endogenous cardiac stem cells. Skeletal myoblasts fit the profile of cardiomyocytes due to their common purpose as muscle cells, but the extent of their similarities seem to end there. Skeletal myoblasts have not been shown to differentiate into cardiomyocytes *in vitro*[13], and incorporation of autologous skeletal myoblasts into infarcted myocardium has typically resulted in poor electrical coupling with intact myocardium[13], leading to the termination of human trials using these cells[14]. A myriad of different bone-marrow derived hematopoietic cells have also been noted for their capacity to differentiate into cardiomyocytes. Mouse hematopoietic stem cells have differentiated into cardiomyocytes when implanted into infarcted myocardium[15], but direct evidence of cardiomyocyte differentiation of human hematopoietic

stem cells has not been presented[16]. Endothelial progenitor cells (EPCs) have also been noted for their ability to improve myocardial function, possibly by improving vascularization of myocardium[17] which promotes the transport of paracrine signals to cardiomyocytes[18], but have not demonstrated the ability to differentiate into cardiomyocytes. Mesenchymal stem cells (MSCs) are a subset of bone marrow derived stem cells and have received ample attention for versatility in multipotency; they have been shown to differentiate into cells that can be used for engineering bone, cartilage, and fat cells[19]. Differentiation of cardiomyocytes from MSCs has been observed when transplanting MSCs into the myocardium of both rats[20] and pigs[21]. However, it has also been shown that MSC's in transplanted mouse hearts differentiated into osteoblasts rather than cardiomyocytes[16], which is an extremely undesirable cell type to have within the heart. Thus MSCs may not be the best option for differentiation of cardiomyocytes. Cardiac stem cells, endogenous in the adult heart, have received attention as a very promising cell type for cardiac differentiation, but they have not yet been fully characterized by a unique marker[16] and thus are difficult to isolate. Furthermore, it is not clear how effectively cardiac progenitor cells may differentiate into cardiomyocytes, leaving cardiac tissue engineers to explore pluripotent stem cells as a source for cardiac derivation.

Pluripotent stem cells possess two major characteristics which endow them with massive potential for engineering tissues. By definition, pluripotent stem cells are capable of differentiating into any of the basic tissue germ layers: endoderm, ectoderm, and mesoderm. The second property which makes pluripotent cells an ideal cell therapy source is their clonality and self-renewability. Under proper culture conditions, which will be addressed, pluripotent cells may divide indefinitely given that they maintain their pluripotent genotype and phenotype. The mechanism for their immortality is attributed to their high telomerase activity thereby allowing

for up to 32 passages over a span of 8 months without losing replication ability[22]. When expanding pluripotent cells for downstream differentiation, however, one major challenge is maintaining proper conditions in an effort to prevent the unwanted or premature differentiation of the cells. The use of feeder cells, such as mitotically inactivated fibroblasts[22,23], and paracrine signals such as leukemia inhibitory factor (LIF) have been commonplace for maintaining pluripotency[22,23]. The immortality of pluripotent cells allows for the expansion of large quantities of them to differentiate into therapeutic engineered tissues, but several major pitfalls exist when using pluripotent cell sources. For example, MSCs are multipotent, meaning they can differentiate into a number of different kinds of tissue, but even multipotent cell differentiation is difficult to control. Specifically, MSCs that were genetically altered to survive and differentiate into cardiomyocytes also displayed unwanted differentiation into osteoblasts[24], which would be detrimental to heart function if present within the heart. Since MSCs are multipotent and not pluripotent, one can imagine that unwanted differentiation becomes a greater concern when using pluripotent cells. In addition to a current lack of understanding of the factors and mechanisms driving differentiation in pluripotent cells, *in vivo* injection of undifferentiated pluripotent cells may result in teratomas, or tumors[23,25]. In addition to the formation of teratomas, pluripotent cells also elicit an immune response[25], which further complicates their therapeutic application. As progress is made with pluripotent cell engineering, however, teratoma formation may be averted by performing differentiation of the therapeutic tissue prior to *in vivo* implantation, or by genetically selecting for the desired cell type, such as cardiomyocytes[26].

The prototypical pluripotent cell is the embryonic stem cell (ESC), which is derived from the inner cell mass of the blastocyst. ESCs have been shown to differentiate into cardiac

tissue[23,25-26, 27,28] in both humans and mice[29]. Along with cardiomyocytes, supporting cardiac tissue cells such as fibroblasts and endothelial cells have also been derived from differentiation of ESCs[30]. Although ESCs have received special attention because of their great potential in tissue therapy, they also carry ethical concerns regarding their derivation. For human ESCS (hESCs) to be acquired, a human embryo must be sacrificed as the cell source, which incites much scrutiny and ethical disapproval. Aside from the ethical quandary of hESC derivation, their procurement is also not convenient for therapeutic purposes, particularly when considering ESC immunogenicity and the need for autologous cell sources. Induced pluripotent stem cells (iPSCs) are adult cells which are genetically reprogrammed to become pluripotent cells. They have recently been shown to successfully differentiate into cardiomyocytes[31,32,33]. iPSC research is relatively new compared to ESC research and thus some issues with iPSC technology still remain to be overcome. Ideally, the genetic modification of iPSCs should result in ESC analogues that are genetically identical to ESCs. However, early reports show that iPSCs exhibit different gene expression patterns from ESCs, although they do display similar morphology, proliferation, and teratoma formation[34]. Regardless, iPSC technology still contains potential for cell therapy, as it has recently been shown that iPSCs are capable of aiding in the formation of neurons and may be tailored to be patient-specific[35].

1.3 *Biomaterial hydrogels and their tissue-engineering applications*

In addition to selecting appropriate cell types to engineer therapeutic tissues, the selection and design of a biomaterial scaffold is also crucial for engineering tissues. Biomaterial scaffolds aid in tissue engineering by acting as a synthetic extracellular matrix (ECM) analogue that provides structure to the engineered tissue and allows for control over the presentation of biological

signals[36]. A vast array of biomaterials have been researched for their efficacy as tissue scaffolds, including hydrolytically degradable poly(lactide-co-glycolide) (PLG)[36], synthetic polymer hydrogels, and naturally-derived polymers. Hydrogels are ideal scaffold materials because they are hydrophilic and have high water content (greater than 30%[36]), which mimics natural ECM. Furthermore, high water content provides hydrogels with ideal transport capabilities, enabling for the diffusion of nutrients and waste to and from tissue. Hydrogel materials of note which have been used in tissue engineering include poly(ethylene glycol) (PEG), poly(vinyl alcohol) (PVA), alginate, hyaluronic acid (HA), and collagen[36]. Hydrogels in tissue engineering typically consist of a polymer in solution and may be processed, or "gelled", under physiologically mild conditions which are conducive to maintaining cell viability. The mechanism of solution to gel (sol-gel) transition often relies on a crosslinking agent, but some polymers such as Pluronic are gelled by undergoing simple temperature phase transition[37].

Natural polymer hydrogels, such as alginate, HA and collagen, are excellent candidates as biomaterials because of their natural biocompatibility and gelling potential. Alginate, a polysaccharide, undergoes sol-gel transition when in the presence of divalent cation crosslinkers, most typically Ca^{2+}, by forming ionic bonds between the cation and guluronic residues in alginate[38]. Alginate undergoes its sol-gel transition under highly biocompatible and simple conditions, and thus has become a popular biomaterial for encapsulating tissues[38]. Although alginate has perhaps the simplest and most biocompatible gelling procedure, its lack of bio-active moieties and lack of diverse modification potential are drawbacks[39]. Alginate can be modified, however, where covalent peptide addition to alginate block polymers is possible via aqueous carbodiimide chemistry[40]. Other naturally occurring polymers, such as HA and collagen, possess greater degrees of bio-functionality than alginate, perhaps due to the fact they are both

ubiquitous ECM components. HA is included in many co-polymer blends as a scaffold material, and can be modified to covalently crosslink with hydrazide derivatives via esterfication or annealing[38]. Collagen, the most prevalent ECM protein in mammalian tissues[41], is a structural component of typical engineered heart tissues (EHT) which has seen promise within the field of cardiac tissue engineering. Endogenous collagen typically arranges itself into triple-helix strands of three protein subunits, forming fibers which make collagen an attractive choice for load-bearing tissue scaffolds. Due to its biological prevalence and load-bearing strength, collagen has seen marked success as an EHT scaffold material. Eschenhagen *et al.* have created highly functional contracting constructs which incorporate collagen and Matrigel along with neonatal rat heart cells[42]. This collagen-based EHT resulted in cardiac tissue with similar mechanical and electrophysiological properties to the native myocardium of rats, and was capable of integrating with host tissue[42]. Their work showed how mechanical stretching and conditioning of the EHT would align collagen fibrils, which highlighted the importance of aligned tissue and its influence on the maturity of the tissue. However, even with the incorporation of a defined material such as Matrigel, the use of constructs derived from only naturally occurring hydrogels has the shortcoming of batch variability. Thus hydrogels in tissue engineering typically will employ synthetic polymers to improve reproducibility.

1.4 *PEG hydrogels and tunable modification potential*

Synthetic polymers such as PVA and PEG are well suited as scaffolding materials because of their low cost (relative to naturally derived polymers), reproducibility, and propensity for modification. Tissue engineers have taken advantage of synthetic polymers' ability to be tailored to meet scaffold design requirements. These scaffolds may be tailored to have specific

mechanical and structural composition and may also deliver paracrine signals to tissues. PEG is a widely used biomaterial in tissue engineering because it is highly biocompatible and it has great potential for modification. Advantages to using this synthetic polymer include its ability to tune the mechanical properties of hydrogels by altering crosslink density or chain size and shape (i.e. linear, or multi-armed), as well as its capability to be conveniently photo-polymerized under physiologically acceptable conditions. PEG has been thoroughly investigated for its crosslinking ability[43,44,45] as well as its ability to be functionalized[46]. PEG has been functionalized via acrylation on both ends of its polymer chain to form PEG-diacrylate (PEGDA), giving the new acrylated polymer the ability to crosslink in solutions of physiologically compliant medium, such as PBS or HBS. In addition to PEG-acrylated polymer hydrogels, PEG may be functionalized with a variety of other end groups such as vinyl sulfone[47] and thiol groups[48]. A review of functional groups which have been conjugated to PEG ends is shown in Figure 1.

Because PEG is hydrophilic and resistant to non-specific protein adsorption, cells cannot adhere to it and are not readily cultured on PEG scaffolds unless the hydrogel is modified with adhesive moieties. The versatility of PEG makes the incorporation of adhesion sites possible by a variety of means. Seliktar *et al.* have performed extensive studies on the functionalization of PEGDA with the ECM protein fibrinogen, and the conjugated PEG-fibrinogen is able to crosslink using photoinitiators. These ECM-functionalized hydrogels have been shown to support adhesion of neonatal rat cardiomyocytes and promote the adhesion and migration of sheep aortic smooth muscle cells[46]. In addition to fibrinogen, peptide sequences with affinity towards specific integrins that promote cell adhesion have also been successfully incorporated

into PEG hydrogels. The most commonly utilized adhesion peptide sequence[49] has been RGD, which is present on collagen.

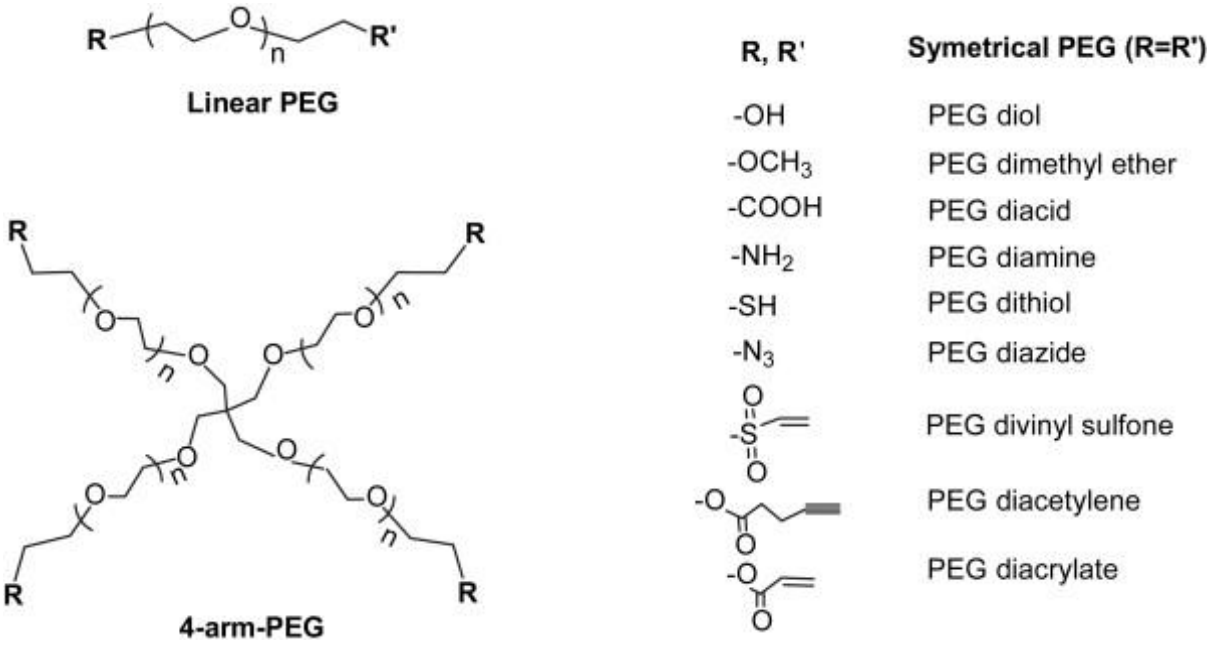

Figure 1: PEG structure and functional groups. PEG structures may be linear or multi-armed. A number of functional end groups that may be conjugated to PEG are also listed. Adapted from Zhu[49] and reprinted with permission.

Crosslinked PEG hydrogels do not readily degrade under physiological conditions unless the polymer is modified to incorporate degradable sequences. Degradable sequences are susceptible to enzymatic cleavage, and the most frequently used sequences are sensitive to cell-secreted matrix metalloproteinase-1 (MMP-1)[49]. Additional work has demonstrated PEG's ability to be modified with multiple bioactive molecules within the same hydrogel. Lutolf *et al* have incorporated into PEG hydrogels both adhesive RGD sequences and degradable sequences sensitive to MMP enzymatic hydrolysis, to enable cellular remodeling of PEG hydrogel scaffolds[50]. A schematic of the remodeling is illustrated in Figure 2. Such bio-functionalization of a hydrogel scaffold is invaluable as cellular remodeling of surroundings mimics the remodeling of native ECM by cells. Cells remodel their surroundings by degrading the ECM via

deposition of enzymes during tissue development in order to create space for cell proliferation. Therefore, a central principle in engineering of functional tissue scaffolds is to balance the rate of degradation and the rate of cell growth. One of the major problems encountered by Magyar *et al* when using alginate microsphere to encapsulate mouse embryonic stem cells (mESCs) was the inability of the stem cells to degrade the matrix, which may have contributed to the inhibition of EB formation in their higher (1.6%) concentration alginate gels as opposed to their lower (1.1%) concentration gels, which enabled EB formation[39]. Given PEGDA's tunable characteristics, the covalent conjugation of a bioactive moiety permits cell-scaffold interaction and remodeling, and allows for the full potential of PEGDA to be realized.

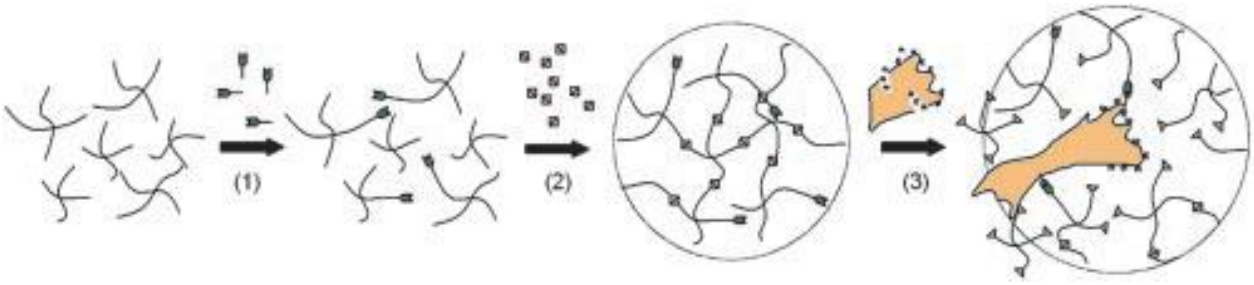

Figure 2: Modified PEG allows for cellular remodeling of crosslinked polymer network. 4-armed PEG initially functionalized with vinyl sulfone groups, and with incorporated adhesion (1) and degradation (2) sites**.** Cellular adhesion and degradation is illustrated (3). Figure adapted from Lutolf *et al.*[51] and re-printed with permission: Copyright 2003 National Academy of Sciences U.S.A.

PEG's modification potential does not end with the covalent conjugation of bioactive adhesion and degradation sites, as morphogenic proteins that induce differentiation may also be covalently attached to functional end groups. Tethering of growth factors via covalent attachment is beneficial in tissue scaffold engineering because it allows for controlled or sustained release, while avoiding the burst release profile seen when factors are simply physically mixed into the hydrogel material. Growth factors that have been shown to induce

cardiomyocyte differentiation include bone morphogenic proteins (BMPs) and transforming growth factor-α (TGF- α)[52].

In addition to the ability to incorporate different bio-active molecules within PEG-based hydrogels, PEG may also be modified to possess unique mechanisms of polymerization. Covalent polymerization of PEG-hydrogels is typically achieved by modifying PEG-chains ends with functional groups such as acrylates or vinyl alcohols, which form covalent crosslinks when exposed to a free-radical photoinitiator. Other than covalently attaching functional groups to PEG-chain ends to achieve gelling, another method of gel formation employs a PEG-based polymer, Tetronic, which allows for reversible physical gelling of the hydrogel polymer. The reversible physical solution-to-gel (sol-gel) transition of Tetronic occurs when the polymer is warmed above its glass transition temperature. The polymer exists as a solution below this transition temperature. Because Tetronic is PEG-based, it may also be further modified to have acrylated ends to promote permanent covalent polymerization of the hydrogel. Acrylated Tetronic thus has the potential to undergo both "fast" physical gelation by temperature transition, and "permanent" covalent crosslinking by free-radical polymerization. This "tandem" gelation method was described by Cellesi *et al* for a unique method of producing Tetronic microspheres for encapsulation applications[62].

1.5 *Embryoid body differentiation*

Protocols for the differentiation of pluripotent cells, particularly ESCs, often require the forced aggregation of stem cells into three-dimensional spheroids, termed embryoid bodies (EB). EB differentiation is a conventional method among stem cell engineers not only because of efficacy, but also due to the EB's similarities to the developing gastrula and the amount of information

which can be ascertained from EB differentiation to better understand factors which drive stem cell differentiation. The developing embryo is a natural model of the EB since it undergoes heterogeneous differentiation into all the different tissues that make up an organism. The challenge for *in vitro* EB differentiation then is finding appropriate measures to manipulate differentiating cells so that they undergo homogeneous directed differentiation into a target tissue type. Derivation of a homogeneous population of cells from an EB is thus a monumental reverse engineering problem in stem cell research. Differentiation is driven by a plethora of extremely intricate factors, including biochemical, mechanical, electrical, and temporal cues. The mechanism for the heterogeneous differentiation of tissues within an EB can be explained simply by diffusion gradients, which create a non-uniform distribution of growth factors, nutrients and wastes within the EB. An EB is a spherical cell aggregate where cells in the interior of the aggregate are not subjected to the same conditions as the cells in the medial region, which are also exposed to different conditions when compared to cells on the outer layer of the aggregate. Efforts have been made to overcome heterogeneous differentiation by studying the mechanisms of development, where studies have investigated the effects of EB size on stem cell fate[53,54,55] as well as the relationship between concentration gradients of signals and cell differentiation[54]. Briefly, Zandstra *et al* controlled the size of EBs using micropatterned culture wells[55] and found that smaller EB colonies (200 μm diameter) preferentially differentiated into definitive endoderm while larger colonies (1200 μm diameter) preferentially differentiated into mesoderm, and similar conclusions were drawn from another study in which EB size was correlated with fate specification[53]. Although control of EB size enabled some control over differentiation, resultant cell types from such differentiation systems still yielded various phenotypes, indicating that factors other than EB size must be controlled to produce

homogeneous populations of stem cells. Additionally, another drawback of this micropatterned EB differentiation system is its lack of scalability.

McDevitt *et al* have demonstrated the importance of homogeneous delivery of morphogenic factors to cells within EBs, where retinoic acid was presented to differentiating stem cells by incorporation of morphogen-containing degradable PLGA microspheres into the EBs[56]. However, the initial study conducted resulted in non-uniform integration of microspheres as well as the production of EBs of various sizes as seen in Figure 3, introducing variability into the EB differentiation system. A follow up study by the same group investigated the differentiation behavior of EBs when microsphere delivery vehicle size was controlled and varied, where the group concluded that smaller microspheres were more easily incorporated into EBs and enabled for more efficient EB differentiation[57].

EB differentiation may be accomplished using a variety of different procedures, where each procedure has a different focus. The conventional method of forming EBs induces aggregation of cells in a hanging droplet and it is referred to as the hanging droplet method of EB formation. This method allows for approximate control over cell aggregate size by suspending stem cells at a specific concentration in culture media, forming droplets of known volume on a culture dish lid, and then inverting the dish lid to allow the forced aggregation (by gravity) of cells at the bottom of the drop. The hanging drop method is widely practiced[55,56,58] because it requires only standard equipment and allows for some control over aggregate size, but its major drawback is lack of scalability due to its time and labor cost. EB formation via micro-well centrifugation produces EBs of uniform size[53-55], but this method is also not highly scalable.

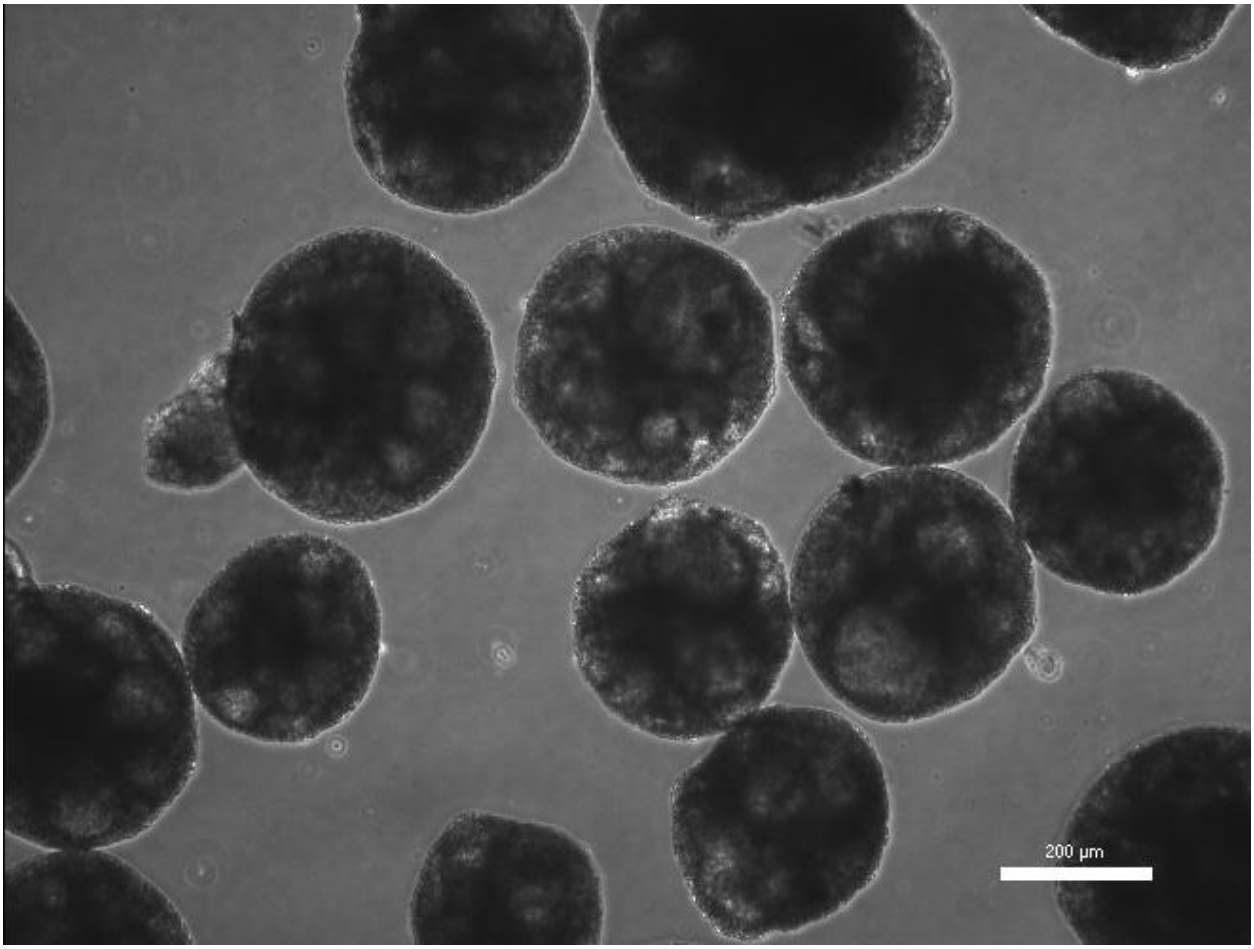

Figure 3: Embryoid bodies undergo non-homogeneous differentiation. EBs formed via hanging droplet method on Day 7 of differentiation. Non-uniform EB sizes can be observed. Scale bar = 200 µm.

Previous work by Zandstra and McDevitt have the central theme of uniformly controlling environmental parameters to which EBs are exposed, either by standardizing structural or morphogenic conditions, respectively. Homogeneous EB differentiation requires an elucidation of the complex differentiation mechanisms of stem cells, whether the stem cells are differentiating in the developing embryo or are sourced from an adult stem cell niche. Regardless, the ECM and supporting cell types are mechanistically involved in providing

physicochemical cues such as mechanical or morphogenic stimulation of stem cells to influence their tissue specification. Presentation of environmental cues is difficult to mimic *in vitro*, as the regulation of such factors require elegant spatiotemporal induction. What the aforementioned differentiation strategies lack is a simultaneous combination of structural control and spatially modulated delivery of differentiation factors. Previous work has shown that mESCs are capable of forming EBs when encapsulated within alginate microspheres and that differentiation may be initiated within the microsphere[39]. Controlled presentation of cardiogenic inducing factors was not included in that study however, nor was there an effort to uniformly distribute the initial number of ESC within the microspheres. Regardless, the work demonstrated a scalable method to expand mESCs into EBs and initiate differentiation when encapsulated within a hydrogel microsphere. Microspheres are commonly used for the encapsulation and delivery of pharmaceutical agents, but they have also been used for the encapsulation of cells[39,59]. Franco *et al.* developed a simple water-in-oil emulsion system for the mass production of cell-laden PEG-based microspheres[59]. This method is highly scalable in that one needs to simply increase the polymer and oil volumes to generate a large quantity of encapsulated cells, which in turn will generate a larger quantity of functional tissue. Additionally, the use of a PEG-based microsphere allows for bio-modification of the biomaterial scaffold, which has not yet been performed in other microsphere systems such as those made of alginate or collagen.

1.6 *Rationale behind the development of a scalable differentiation system*

It is exciting to see the current progress in engineering cardiac tissue, stem cells and biomaterials. Different approaches to engineering cardiac tissue typically focus on one aspect of environmental regulation, such as controlling EB size or selecting an appropriate biomaterial to

form functional tissue, but few proposed design strategies have engineered tissue products with scale-up as the a central goal. The rationale for this study is thus to design a system for the differentiation of pluripotent cells into cardiac tissue by using a biomaterial carrier which can be processed in a highly scalable fashion. This study is innovative in that it combines EB structural regulation with microsphere encapsulation technology using a biomaterial which is highly flexible in terms of its capacity for modification. The biomaterial used in this study is a PEGylated fibrinogen which provides encapsulated stem cells with adhesion and degradation sites, allowing for matrix remodeling, while the PEG may allow for further modification such as the tethering of growth factors or peptide sequences that may promote cardiogenesis or other reactions.

II. Materials and Methods

2.1 *mESC expansion and maintenance*

D3 line mouse embryonic stem cells (mESC) genetically modified for neomycin resistance on the α-sarcomeric actinin promoter and primary mouse embryonic fibroblasts (MEFs) were a generous gift from Drs. John Gearhart and Leslie Tung of Johns Hopkins University. MEFs were mitotically inactivated by exposure to gamma radiation up to 9000 rads. mESCs were expanded on inactivated MEF feeder layers in mESC culture medium, composed of DMEM with 10% (v/v) ESC defined FBS (Atlanta Biologicals). All media components were from Gibco, unless otherwise noted: Glutamax, non-essential amino acids, sodium pyruvate, gentamycin (Lonza), β-mercapto ethanol (Gibco), and LIF (Esgro). mESCs were further expanded in feeder-free conditions on gelatin coated tissue culture treated dishes using the same LIF-supplemented media prior to differentiation experiments. Differentiation media was the same as mESC expansion media except it did not include LIF.

2.2 *Preliminary experiments for selection of biomaterial*

Tetronic (BASF) was tested for its reverse gelation kinetics by dissolving it in PBS. Solutions ranged in concentration from 5 to 40% (w/v). Complete dissolution was achieved by stirring at 4°C. To assess the crosslinking ability and hydrogel stability of Tetronic-PEGDA mixtures, Tetronic and PEGDA were both dissolved in PBS at varying ratios, and a photoinitiator solution was added at the concentration of 5μL per mL of polymer solution. Acetophenone photoinitiator solution was made of 2,2-dimethoxy-2-phenyl acetophenone (Acros Organics) in 1-vinyl-2-pyrrolidinone (NVP, Sigma) at 300 mg/mL. Polymer solutions were dropped in 48-well plates and crosslinked under a 365 nm lamp for 5 minutes. The polymerized discs were transferred to

24-well plates and swelled with PBS. Swelling ratios were taken by measuring the weight of the discs prior to swelling and at different time points after swelling was initiated.

Pluronic F127 (Sigma) was also tested for its reverse gelation ability, where solutions in PBS were made ranging in concentration from 10 to 40% (w/v). Mixing was achieved by stirring at 4°C. Pluronic F127 was also mixed with Tetronic at varied ratios to assess for reverse gelation.

2.3 *Synthesis and characterization of biomaterials*

Poly(ethylene glycol) diacrylate (PEGDA) was synthesized by reacting 10,000 MW PEG (Sigma) with 2M excess acryloyl chloride and 1M excess triethyl amine in anhydrous dichloromethane (Acros Organics) in argon overnight. The acrylated PEG solution was then mixed with 2 M K_2CO_3 at 3M excess compared to PEG and was allowed to separate in a separation funnel for several days. Following the separation of organic and aqueous phases, the organic phase was collected, mixed with magnesium sulfate, and filtered using a Buchner funnel. The filtered solution of PEGDA was then precipitated in cold diethyl ether, filtered, and oven dried. Acrylation efficiency was assessed by dissolving 50 mg PEGDA into deuterium oxide (d_2O, Acros Organics) and analyzing it using NMR.

PEGDA was conjugated to fibrinogen as previously described by Seliktar *et al*[46,47,50]. Briefly, fibrinogen from bovine plasma (Sigma) was dissolved in 8 M urea (Sigma) solution (in PBS), and TCEP (Acros Organics) was added in 1.5 M excess to fibrinogen cysteines to expose cysteines on the fibrinogen. The pH of the solution was then adjusted to 8 using 0.1 M NaOH to further unfold the protein. 10,000 MW PEGDA was added to the denatured protein solution at 4 M excess to cysteines and reacted for 3 hours. The conjugate solution was then diluted to 3 mg

protein/mL, and then the resultant solution was precipitated by mixing with 4 equivalent volumes of acetone and separated in a separation funnel. The precipitate solution was centrifuged and the precipitate pellet was resuspended in 8M urea solution and homogenized. The solution was then placed in dialysis tubing with a 12-14 kDa cutoff and was dialyzed for 2 days in cold PBS, with 2 PBS changes per day. Three separate batches of PEG-fibrinogen (PF) were used in experiments, one of which was synthesized by Seliktar *et al* and shipped to our lab. One batch of PF had such low PEG content that it required additional PEGDA to be added at a concentration of 20 mg PEGDA/mL PF (referred to as Batch-2 PF) to facilitate photo-crosslinking. Protein content was measured using a Pierce BCA protein assay kit (Thermo Fisher). Dry content of PF was measured by weighing lyophilized PF. PEGDA percentage was calculated by subtracting calculated protein content from total dry content, with the assumption that PF dry content was composed entirely of protein and PEGDA.

2.4 *Preliminary experiments for design of microsphere formation process*

Initial experiments conducted to form microspheres tested the principle outlined by Cellesi *et al*[62] and were performed by dropping solutions of 150 mg PEGDA/mL of 30% Tetronic (in PBS) into a hardening bath composed of 10% (w/v) Pluronic F127, Tween 80 (Sigma) and n-hexane (Acros Organics). 5 µL acetophenone photoinitiator solution was added per mL of polymer solution to enable crosslinking by exposing to a 365 nm lamp for 2 minutes. Polymer solution was extruded into the hardening bath using either pipette or syringe.

Microspheres were produced via emulsion with varied formulations to achieve disperse microspheres in mineral oil (Sigma). Solutions of 100-150 mg PEGDA/mL PBS and PF (Batch 1) were initially used as a polymer precursor solution to act as the microsphere material. The

photoinitiators acetophenone, Eosin Y (Fisher), and Irgacure 2959 were tested for crosslinking efficacy by mixing with polymer precursor solutions. Acetophenone was always dissolved in NVP at the previously mentioned concentration, while Eosin Y was dissolved in NVP at a concentration of 20 mg/mL. Irgacure 2959 photoinitiator solution was always dissolved in 70% ethanol at 10% (w/v). The surfactants Pluronic F127, Pluronic F68 (Sigma), Span 80 (Sigma), Tween 80, and Triton X-100 (Sigma) were incorporated into the oil phase for microsphere dispersion. A stock oil-surfactant solution previously described by Griffiths *et al*[60] was mixed as follows: 95.05% (v/v) mineral oil, 4.5% (v/v) Span 80, 0.4% (v/v) Tween 80, and 0.05% (v/v) Triton X-100.

2.5 *Scanning electron microscopy of spheres*

SEM was conducted on spheres to investigate surface morphology and sphere size. The first samples tested were PEGDA spheres produced via emulsion and Tetronic/PEGDA spheres produced via hardening bath. Briefly, crosslinked spheres made of either PEGDA or Tetronic/PEGDA mix were freeze dried in a lyophilizer overnight. Dried spheres were then placed on an aluminum SEM stub and sputter coated with gold using an EMS 550X Sputter Coating Device. SEM images were taken using a Zeiss EVO 50 Variable Pressure Scanning Electron Microscope.

SEM images were also taken of PEG-fibrinogen microspheres created via emulsion. Due to the presence of a biological component, these spheres required additional processing prior to SEM. First, spheres were placed in microporous specimen capsules (30 μm pores, EMS) and fixed in 4% paraformaldehyde solution overnight at 4°C. Capsules were then washed with PBS and fixed with 1% osmium tetroxide (EMS) solution for 30 minutes at room temperature and

then washed again briefly in PBS. Capsules were then subjected to a graded dehydration series, spending 10 minutes in ethanol solutions of the following concentrations: 30%, 50%, 70%, 80%, 90%, 95%, 100%, and 100%. The capsules were then placed in an EMS 850 Critical Point Dryer and were sputter coated and imaged as described previously.

2.6 *Encapsulation of mESCs in PF constructs*

mESCs were biochemically released from gelatin dishes using trypsin (GIBCO) and resuspended in PF precursor solution composed of Batch-1 PF with 2% (v/v) Irgacure 2959 photoinitiator solution and 0.1% (v/v) triethanolamine (TEA, Acros Organics). PF constructs were shaped by encapsulating mESCs at 4 different cell densities and pipetting 35-50 μL per well of the polymer-cell mixture into a 96-well plate. Cell-laden PF constructs were photo-crosslinked by exposing to a metal halide lamp for 5 minutes and were subsequently transferred to a 24-well or 48-well plate containing 1 mL or 300 μL of differentiation media, respectively. Media was changed every day up to 37 total days of differentiation. Ascorbic acid (sterile stock solution composed of 10 mg/mL DI water, Sigma) was added as a media supplement at a concentration of 10 μL/mL of differentiation media on the fourth day and every day after. Constructs were observed using an inverted Nikon Eclipse TS100 microscope and imaged using a Nikon D40X DSLR camera.

2.7 *Microencapsulation and differentiation of mESCs*

mESCs were trypsinized and resuspended in PF precursor solution. Hydrogel precursor solution was a combination of PEG-fibrinogen solution, 0.1% (w/v) Pluronic F68, 2% (v/v) Irgacure 2959 photoinitiator solution, and 0.1% (v/v) triethanolamine. Irgacure 2959 photoinitiator solution

was composed of 10% (w/v) Irgacure 2959 in 70% ethanol solution. A hydrophobic photoinitiator solution (2,2-dimethoxy-2-phenyl acetophenone in 1-vinyl-2-pyrrolidinone, 300 mg/mL) and triethanolamine were mixed with embryo-tested sterile mineral oil (Sigma) at 5 µL/mL oil and 1.5 µL/mL oil, respectively. Two different batches of PF were used for microsphere differentiation experiments: Seliktar's PF and Batch-2 PF. Cells were suspended in the aqueous PF hydrogel precursor, and this hydrogel precursor solution-cell mixture was dropped into the hydrophobic mineral oil-phase to form a water-in-oil single emulsion. Microspheres were formed by vortexing the emulsion for 2 seconds and the spheres were simultaneously crosslinked by exposure to UV light via metal halide lamp for a total of 40 seconds (see Figure 4). The crosslinked microsphere portion of the emulsion was separated from the oil phase with 3 subsequent cycles of centrifugation and DMEM washing before the microspheres were suspended in differentiation media in a tissue culture dish. Encapsulation of mESCs was designated as the initiation of differentiation, or Day 0 of differentiation. Viability was assessed by incubating freshly encapsulated cell-microspheres in PBS containing Live/Dead Viability/Cytoxicity kit dye (Invitrogen L-3224) for 30 minutes, followed by fluorescent imaging. Live/Dead dye was administered at a concentration of 2µM calcein AM (live signal) and 4 µM ethidium homodimer-1 (dead signal). Media was changed by the fifth day of differentiation and every 2-3 days following the first change as cells proliferated and required fresh media. Media was changed by passing the microsphere suspension through a BD Falcon 40 µm cell strainer to collect the spheres while removing spent media. The cell strainer was then inverted to pass fresh media and the spheres into a culture dish. Alternatively, after 7 days of differentiation, media was changed by transferring the suspension culture to a centrifuge tube to allow the microspheres to settle at the bottom of the tube. The supernatant was then exchanged

with fresh media and the suspension was transferred back to a culture dish. mESCs encapsulated using Seliktar's PF degraded their microsphere carriers after roughly 9-10 days of differentiation and attached to the dish bottom. Unattached EB-microspheres that remained in suspension were transferred to separate dishes, while dishes laden with attached colonies were continuously cultured in parallel to the microspheres in suspension to observe contracting attached colonies.

2.8 *Characterization of microspheres and differentiation*

Phase contract images and videos taken of microspheres with encapsulated mESCs were imaged using a Nikon Eclipse inverted microscope equipped with an Andor camera. Live imaging was performed immediately after encapsulation or up to 3 weeks after initiation of differentiation. Microsphere diameter was measured using Nikon Elements software's analysis tools.

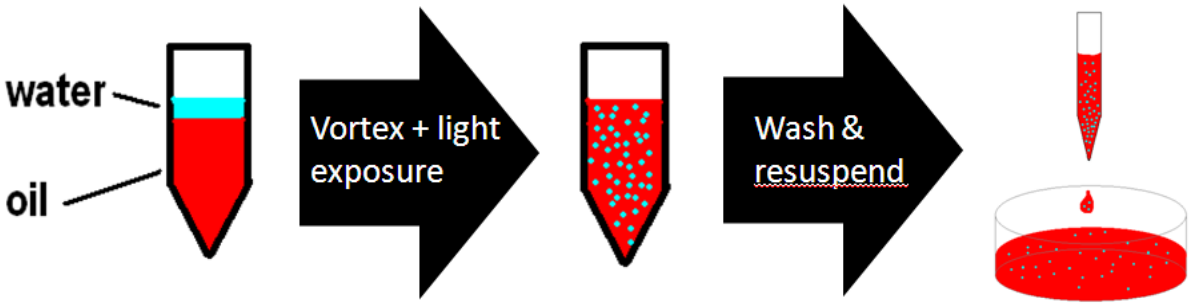

Figure 4: Process illustration of emulsion-generation of microspheres. An emulsion is formed by dropping the aqueous cell-polymer mixture into mineral oil. Microspheres are formed by vortexing the emulsion with simultaneous UV light exposure for photo-crosslinking. The polymerized spheres are then washed with DMEM and resuspended in differentiation media.

2.9 *Microsphere contraction and epinephrine study*

The development of encapsulated mESC colonies and attached EB-microspheres were monitored daily for spontaneous contraction. Encapsulated and attached EBs' responses to epinephrine were assessed on their 28^{th} and 16^{th} days of differentiation, respectively. Percentage of

spontaneously contracting EBs was assessed immediately prior to drug exposure, several hours following dosing, and then again overnight. Epinephrine stock solution was comprised of 0.18% (w/v) epinephrine and 0.32% (w/v) ascorbic acid in 0.04 N HCl. To dose the differentiated tissue with epinephrine, differentiation media was replaced with differentiation media supplemented with epinephrine stock solution at a total epinephrine concentration of 0.2 mM. EB-microspheres were incubated in the epinephrine-supplemented medium, and this medium was not replaced throughout the study.

2.10 *RNA isolation and qPCR*

RNA was isolated from cells using RNA isolation kits from Qiagen (RNA-Micro Isolation Kit). Encapsulated cells were removed from microspheres by enzymatically degrading cell-laden microspheres in trypsin solution, centrifuging the solution, and removing the supernatant to obtain only cell material. Single cell suspensions, whether they were un-differentiated cells from 2-D culture or differentiating, microsphere-encapsulated cells, were lysed using the kit's lysis buffer and centrifuged through the Qiashredder column. The lysed solution was then transferred to the RNA collection tube and RNA was isolated by following the kit's instructions. Approximately 14 µL of RNA solution was isolated per sample. The samples were stored in a freezer prior to qPCR. RNA concentration was analyzed using a NanoDrop Spectrophotometer (Thermo), and then was mixed at appropriate concentrations with specific gene promoters (Oct4 and Nkx2.5) to create a cDNA library using a thermocycler (Thermo). The cDNA libraries were then quantified for genes of interest by adding the cDNA to CyberGreen analyzed by qPCR (BioRad). Gene expression was normalized to GAPDH expression and $\Delta\Delta C_t$ method was used to assess relative expression.

2.11 *Immunohistochemistry*

Pluripotency of mESCs was assessed by staining for pluripotency marker Oct4. Briefly, mESCs were plated onto gelatin-coated microscope slides and allowed to attach overnight in mESC expansion media containing LIF. The slides were then washed with PBS and the attached cells were fixed with 4% paraformaldehyde for 10 minutes at room temperature. Slides were then washed with PBS for 3 minutes before the cells were permeated with PBS-T (PBS with 0.1% Triton X-100) for 50 minutes at room temperature. The slides then underwent antigen retrieval by boiling in citric acid (pH 6) for 15 minutes. After cooling and PBS rinse, the samples were blocked in 3% FBS blocking buffer for 25 minutes. Primary antibody containing 1:100 Oct4 antibody (Abcam) was applied for 1 hour. The samples were triple rinsed with PBS and then exposed to the Oct4 secondary antibody at a 1:500 dilution for 1 hour. Following the secondary antibody incubation, the samples were fixed with Vectashield mounting medium with DAPI (Vector Laboratories) and stored in a humidified container for fluorescent imaging. Imaging was performed on a Nikon TE-2000U inverted microscope using the Nuance FX multispectral imaging system.

III. RESULTS

3.1 *Assessment of Tetronic and Pluronics*

Tetronic and Pluronic F127 were dissolved in PBS at a range of concentrations and their reverse gelation kinetics were examined. Reverse gelation has been shown in literature[62] to occur with these polymer solutions when they are at least 20% (w/v) concentrated and removed from a refrigerated environment, generally around 4°C. The saturation limit for dissolving the polymers was 40% (w/v), where at 4°C the saturated solutions were highly viscous. The high viscosity of the saturated solutions was not measured, but could be comparable to molasses, and made the polymer extremely difficult to handle. At concentrations ranging between 20-30%, the polymers were still very viscous at 4°C and difficult to manipulate using precise volumes due to their propensity to stick to the inside of pipettes and containers. Pluronic polymer solutions were more difficult to handle than Tetronic solutions at the same concentrations. Due to the high viscosity of the polymers and the cold conditions at which they had to be handled, they were not used for encapsulation experiments.

Although Tetronic was not used for encapsulation, initial studies were conducted to assess its reversible physical gelation behavior. Non-functionalized Tetronic was mixed with PEGDA and its swelling ratio was assessed by weighing gelled discs prior to and after swelling. Excess liquid was removed from swelled disc samples by gently dabbing the discs with a Kim wipe. Swelling ratio results can be seen in Figure 5. It appeared that hydrogels composed of PEGDA only resulted in gels with increased weight with swelling, while gels containing any Tetronic resulted in gels with decreased weight. This may be attributed to the nature of each polymer's crosslinking; the PEGDA was covalently crosslinked while the Tetronic was only physically gelled. Thus swelling the gels containing Tetronic diluted them, allowing the

Tetronic polymer to diffuse out within the first 30 minutes of swelling. This is evident as the weight of the gels containing Tetronic did not fluctuate after the first 30 minutes of swelling.

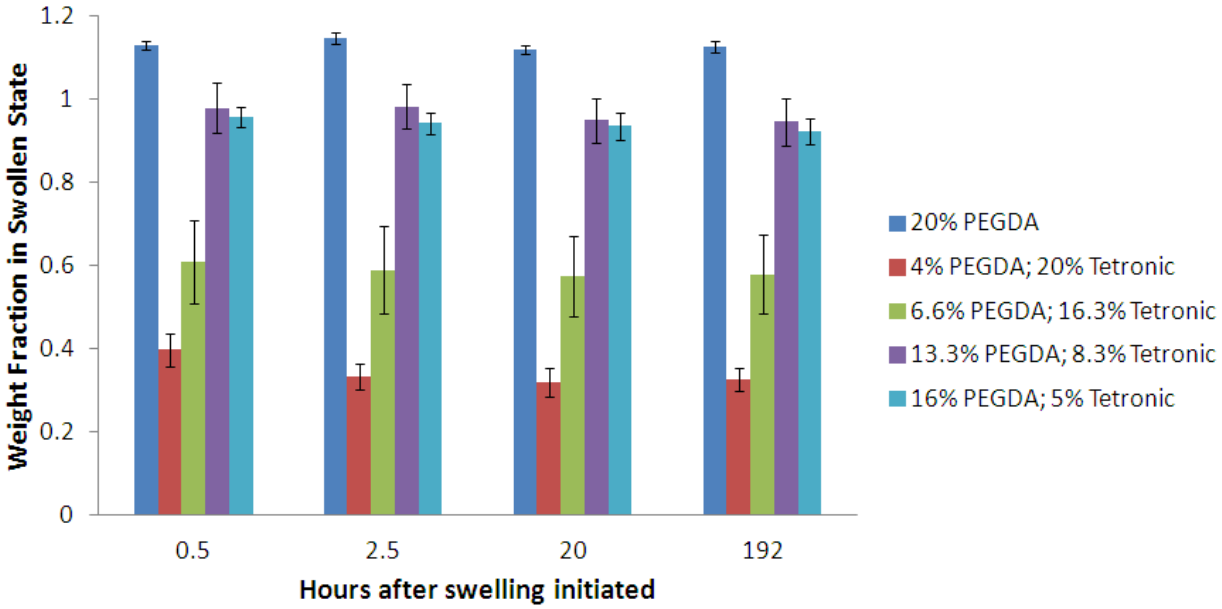

Figure 5: **Swelling ratios of Tetronic-PEGDA hydrogels.** Three gels of each polymer composition were weighed after crosslinking and subsequently reweighed 0.5, 2.5, 20, and 192 hours after the initiation of swelling. Weight fraction in swollen state is calculated as $Weight_{Swollen\ Polymer}/Weight_{Dry\ Polymer}$. Error bars reflect standard deviation of averaged ratios for each hydrogel composition.

The sphere formation method outlined by Cellesi *et al.*[62] was tested by dropping 30% Tetronic-PEGDA solution into a hardening bath. It was found that spheres would not form upon impacting the surface of the hardening bath unless both Tween 80 and a layer of n-hexane were added to the bath with stirring. This brought to our attention how crucial a surfactant would be for forming a sphere. While this method was exciting, Tetronic's reverse gelation kinetics were simply too difficult to control at room temperature and the smallest spheres which could be produced with the viscous polymer were greater than one millimeter in diameter.

3.2 *SEM characterization of materials and processes*

A crosslinked Tetronic-PEGDA sphere formed via hardening bath method was characterized by SEM, and the sphere's size and surface can be seen in Figure 6. The diameter of the dehydrated sphere was roughly 1700µm (Figure 6).

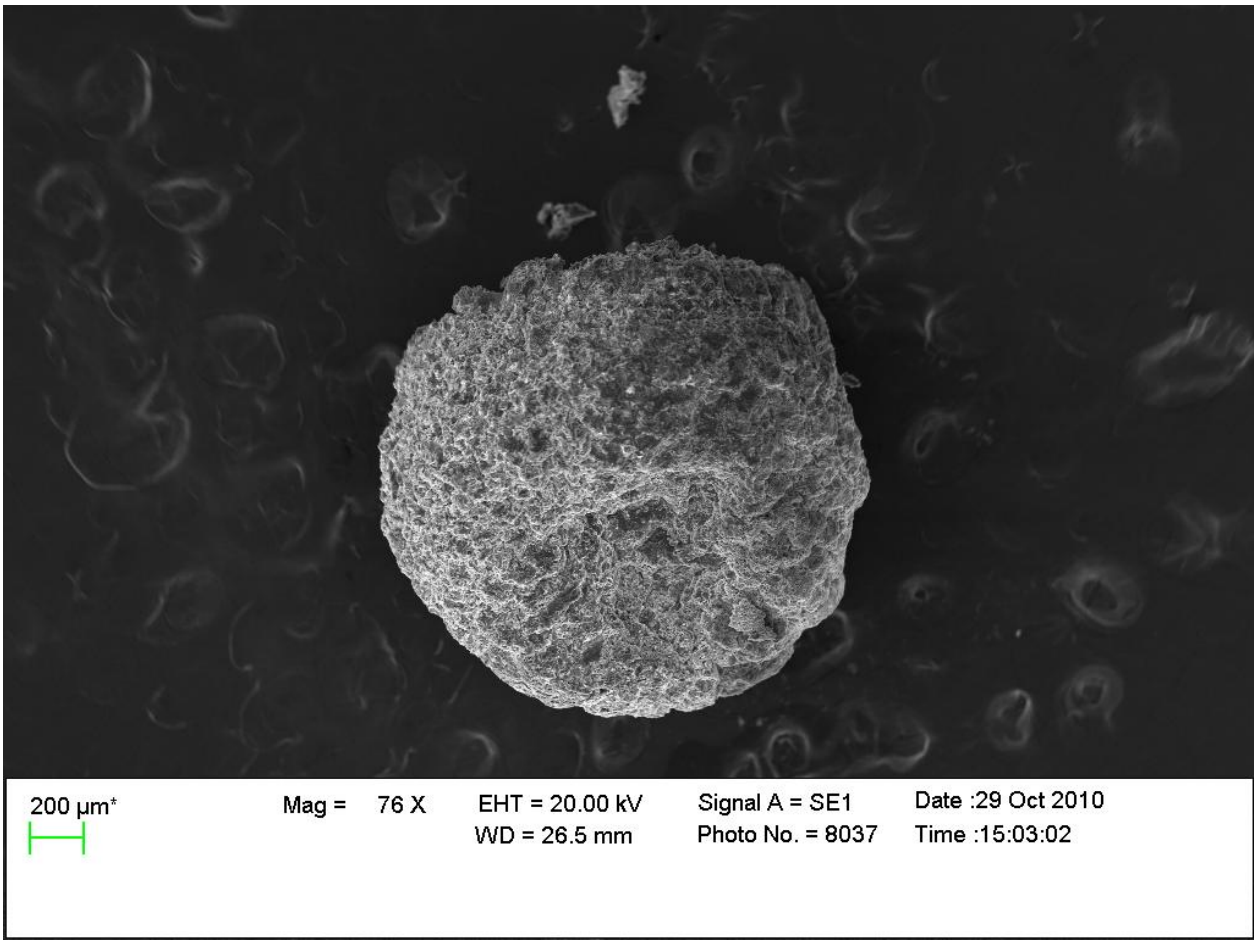

Figure 6: A Tetronic-PEGDA sphere. An SEM image of a single Tetronic-PEGDA microsphere formed by dropping into a hardening bath containing surfactant. The polymer solution was composed of 150 mg PEGDA/mL of 30% Tetronic solution in PBS, with acetophenone as the photoinitiator.

The porous Tetronic-PEGDA polymer matrix can be seen at the higher magnifications (Figure 7 A & B), where the pores appear to form a hierarchical network of larger pores, roughly 100µm in size, to smaller pores with sizes on the order of tens of microns.

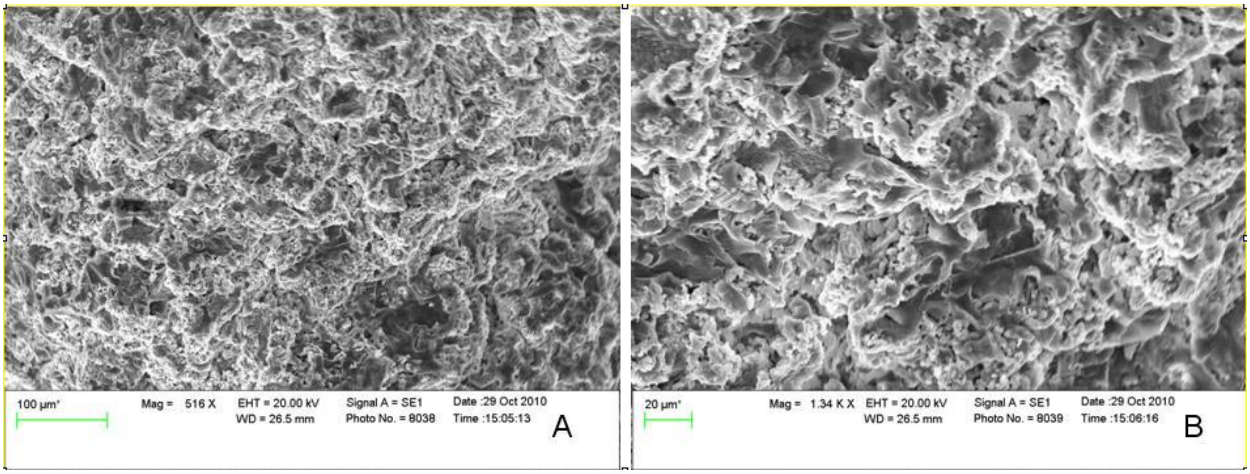

Figure 7: Tetronic sphere surface exhibited crosslinked polymer network. High magnification SEM images of Tetronic-PEGDA microsphere surfaces. Pores can be seen within the dried polymer matrix. A) At 516x magnification. B) At 1340x magnification. Scale bars are 100 and 20 µm, respectively.

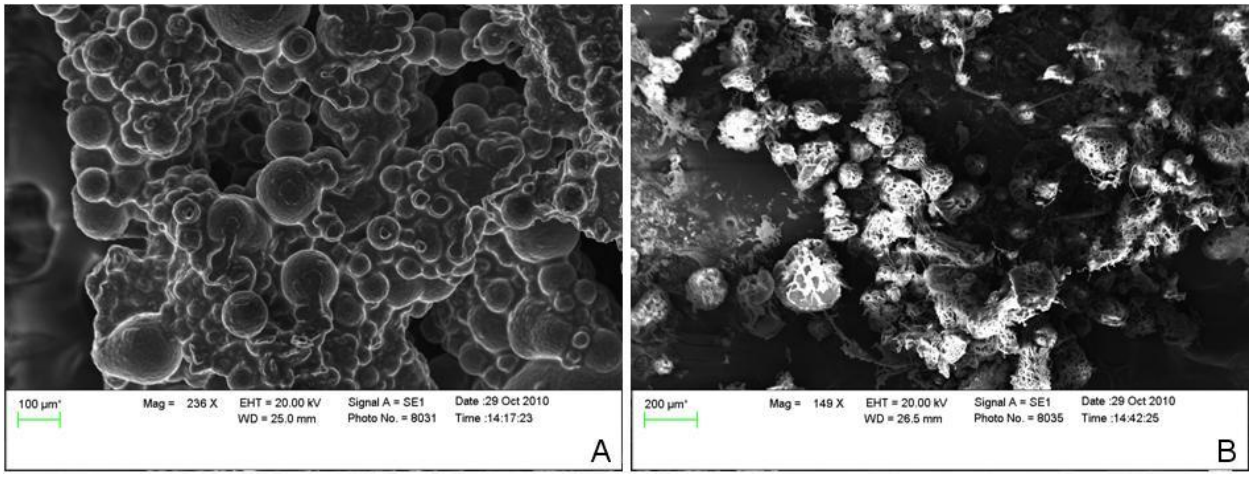

Figure 8: SEM images of PEGDA spheres. SEM images of PEGDA spheres formed in early emulsion trials without the use of surfactant. Spheres were A) unwashed and oil coated or B) washed. Scale bars are 100 and 200 µm, respectively.

Crosslinked PEGDA microspheres which were produced via emulsion are shown in Figure 8. These spheres were either washed (8A) or unwashed (8B). It was seen that a significant amount of oil was present on the unwashed spheres, which acted to encapsulate the

spheres. Furthermore, these unwashed spheres are representative of the typical clumped spheres which were obtained initially without the use of a surfactant and an optimized emulsion procedure (see Section 3.3). These spheres appeared to range in diameter from roughly 50-100 microns. On the other hand, the washed spheres exhibited a porous matrix similar to that seen in the large Tetronic sphere. These washed spheres appeared to have a diameter between 100 and 200 microns, larger than the unwashed spheres. This apparent difference in diameter may be attributed to variability in sphere-size seen from emulsion to emulsion, or due to the sphere swelling which resulted from the washing process.

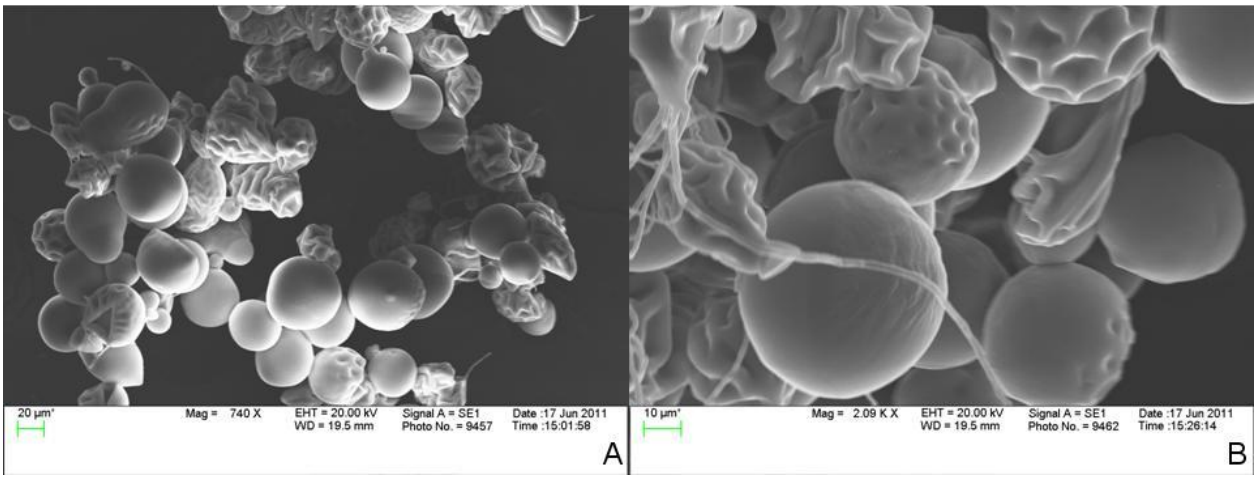

Figure 9: SEM images of PEG-fibrinogen microspheres. Spheres were formed using the optimized emulsion procedure. A) 740x magnification shows the relative sizes of the spheres and different surface morphologies among different spheres (scale 20 µm). B) 2,090x magnification shows smooth and shriveled morphologies more closely (scale 10 µm).

PEG-fibrinogen spheres were fixed in 4% paraformaldehyde solution to stabilize the protein component of the hydrogels and were dehydrated thoroughly using both ethanol dehydration and critical point drying. These spheres exhibited a unique morphology in comparison to spheres composed of only PEGDA. There were no pores visible in these PF spheres, most likely due to the presence of fibrinogen (Figure 9). The PF spheres exhibited

completely smooth and round surfaces or a "shriveled" yet still smooth morphology. This difference in surface morphology is not fully understood, but may be explained by varied degrees of biomaterial drying, or inhomogeneous distribution of protein and PEG. PF microspheres appeared to be relatively uniform in diameter, with a range between roughly 50-100 microns. This diameter range agreed with rigorous measurements of microsphere sizes analyzed via phase contrast imaging (as will be discussed in Section 3.7), although the slightly decreased diameters may be explained by the dehydrated state of the spheres.

3.3 *Preliminary emulsion experiments highlighted the necessity of a surfactant*

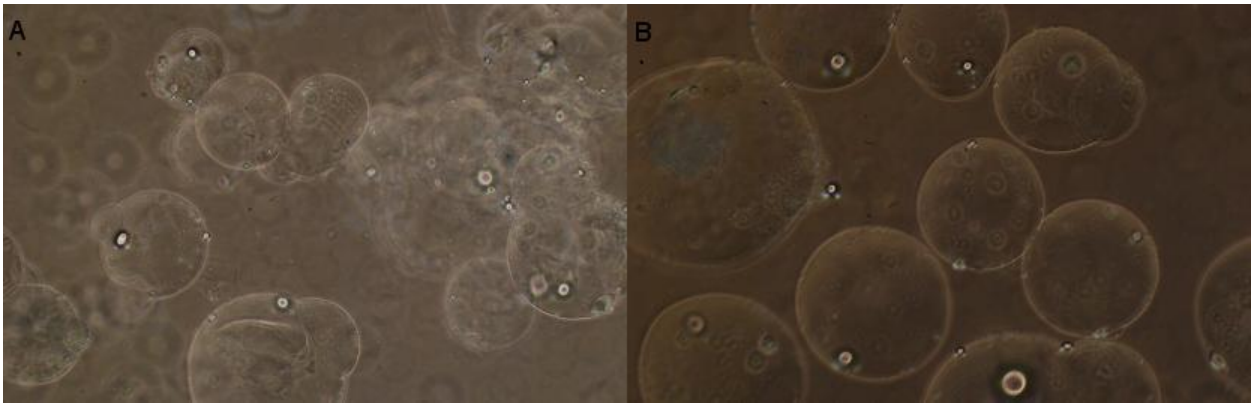

Figure 10: PF microspheres produced in early emulsion trials. 10x magnification phase contrast images of PF microspheres formed via standard emulsion (without surfactant) using 40 seconds of total crosslinking time. (A) An emulsion vortex time of 20 seconds yielded clumped particles. (B) An emulsion time of 40 seconds yielded non-clumped particles.

Preliminary experiments were conducted in order to establish the conditions needed for microsphere encapsulation of cells. Initially, the concentrations of photoinitiators Eosin Y and acetophenone were varied along with the ratio of polymer solution volume to oil volume. Vortex and UV crosslinking times were also varied, typically with vortex times between 20 to 40 seconds. These initial emulsion tests were performed using VWR 1.5mL microcentrifuge tubes,

which are conical in shape. It was found that regardless of how those parameters were varied, spheres were poorly dispersed and would crosslink in clumps (refer to Figures 8A, 10A, and Appendix Section 6.2). Given long vortex times, dispersion of spherical spheres was achieved (see figure 10B), yet long vortex times would not be appropriate for live cells. Because of this, surfactants were tested for their efficacy in dispersing microspheres in order to eliminate the need for long vortex times.

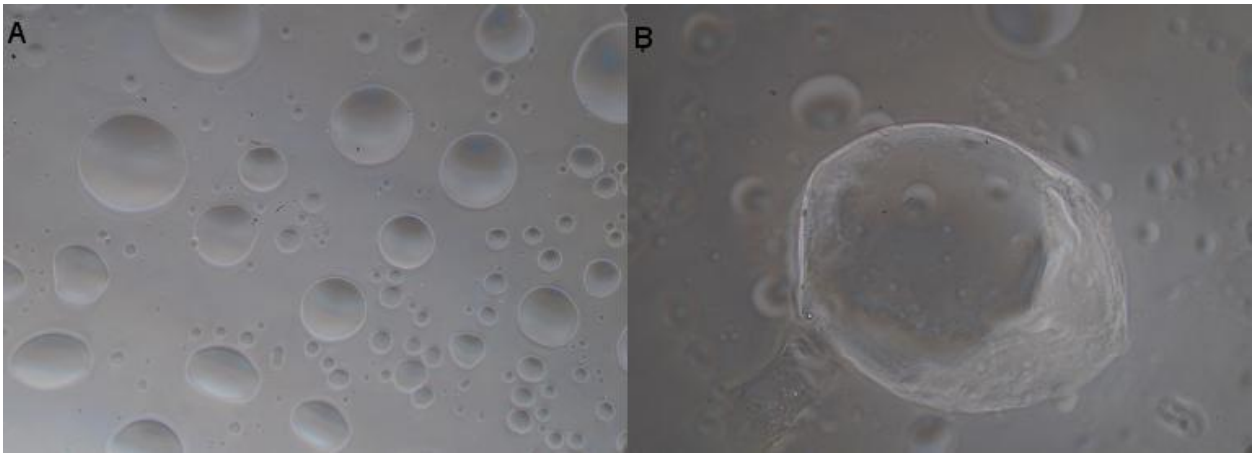

Figure 11: Spheres formed using diluted Griffiths' surfactant. 10x magnification phase contrast images of PEGDA spheres formed using Griffiths' surfactant. (A) Non-spherical particles with a large size distribution were achieved. (B) A large particle formed with partial polymerization.

During the process of exploring surfactants to disperse spheres, different surfactants were tested. Tested surfactants included Griffiths' surfactant, Pluronic F127 and Pluronic F68. "Griffiths' surfactant"[60] was investigated for its efficacy in microsphere dispersion using its undiluted state (1x), and dilutions ranging from 10x-500x in mineral oil. It was found that this surfactant was too effective in dispersing the aqueous-phase within the oil-phase, even at the highest dilution investigated. In other words, the surfactant was "powerful" due to its maximization of interaction between water and oil phases by minimization of surface tension.

This created a high interfacial surface area between the water and oil phases, which resulted in highly dispersed, small polymer particles. When polymer precursor solutions, composed of either PEGDA or PF, were dropped into the surfactants, the emulsion would immediately become cloudy without the input of mechanical energy. The aqueous-phase in these emulsions was photo-crosslinked via metal halide lamp exposure for 2 minutes and spheres were imaged. Images of photo-crosslinked emulsions using Griffiths' surfactant are shown in Figure 11. The particles that were generated appeared to be mostly spherical but it appeared that the surfactant interfered with crosslinking (Figure 11B). Additionally, it appeared that some particles formed were not composed of polymer, but rather oil droplets (Figure 12), which was an unwanted result for this application. It was discovered that the addition of an appropriate surfactant would mitigate the issue of generating poorly dispersed spheres while only requiring a greatly reduced vortex time of 2 seconds (refer to Appendix Section 6.2). Pluronic F68 was chosen as the surfactant at a concentration of 0.1% (w/v) in the polymer precursor solution for the optimized emulsion method of microsphere formation for cell encapsulation.

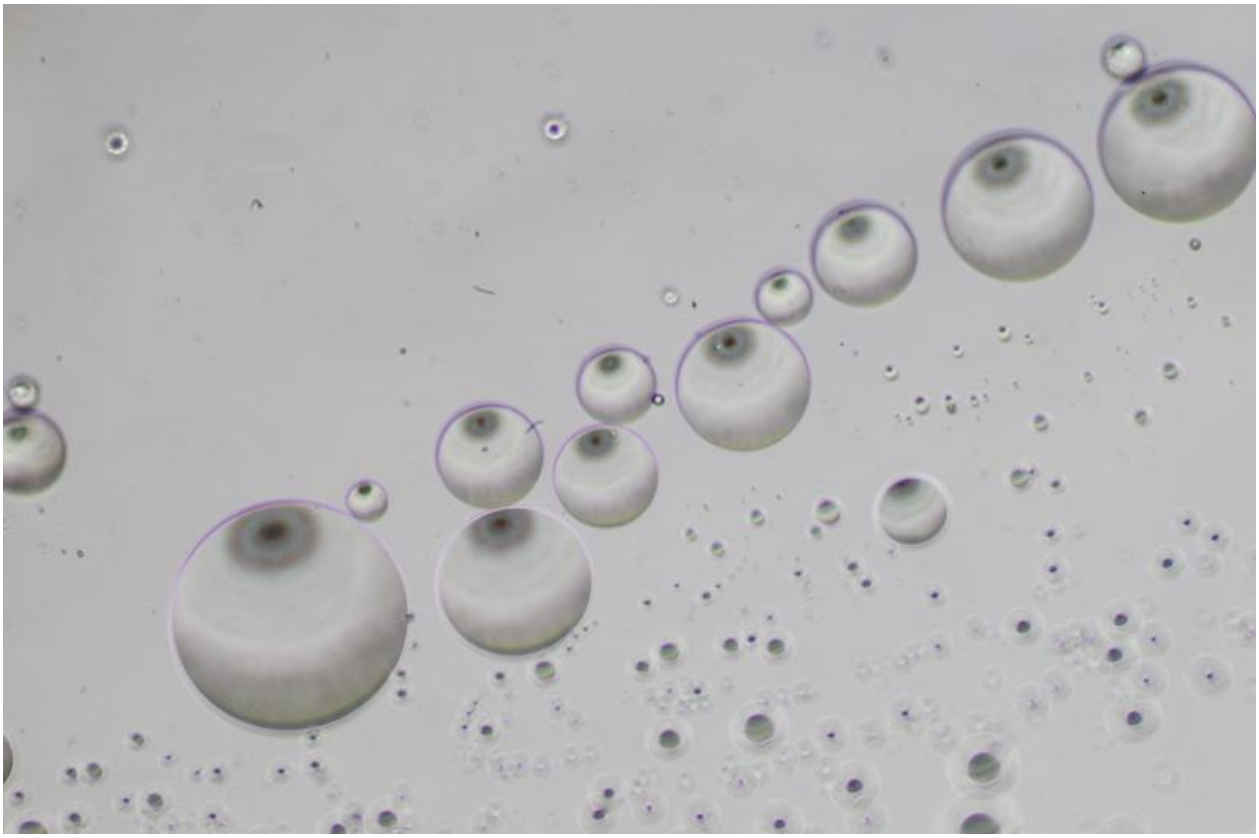

Figure 12: Oil spheres produced via emulsion. Oil spheres resulted when PEGDA was emulsified in Griffiths' oil-surfactant. The pattern that appeared on each particle is an optical effect of the phase contrast and oil. This image is a phase contrast image taken using the Nikon D40X camera.

3.4 *Material characterization*

Acrylation efficiency of synthesized PEGDA (10,000 MW) was assessed by NMR measurements. Acrylation efficiency was calculated by dividing the average number of moles of acrylate groups by the mole number of PEG end groups (2 per PEG chain). An acrylation efficiency of 93.25% was achieved.

Variation was a major concern when using PF as the hydrogel material. PEG-fibrinogen hydrogel protein content and dry weight content were analyzed and are shown in Table 1. Batch 2 yielded such low PEG content that it would not crosslink without the addition of extra PEGDA

at a concentration of 20mg PEGDA per mL of Batch-2 PF. With the addition of un-conjugated PEGDA to batch 2, the material became resistant to enzymatic degradation, which was observed during differentiation trials and when attempting to degrade hydrogels with trypsin in order to isolate cells for RNA isolation.

Batch	0.5mL weight [mg]	Dry weight [mg]	Dry weight %	Protein content [mg/mL]	Raw PEG weight [mg/mL]
1	484.5	15.0	3.1	12.81	17.19
2	486.2	6.7	1.4	7.17	6.23
Seliktar's	451.3	18.8	4.2	12.81	24.79

Table 1: PEG-Fibrinogen batch variation. Material content of three different batches of PF that were used for experiments

3.5 *mESCs in PF constructs yielded cardiac sheets*

mESCs encapsulated in PF constructs formed in 96-well plates were cultured for up to 37 days and were observed daily for spontaneous contracting tissues. Colony sizes of encapsulated mESCs were quantified on Day 5 of differentiation by taking images of constructs and measuring their cross-sectional area using ImageJ. Colony areas varied greatly and are represented graphically in Figure 15. There did not appear to be a distinct trend in colony area versus cell encapsulation density, but the two lower encapsulation densities yielded larger mean cross sectional areas and higher variability of those areas while the higher encapsulation densities yielded smaller colonies with smaller variability. Figures 13 and 14 show representative images of Day 5 encapsulated colonies, at the varied investigated densities, which were used for colony area quantification.

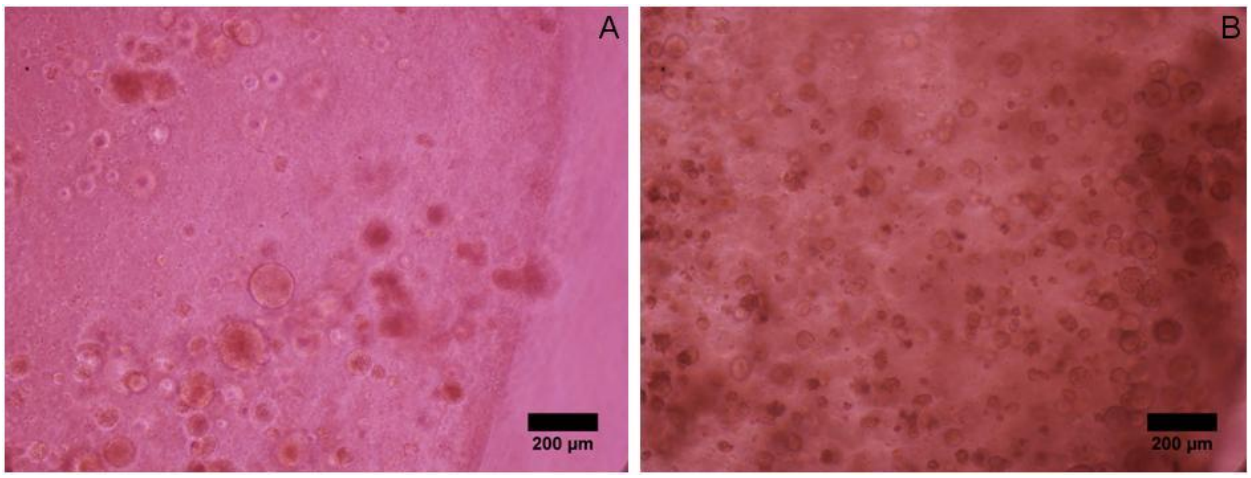

Figure 13: mESCs encapsulated at low concentration within PF constructs. 10x magnification phase contrast images of mESC colonies proliferating within PF constructs on Day 5 of differentiation. Initial cell densities of A) 3.2 and B) 6.4 million/mL PF are shown. Images were captured using a Nikon D40X DSLR camera.

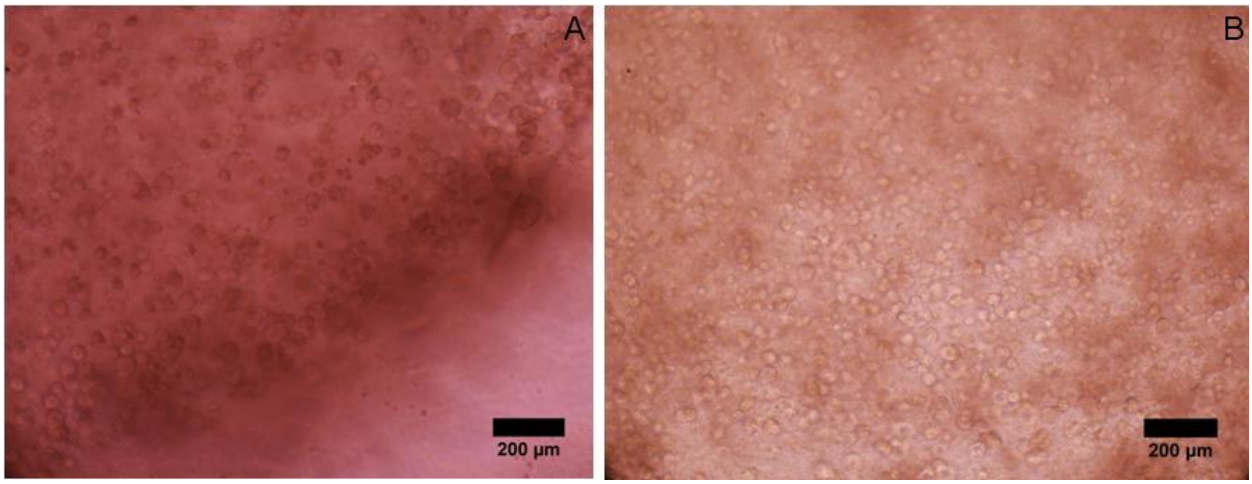

Figure 14: mESCs encapsulated at high concentration within PF constructs. 10x magnification phase contrast images of mESC colonies proliferating within PF constructs on Day 5 of differentiation. Initial cell densities of A) 12.8 and B) 25.6 million/mL PF are shown. Images were captured using a Nikon D40X DSLR camera.

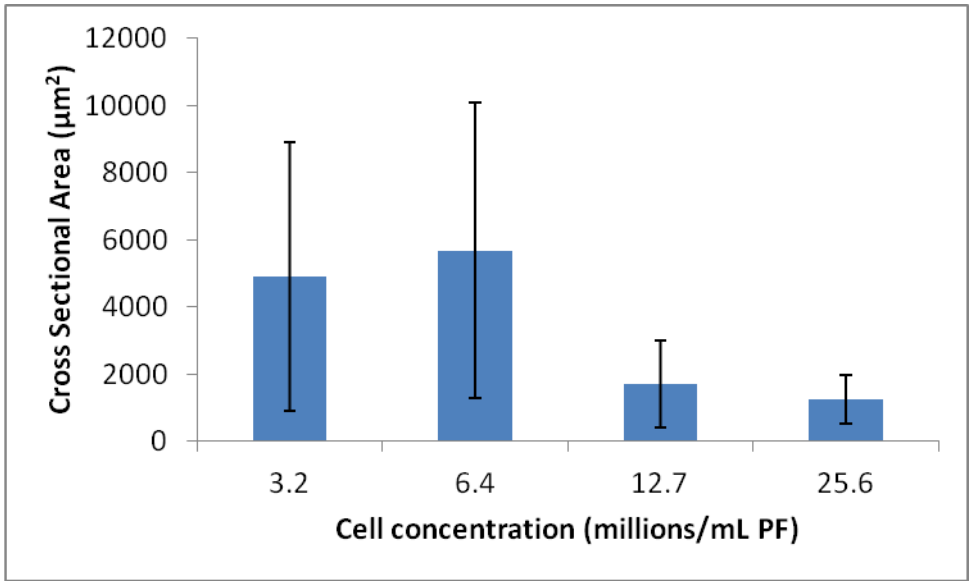

Figure 15: Cross-sectional areas of mESC colonies encapsulated within PF constructs. Cross sectional area of mESC colonies encapsulated within PF constructs on Day 5 of differentiation was assessed against initial cell encapsulation concentration. Bars indicate the mean measured cross-sectional colony area and error bars represent standard deviation. A minimum of 118 colonies were measured for each condition.

Table 2 summarizes observations of contraction made during the course of differentiation. Colonies appeared to originate from single cells and differentiated into contracting cardiac sheets at a low percentage. Spontaneously contracting tissue was observed in 6 of a total of 30 constructs, of which only 2 contracting constructs had the same initial cell encapsulation density. It should be noted that these two constructs which exhibited contracting tissue had the highest encapsulation density used for these experiments (27.5 million cells/mL PF), and spontaneous contraction was first observed in these constructs 27 days following the initiation of differentiation, which was a significant delay in onset of contraction time as compared to the other contracting constructs. The spontaneously contracting tissues formed by the cells and constructs, shown in Figure 16, were also the only ones which resembled cardiac cell sheets attached to the tissue culture dish, as opposed to the embryoid body-like tissues seen

in the other 4 contracting constructs. The lowest cell encapsulation density that yielded spontaneously contracting tissue was 6.4 million cells/mL PF. From these results, it did not appear that initial cell encapsulation density was a principle factor leading to contraction. Instead, all contracting tissues were somehow tethered to the tissue culture dishes, which underscored the contracting tissues' requirement of having a mechanical interface to push against. A whole construct (construct ID #4) was seen to contract and its tether to the culture dish is readily visible in Figure 17.

These experiments using PF constructs were a valuable demonstration of the behavior of encapsulated mESCs within the PF material for the purpose of generating cardiac tissue. The results showed that encapsulated mESCs were capable of surviving the encapsulation procedure and subsequent photo-polymerization, and were able to proliferate, form colonies and differentiate into cardiac tissue.

Construct ID	**Initial cell density (millions/mL PF)**	**Differentiation days where contraction was observed**	**Contracting tissue morphology**	**Range of number of distinct contracting areas**	**Range of contraction frequency (Hz)**
1	6.4	9	EB within construct	2	N/A
2	6.875	9-11, 14, 19-22	EB within construct	1-7 colonies	1-2
3	12.7	9-23	EB, full construct	1-6 areas	0.3-3
4	25.6	13-21	Full construct	Very many	1-2.5
5	27.5	27-37	Sheets	2-6	1-2
6	27.5	27-33	Sheets	1-3	1-2

Table 2: Summary of Differentiation of mESCs within PF constructs. Six PF constructs yielded spontaneously contracting tissues. Range of number of distinctly contracting areas was quantified by counting the number of contracting areas that beat asynchronously.

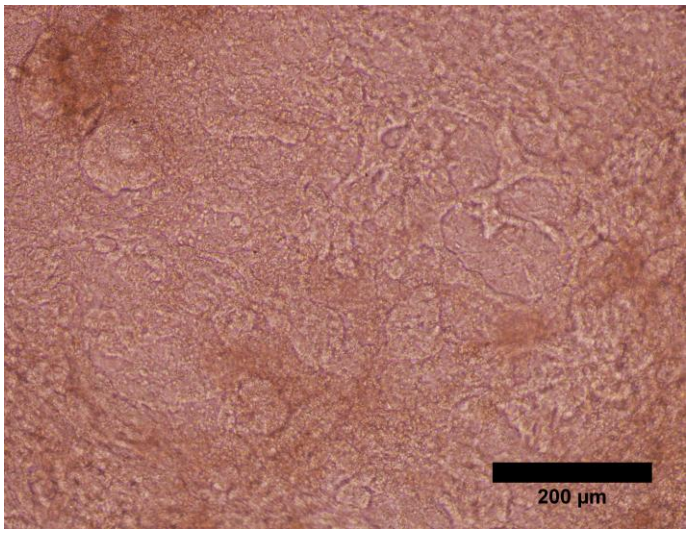

Figure 16: Contracting cell sheets formed from mESCs differentiated in PF constructs. A 20x magnification phase contrast image of a spontaneously contracting cardiac cell sheet on Day 30 of differentiation. The sheet was attached to the bottom of the culture dish and came from construct ID #5. Image were captured using a Nikon D40X DSLR camera.

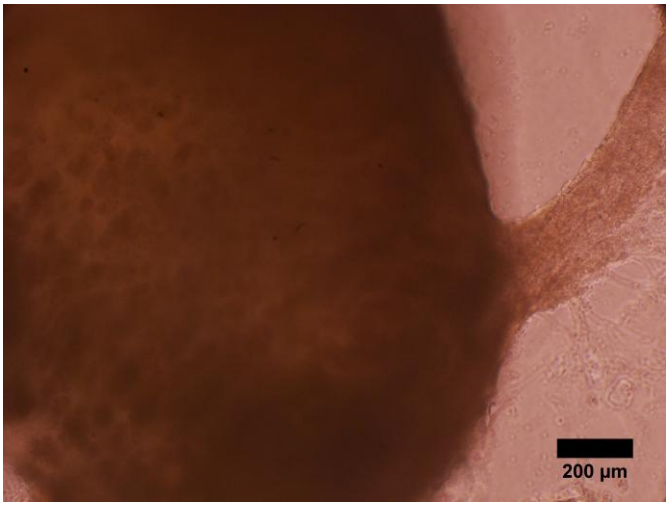

Figure 17: A whole-PF construct contracted. A phase contrast image of a PF construct (ID# 4) that was tethered to its culture dish. The tether can be clearly seen on the right as a structure composed of cells and extracellular matrix. Colonies can also be seen within the construct itself. The entire construct appeared to contract, and the origin of contraction was located where the tether appears to connect to the rest of the construct. This image was taken with a 10x objective and Nikon D40X DSLR camera on Day 14 of differentiation.

3.6 *Encapsulated cell viability*

To determine the viability of cells encapsulated within microspheres using the optimized encapsulation procedure, viability of cells encapsulated within PF spheres was assessed using a Live/Dead viability stain. The "live" stain was calcein AM, which is specific for live cells with esterase activity, while the dead stain was ethidium homodimer-1, which only enters the ruptured cell membranes of dead cells. Calcein AM live signal was detected by using a FITC fluorescent filter and ethidium homodimer-1 dead signal was detected using a TRITC fluorescent filter. The live and dead probes have peak excitation/emission wavelengths of 494/517 nm and 528/617 nm, respectively. Freshly encapsulated microspheres were incubated in dye solution for 30 minutes at room temperature and were subsequently imaged. Cells used for viability staining were encapsulated at a density of 20 million cells/mL PF using Batch-1 PF. Live and dead signals were attenuated using Nikons Elements software look up table (LUT) adjustments. Figures 18 through 21 illustrate the live dead staining of the cells. Mixed viability was seen, where greater than 90% viability was observed in one trial (shown in Figures 18 and 19), and lower than 50% viability was seen in the following trials (shown in Figures 20 and 21). The percentages of live cells and dead cells were not explicitly quantified due to the unreliability of quantifying live and dead signals in a three-dimensional hydrogel due to Z-dimension bleed-through of signal. However, all trials other than the first trial, which yielded very high viability, appeared to have less than or roughly 50% viability. The first trial's high viability cannot be explained except by saying that the fraction of viable encapsulated cells using this method was not controllable, since cells were encapsulated under identical conditions for all viability experiments. It should be noted that viability was assessed only after the optimized encapsulation procedure was formulated and after microsphere-encapsulated cells using the optimized procedure first showed

any signs of colony formation. Before the optimized encapsulation procedure was developed, microsphere-encapsulated cells would not proliferate following encapsulation and had a dark, shriveled morphology within the microsphere. This was due to the harsh processing conditions to which the cells were subjected; long vortex times and insufficient oil-washing resulted in rampant encapsulated-cell death. On the other hand, viable encapsulated cells typically exhibited a bright, smooth and round morphology.

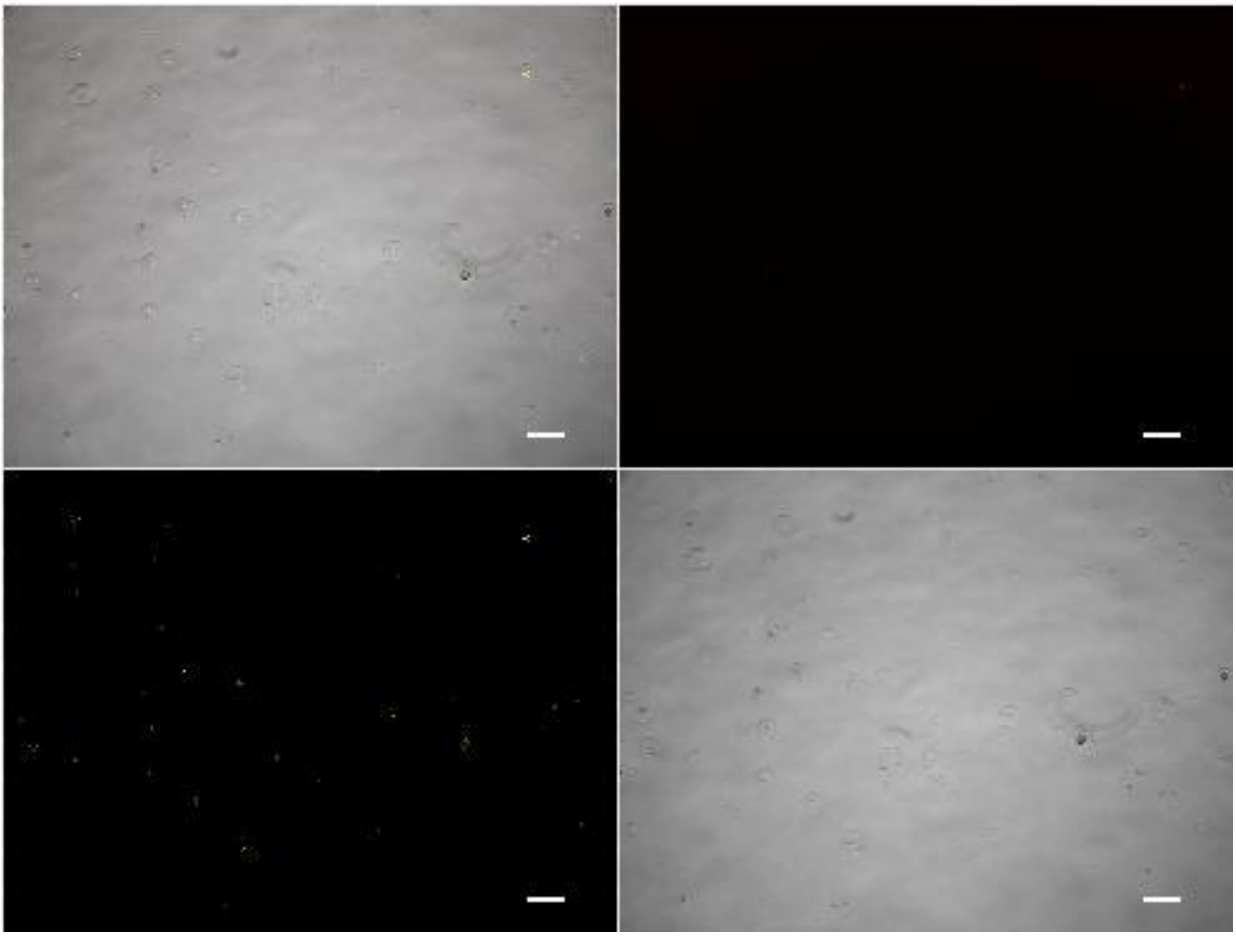

Figure 18: Live Live/Dead images of microsphere-encapsulated mESCs with high-viability. 4x magnification images of freshly encapsulated mESC in Batch-1 PF microspheres. Images are, clockwise from top left: 3 channels overlayed, dead, phase contrast, and live. These images were taken from the first live/dead encapsulation trial, where cell viability was high, which is evident in the high ratio of live cells to dead cells. Scale bars: 200µm.

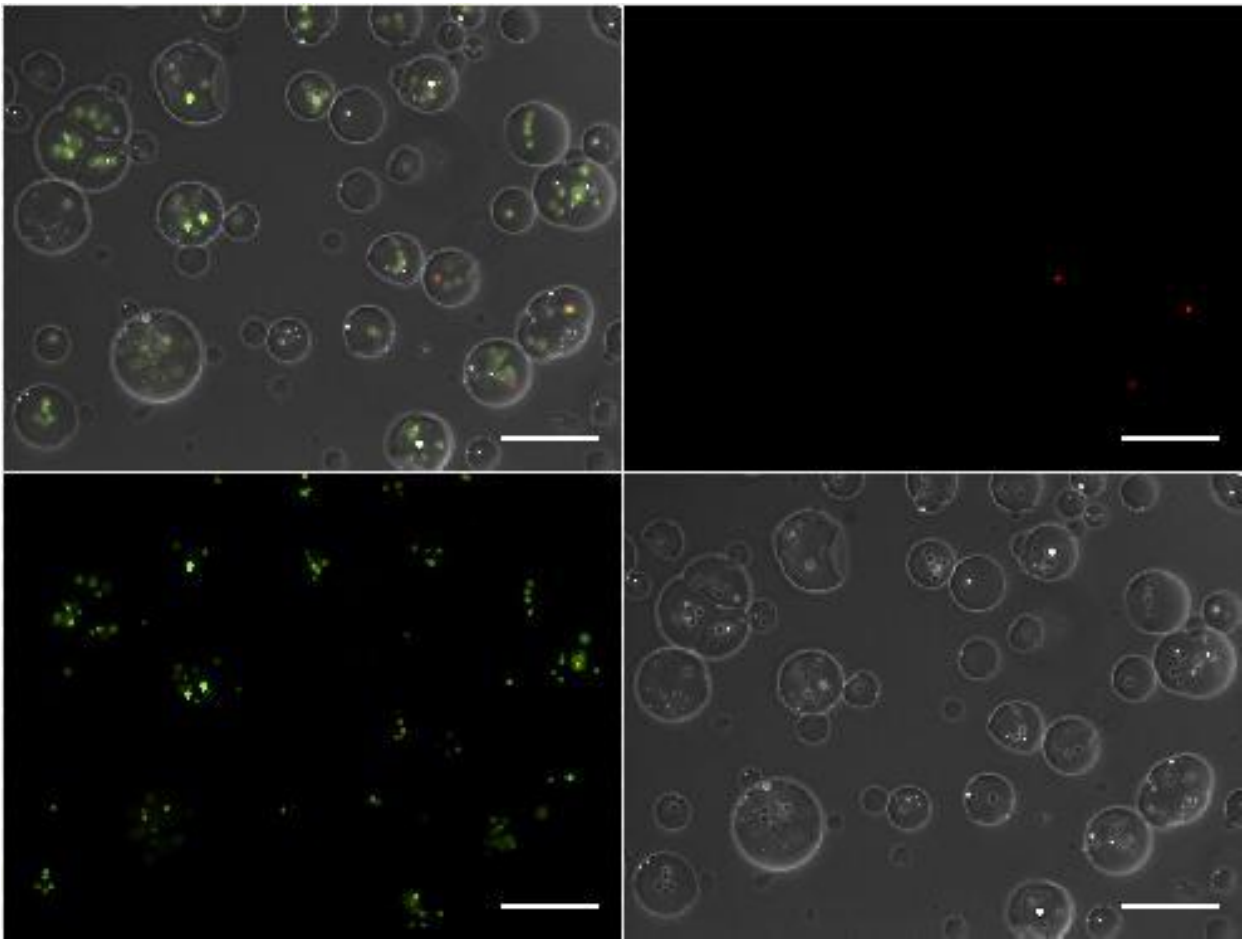

Figure 19: Live/Dead images of microsphere-encapsulated mESCs with high-viability. 10x magnification images of freshly encapsulated mESC in Batch-1 PF microspheres. Images are, clockwise from top left: 3 channels overlayed, dead, phase contrast, and live. These images were taken from the first live/dead encapsulation trial, where cell viability was high, which is evident in the high ratio of live cells to dead cells. Scale bars: 200µm.

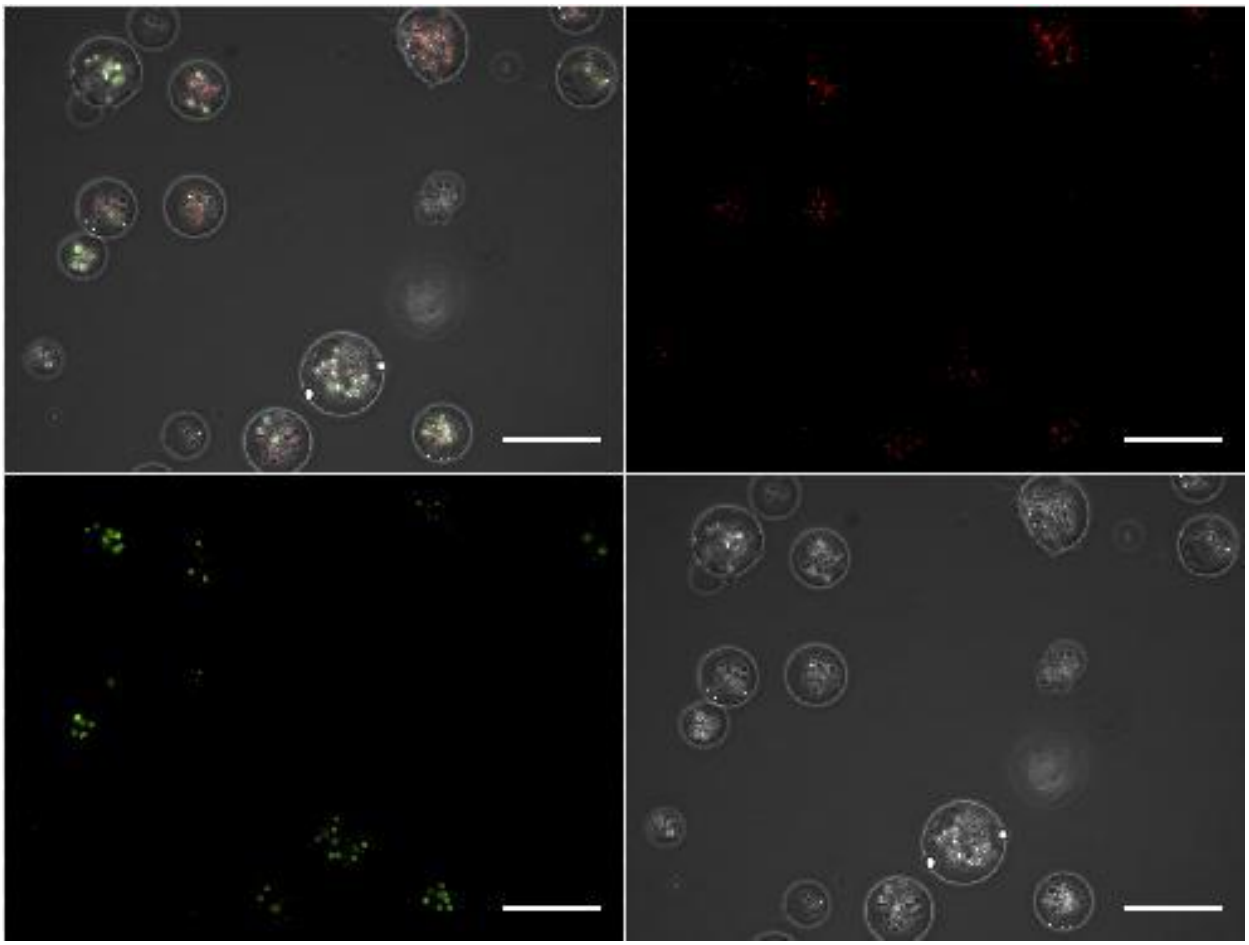

Figure 20: Live/Dead images of microsphere-encapsulated cells. 10x magnification images of freshly encapsulated mESC in Batch-1 PF microspheres. Images are, clockwise from top left: 3 channels overlayed, dead, phase contrast, and live. It can be seen that the ratio of live cells to dead cells is roughly equivalent. Scale bars: 200µm.

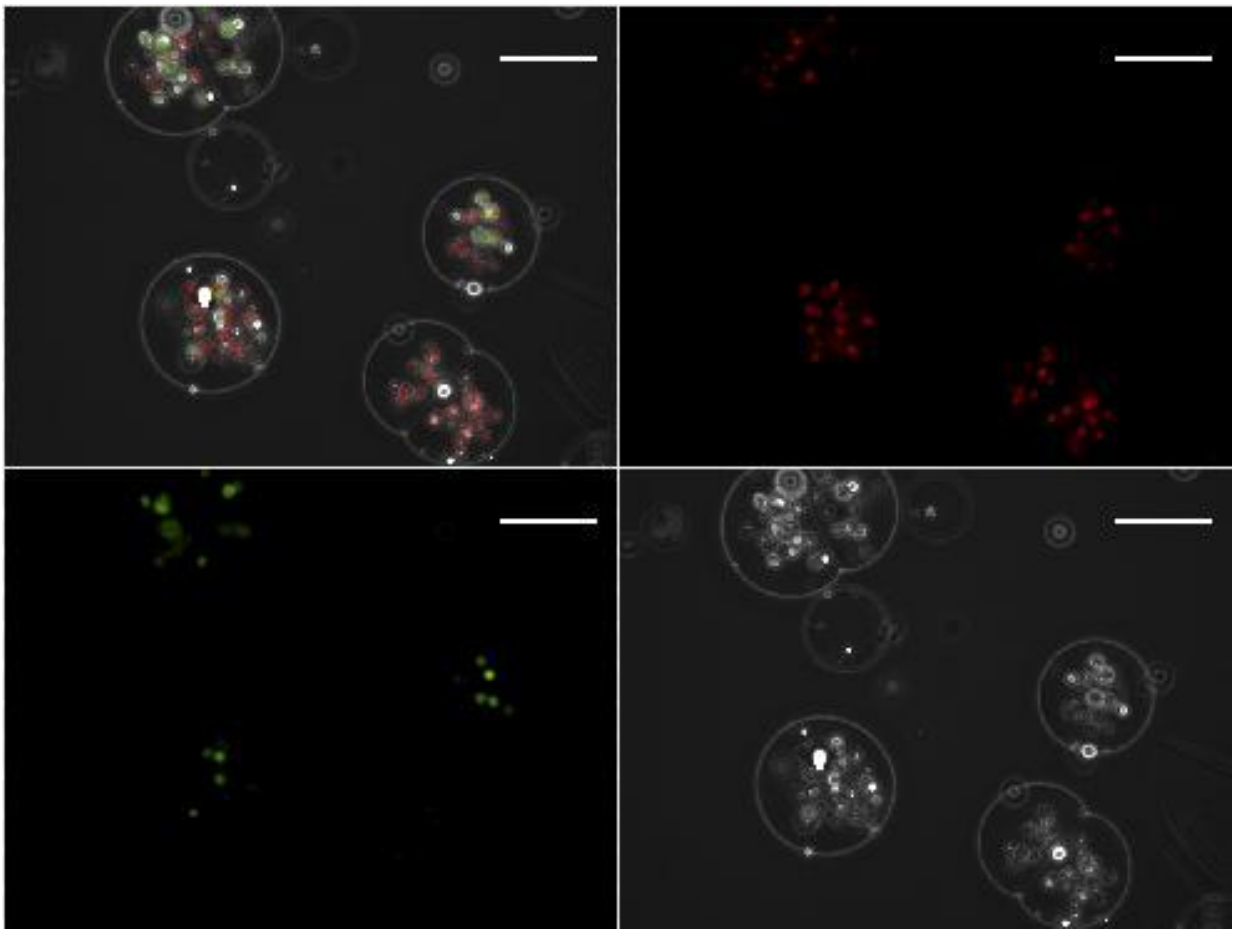

Figure 21: Live/Dead images of microsphere-encapsulated cells. 20x magnification images of freshly encapsulated mESC in Batch-1 PF microspheres. Images are, clockwise from top left: 3 channels overlayed, dead, phase contrast, and live. It can be seen that there are more dead cells than live cells. Scale bars: 100μm.

3.7 *Sphere size distribution*

The diameters of microspheres were measured with Nikon Elements imaging software by analyzing images taken of microspheres immediately after encapsulation via the optimized emulsion procedure. Size distribution was correlated to mESC encapsulation density, shown in Figure 22. Mean diameter of spheres was similar for all encapsulation densities except for the highest concentration of 60 million cells per mL hydrogel precursor solution. Despite a roughly

50% increase in mean diameter in the most concentrated spheres, the mean diameters amongst all five measured encapsulation densities did not show a statistical significant difference, which was shown by error bar overlap among all five densities. Histograms of sphere diameter distribution using Seliktar's PF are shown in Figures 23 and 24. Microspheres formed using Seliktar's PF produced spheres with a mean diameter of 166.8 ± 59.0 µm.

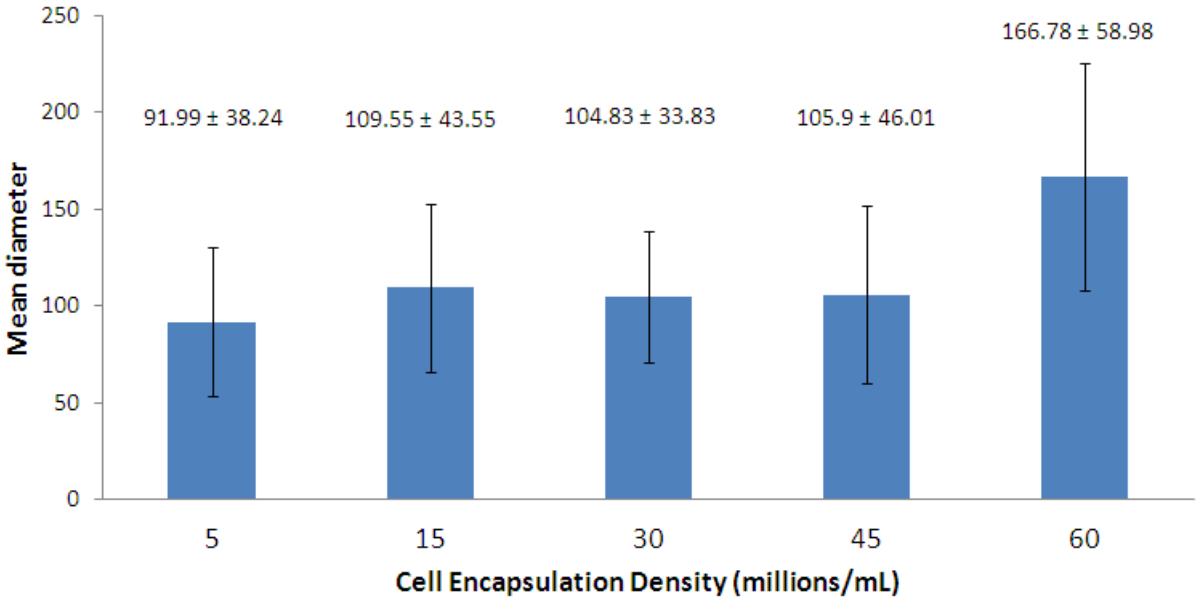

Figure 22: Cell encapsulation density and effect on microsphere size. Cell encapsulation density did not have a significant impact on mean sphere diameter. However, the highest encapsulation density of 60 million cells/mL yielded a higher mean diameter, although not statistically significant due to large standard deviation. n ≥300 for each density.

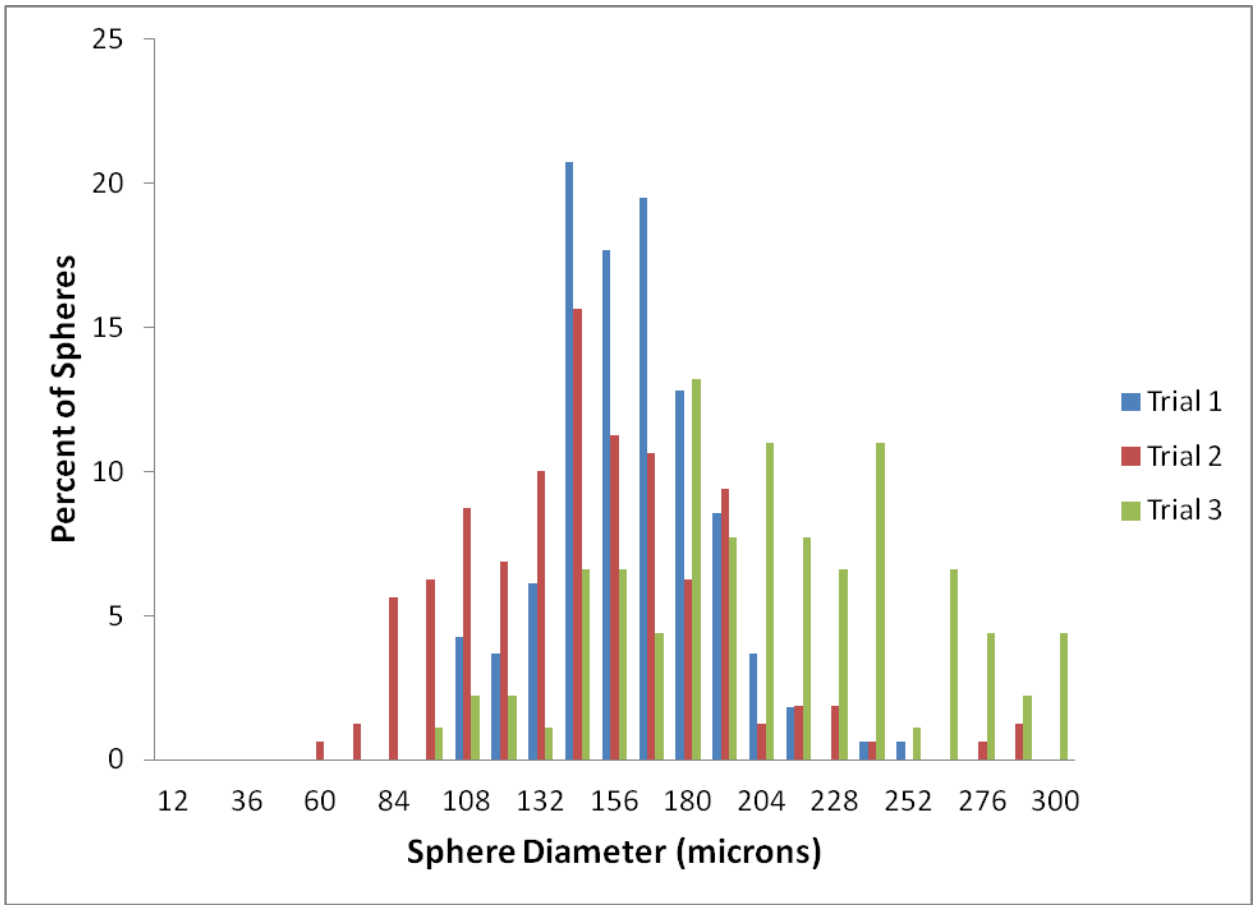

Figure 23: Representative diameter distribution of PF microspheres. This representative histogram illustrates size distribution of Seliktar-PF microspheres with cell encapsulation density of 60 million/mL precursor, produced using the optimized emulsion technique. Variance in size distribution is present among different emulsion trials using the same precursor solution, where Trials 1 and 2 share a similar peak diameter but Trial 2 has a broader distribution than Trial 1. Trial 3 shows a very broad diameter distribution with a greater mean diameter than the first two trials. Mean diameters of the separate trials are: Trial 1 = 155.1 ± 25.4 µm (n = 164); Trial 2 = 141.7 ± 41.3 µm (n = 160); Trial 3 = 223.3 ± 78.8 µm (n = 105). Mean diameter of three trials combined was =166.8 ± 59.0µm (n = 429).

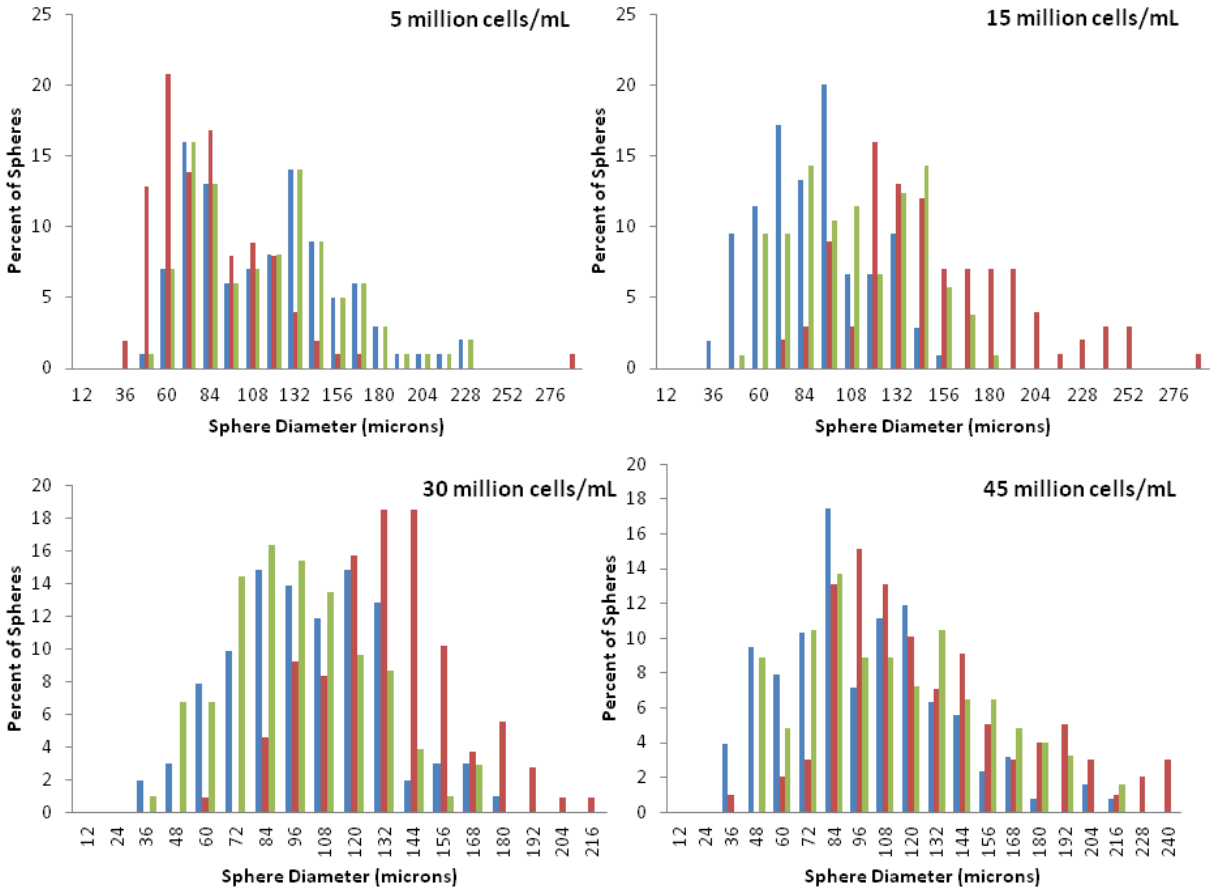

Figure 24: PF microsphere diameter distributions with varied cell density. Histograms of microsphere size distributions formed using Seliktar's PF at four separate encapsulation densities. Different peak diameters can be seen amongst trials in each density condition. The data from these measurements were used to determine mean sphere diameter for each encapsulation concentration. $n \geq 100$ for each trial of each condition.

With an addition of PEGDA at 2% (w/v) with Batch-2 PF, mean diameter decreased and size distribution tightened to produce a mean diameter of 89.8 ± 27.8μm (Figure 25) at an encapsulation density of 60 million cells/mL. Similarly, the microsphere size distribution generated using Batch-2 PF with additional PEGDA at a lower encapsulation density of 45 million cells/mL (Figure 26) yielded more reproducible size distributions across different trials than Seliktar's PF alone.

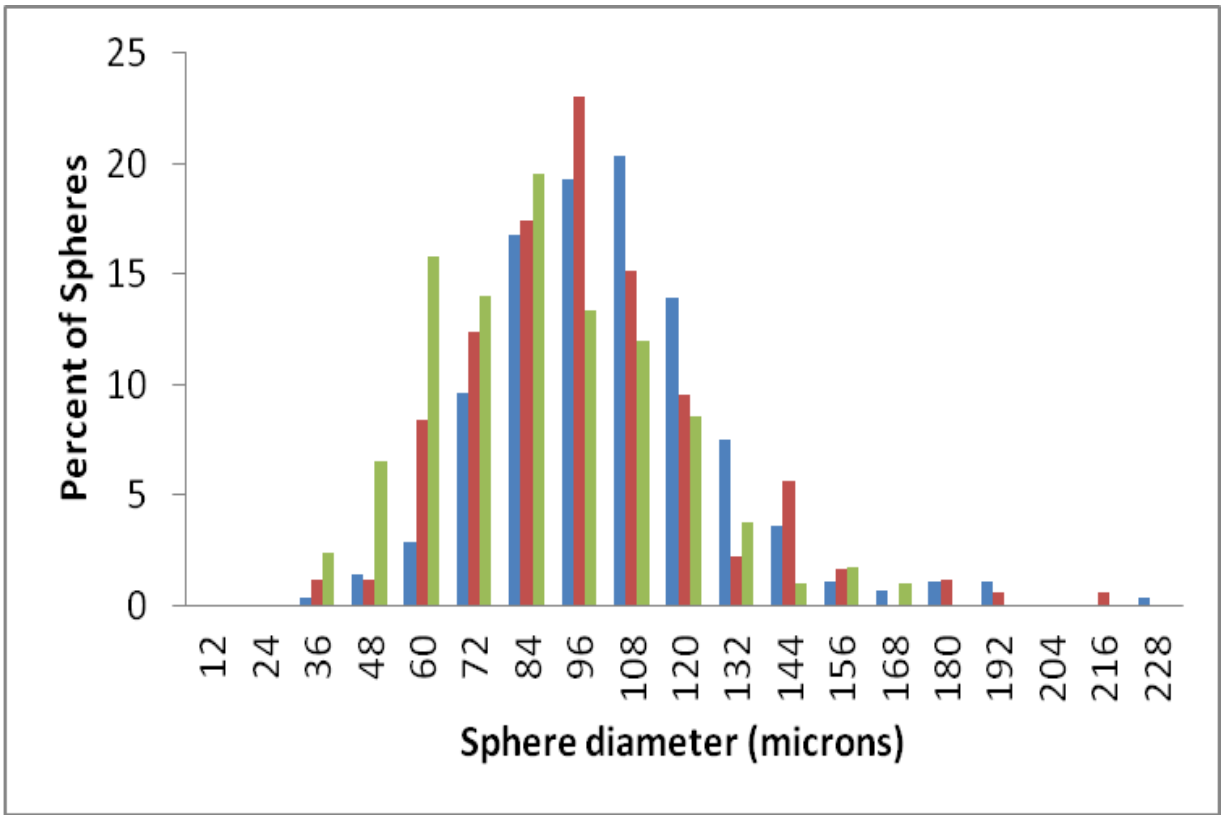

Figure 25: Sphere diameter distribution of Batch-2 PF with 60 million cells/mL. Size distribution of Batch-2 PF microspheres with additional PEGDA at 2% (w/v), at an encapsulation density of 60 million cells/mL precursor. More reproducible size distribution was achieved with the addition of unconjugated PEG. Mean diameters of the separate trials are: Trial 1 = 97.7 ± 26.2 µm (n=280); Trial 2 = 91.4 ± 27.8 µm (n=178); Trial 3 = 81.4 ± 27.0 µm (n=292). Mean diameter of three trials combined was = 89.8 ± 27.8µm (n=750).

Diameter measurements were taken from three trials at each condition (with a minimum of 100 sphere diameters measured for each trial) and variance among trials was more evident in the spheres formed using Seliktar's PF. Furthermore, only two conditions were tested for Batch-2 PF. Although these results indicate that Batch-2 PF with 2% additional PEGDA allows for greater reproducibility in size than Seliktar's PF, more trials would need to be carried out for verification due to the variability of size distribution among trials.

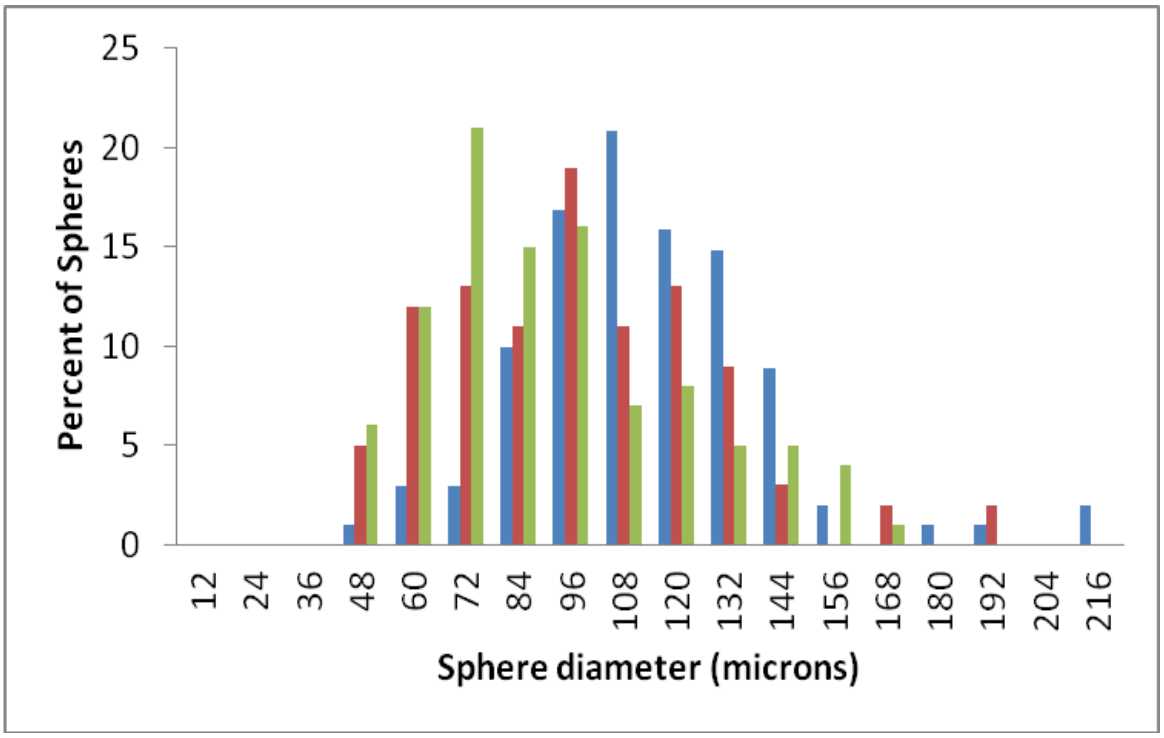

Figure 26: Sphere diameter distribution of Batch-2 PF with 45 million cells/mL. Size distribution of Batch-2 PF microspheres with additional PEGDA at 2% (w/v), at an encapsulation density of 45 million cells/mL precursor. Similarly to the 60 million encapsulation concentration using the same material, the size distribution was similar among three trials. Mean diameters of the separate trials are: Trial 1 = 107.7 ± 28.2 µm (n = 101); Trial 2 = 91.4 ± 30.6 µm (n=100); Trial 3 = 86.2 ± 29.8 µm (n=100). Mean diameter of three trials combined was 95.2 ± 31.0 µm (n = 301).

3.8 *Characterization of colony formation*

Cell encapsulation concentration had a significant effect on the ability of encapsulated cells to proliferate and differentiate. Concentrations within the range of 5 to 60 million cells/mL precursor solution were examined for their differentiation efficacy. The effect of encapsulation density on the number of cells per sphere can be seen in Figure 27. Low cell encapsulation concentrations of 5, 15, and 30 million cells/mL Seliktar's PF yielded poor colony formation and resulted in a halt of proliferation and differentiation 3 days post-encapsulation. Conversely,

continued proliferation and differentiation was observed at higher encapsulation concentrations of 45 and 60 million cells/mL of the same material. The relative successes of colony formation as a function of encapsulation density within the first 5 days of differentiation are shown in Figures 28 and 29. The dependence of successful differentiation on encapsulation density can be attributed to the ability of the mESCs to recognize the presence of nearby cells via cell signal diffusion through the hydrogel matrix, and the necessity of a threshold cell density to facilitate further differentiation. Thus for further cardiac differentiation experiments using both materials, cells were encapsulated at either 45 or 60 million cells/mL. However, successful colony formation was also achieved in an earlier trial using a low encapsulation density. 2 out of 3 trials resulted in successful colony formation and resulted in spontaneously contracting tissue when cells were encapsulated at a density of 15 million cells/mL of Batch-2 PF with 2% additional PEGDA. Those three encapsulations at the density of 15 million cells/mL were carried out before the study that examined the effect of encapsulation density was conducted. One likely explanation for this is that the study which examined the effect of encapsulation density on colony formation was performed in parallel in one sitting. To elaborate, triplicate encapsulations of cells at the densities of 5, 15, and 30 million cells/mL Seliktar's PF were all conducted in parallel for a total of 9 encapsulations and wash steps in one sitting. This totaled roughly 3.5 hours, beginning with the trypsinization of all the cells used and ending in the resuspension of the final dish of microsphere-encapsulated cells in differentiation media. This long processing time likely resulted in significant cell death due to the extended times that some conditions spent without culture media. However, the three different concentration conditions in this particular study were encapsulated and processed in parallel, meaning that the conditions were encapsulated in three sequential series of the three conditions in the order of 5, 15, 30 (cells/mL),

so that any negative effect of long processing time should only have affected one trial from each condition. This is because typical encapsulation procedures totaling 3 encapsulation trials lasted about 2.5 hours in one sitting.

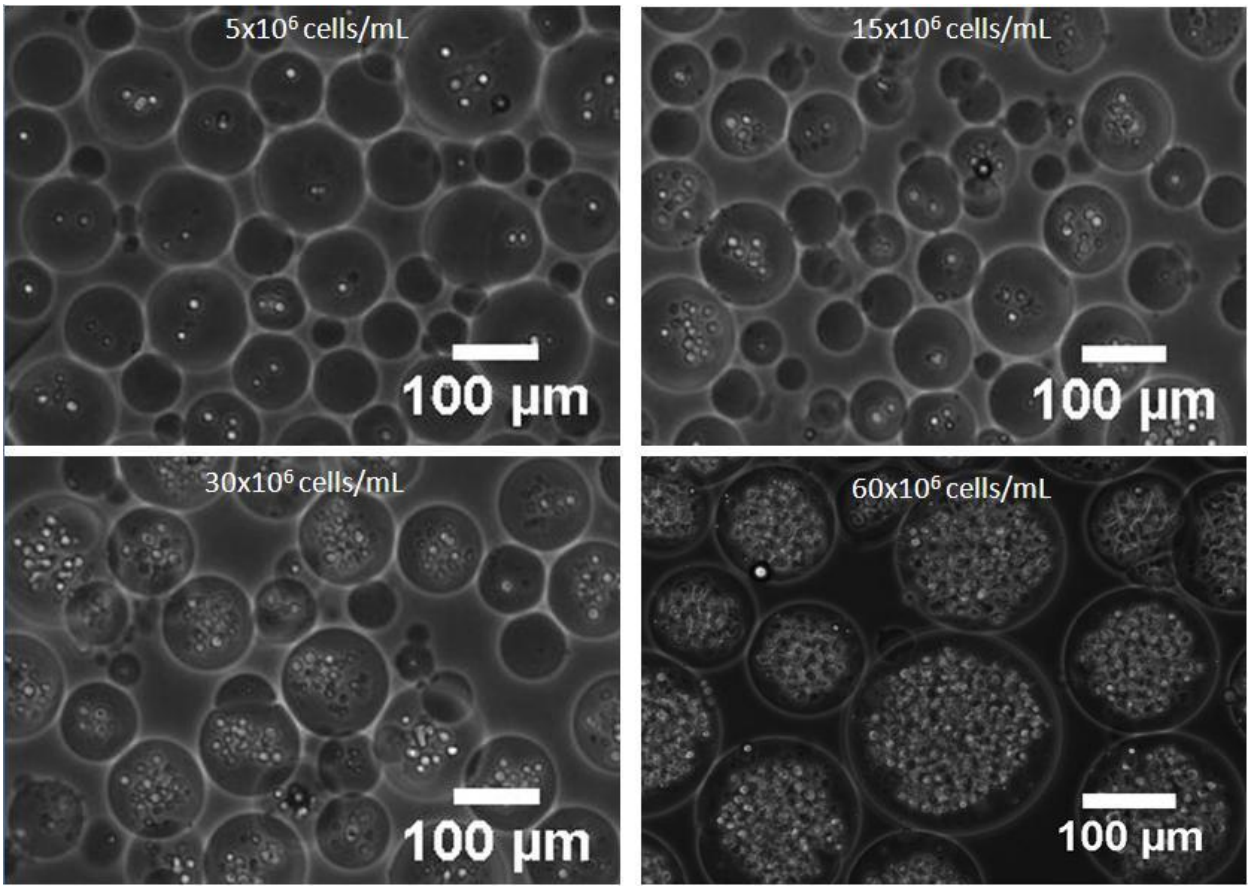

Figure 27: Encapsulated density was reflected in number of cells per microsphere. Phase contrast images of mESCs immediately after microsphere encapsulation using Seliktar's PF. The graded effect of cell encapsulation density upon the cell density per microsphere is visually evident.

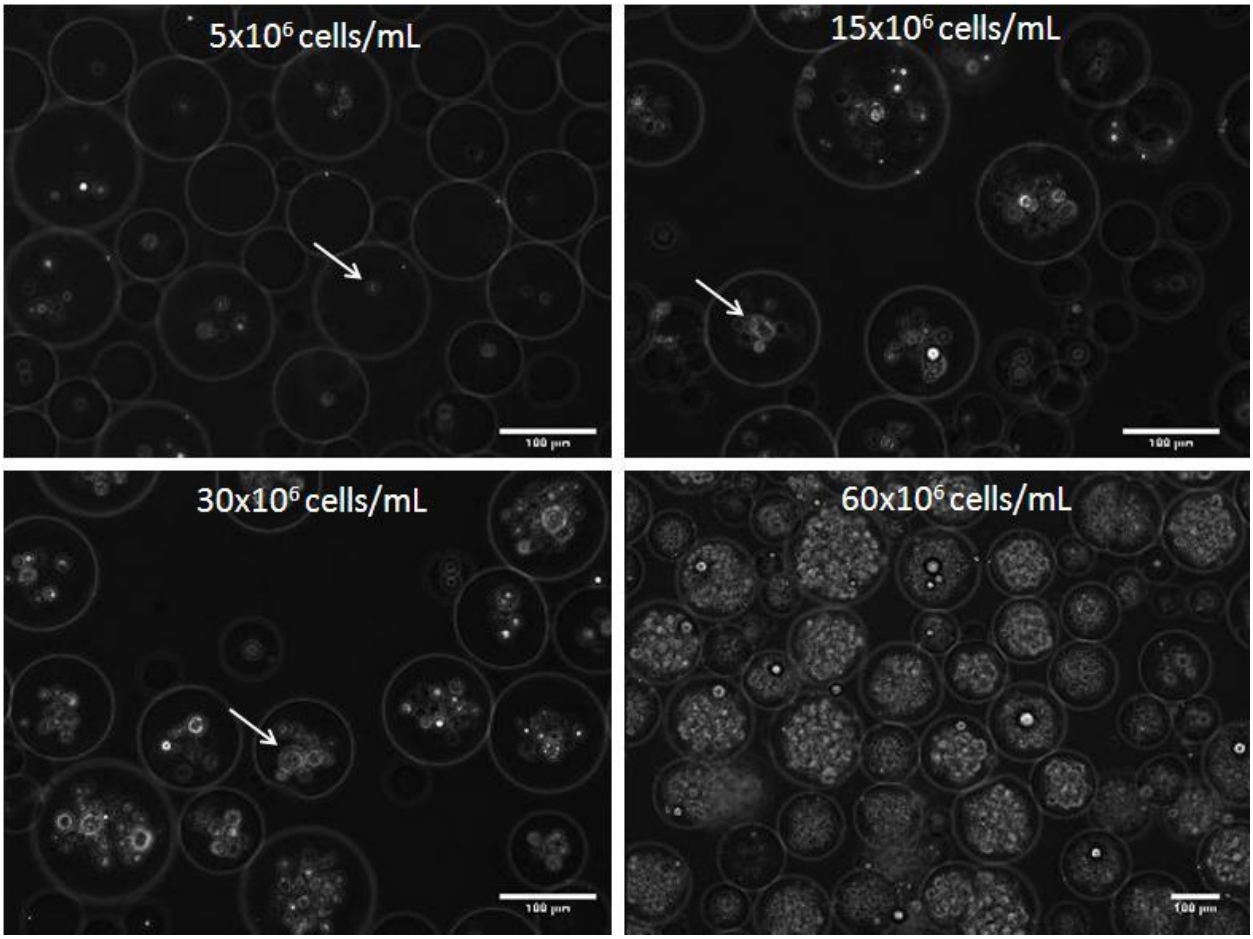

Figure 28: Day 2 Colony formation in microspheres. Representative images of colony formation on Day 2 of differentiation. These images represent the more robust cases of colony formation at each condition. It can be seen that at or below an encapsulation density of 30 million cells/mL, mESC proliferation is limited, whereas colony formation is robust at the highest density. Arrows indicate proliferating encapsulated cells. It can also be noted that many non-proliferating cells are present within many microspheres, which is particularly clear in the lower encapsulation densities.

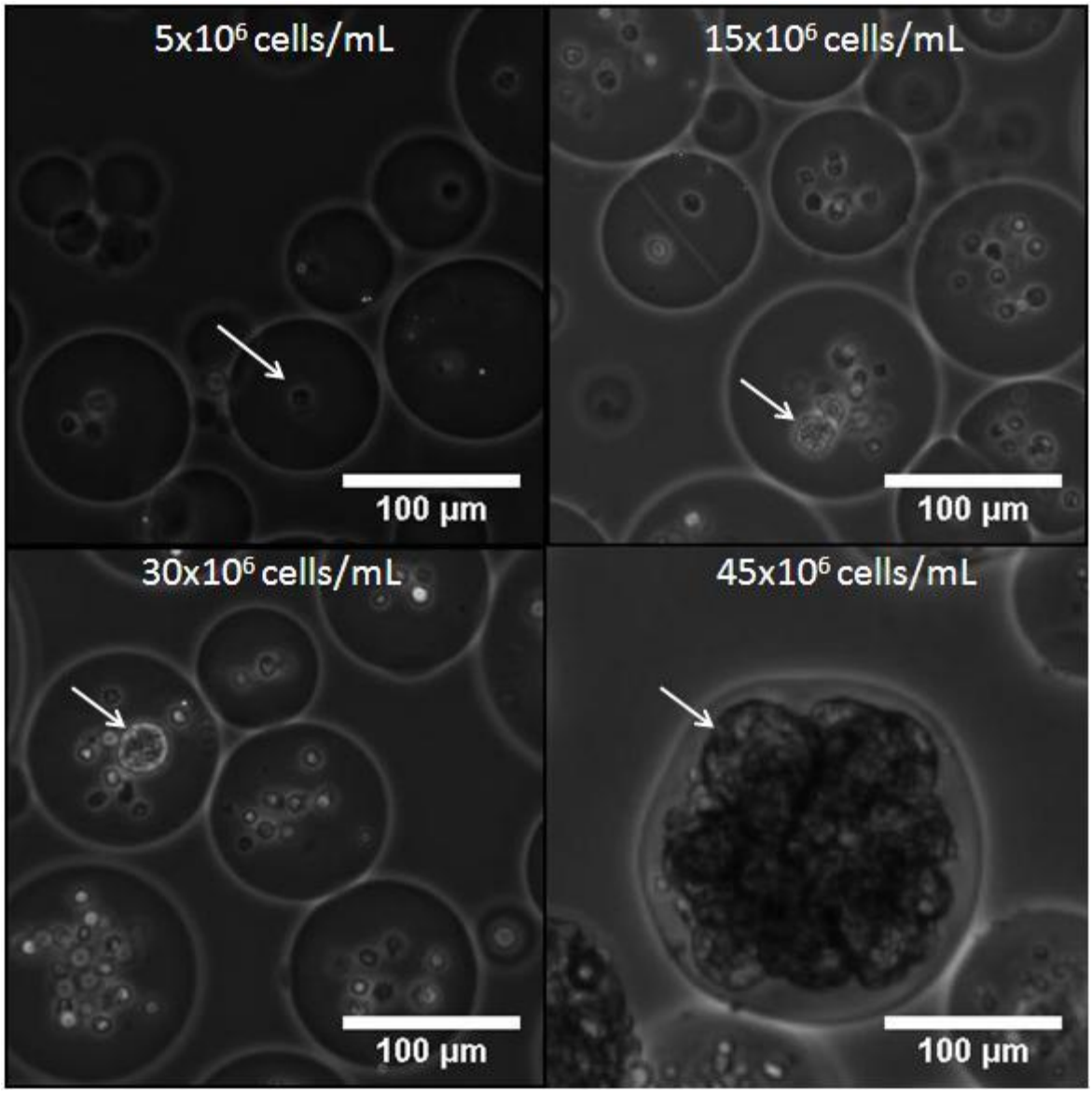

Figure 29: Day 5 Colony formation in microspheres. Images of colony formation on Day 5 of differentiation. These images represent the more robust cases of colony formation at each condition. Arrows indicate representative proliferating colonies; note that colonies did not proliferate in the low-encapsulation condition (5 million cells/mL). By Day 5 of differentiation, cell proliferation had not changed significantly from Day 2 except in the higher encapsulation condition of 45 million cells/mL.

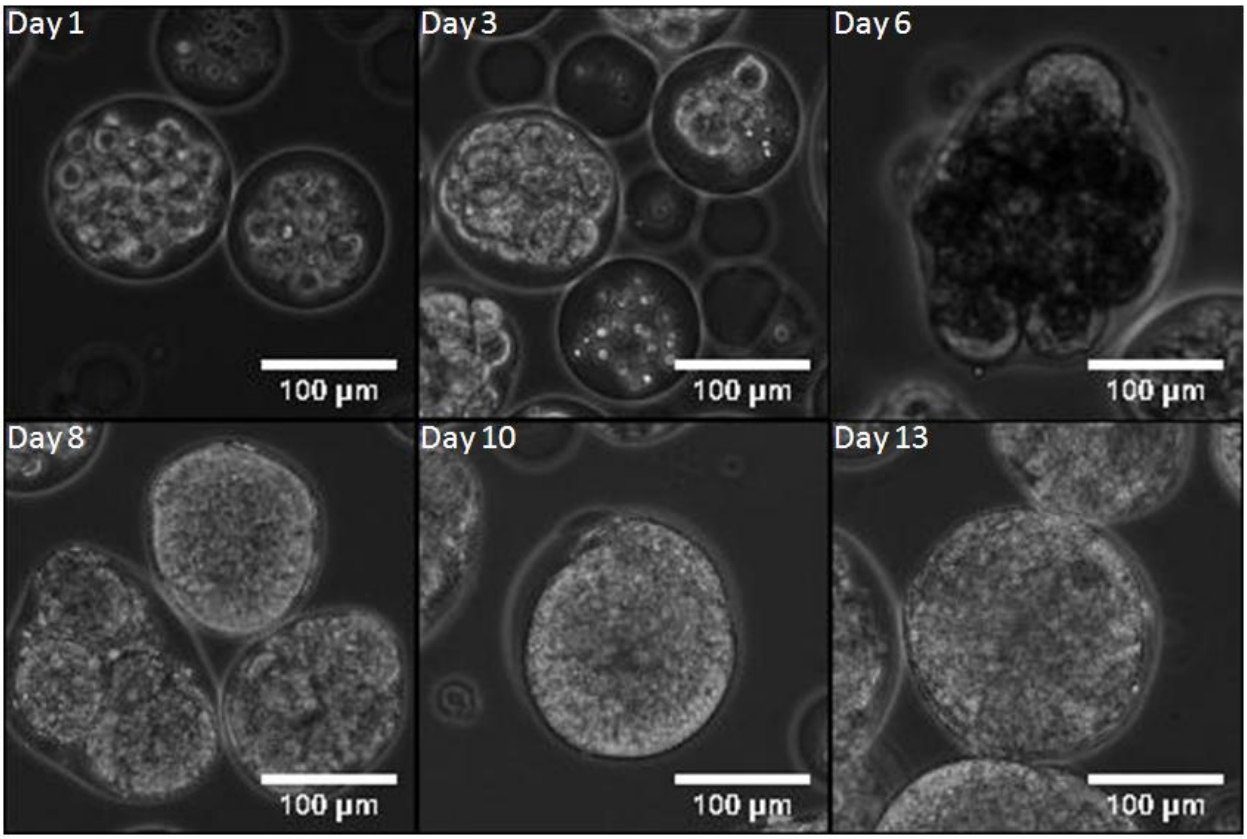

Figure 30: Development of EBs in microspheres over time. Phase-contrast images of encapsulated cells differentiating over time. Many spheres yielded multiple differentiating colonies. Proliferating colonies remodel the microspheres with time; it can be seen that some spheres do not appear spherical as they are deformed. Smooth-edged colonies that resemble EBs are evident by Day 8, and these EBs continued to grow in size. These images are from PF microspheres with 2% (w/v) additional PEGDA with a cell encapsulation density of 60 million/mL. The EBs did not completely degrade the microsphere hydrogel, which is particularly clear on Day 13, due to the presence of the unconjugated PEGDA in the biomaterial.

mESCs encapsulated in both batches of PF used for microsphere encapsulation proliferated in microsphere hydrogels and formed EB-like cell aggregates within the microspheres while degrading and remodeling the hydrogels. Figure 30 illustrates the formation of colonies that began to resemble EBs over roughly two weeks of differentiation. As cells were both proliferating and differentiating, they deformed and stretched their hydrogel matrix. The

effect of this remodeling was quantified by measuring the maximum diameter of encapsulated colonies. Note that Figure 30 illustrates remodeling of microspheres composed of Batch-2 PF with additional PEGDA. Encapsulated colonies in microspheres composed of Seliktar's PF would not typically remain in solution past Day 10 of differentiation. Regardless of the batch of PF used for encapsulation, the cells would remodel the microsphere material. A representative upward shift in sphere size and distribution is illustrated in Figure 31.

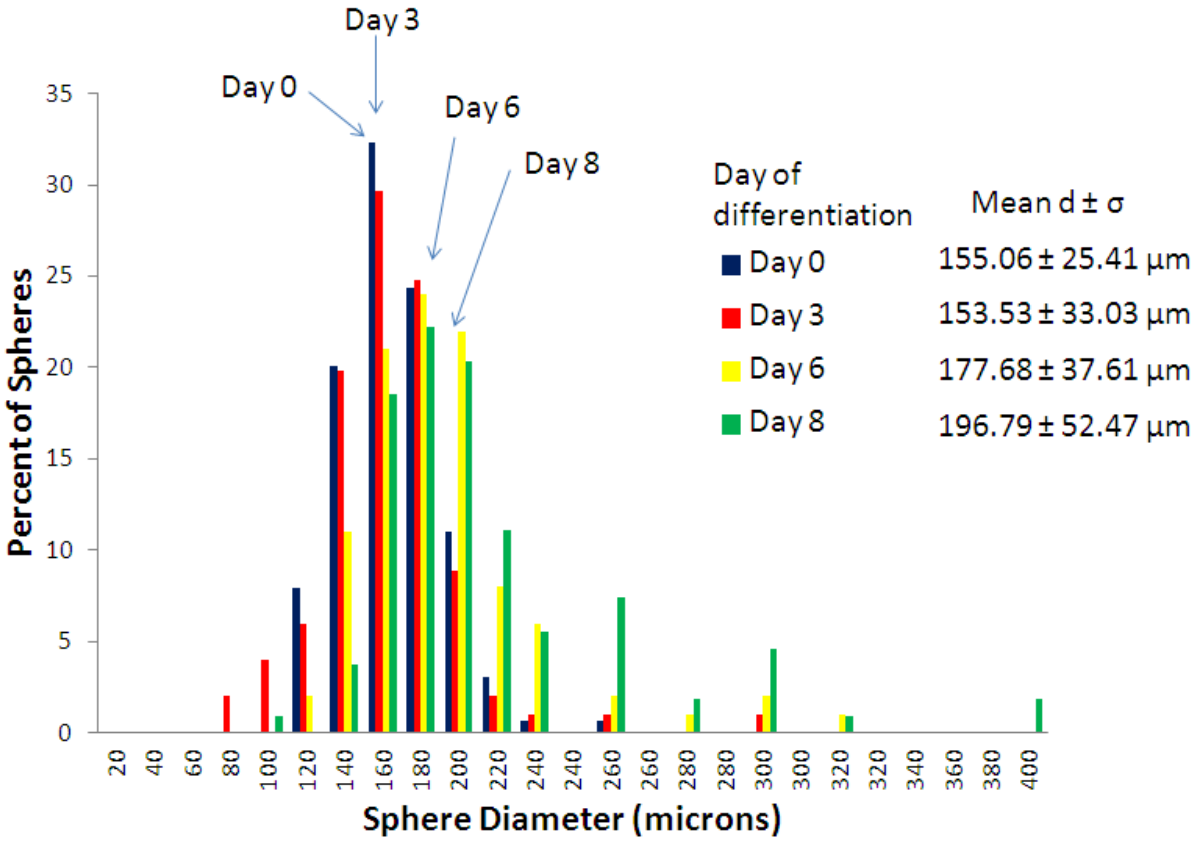

Figure 31: EBs remodeled microspheres and increased microsphere size. Sphere size distribution as a function of differentiation day. By Day 6 of differentiation, an upwards shift in the mean diameter of microspheres increased. Additionally, the appearance of very large spheres above 300 microns in diameter was seen by Day 3, and the number of large spheres increased as colonies grew. This data is from Seliktar's PF spheres (without additional PEGDA), at a cell encapsulation density of 60 million/mL.

3.9 *Enzymatic degradation of hydrogel and batch-to-batch variation*

mESCs encapsulated within Seliktar's PF demonstrated the material's degradability by remodeling the polymer matrix to the point that encapsulated EBs would escape from the microsphere and attach to their culture dish. Proliferating encapsulated EBs typically degraded hydrogels to the point of reaching the outer layer of the microspheres by Day 10 of differentiation and enzymatic degradation of the PF material allowed for cellular extensions to attach to the tissue culture-treated dish. EB-microspheres using Seliktar's material began to attach to the culture dish by Day 10 of differentiation and would continue to do so for the next 6 days of differentiation (up to Day 16). By Day 16, it was found that nearly all encapsulated proliferating EBs had attached to the dish. Attached colonies were counted and spontaneously contracting attached colonies were circled on the bottom of the dish. Representative images of attached EB-microspheres are shown in Figures 32 and 33.

Conversely, encapsulated mESCs using Batch-2 PF did not escape from their microspheres nor did they attach to their culture dishes. This may be attributed to the addition of unconjugated PEGDA (2% w/v) to the polymer precursor solution, which made the biomaterial resistant to enzymatic degradation. The encapsulated colonies in Batch-2 PF spheres stretched the biomaterial (see Figure 30) rather than degrading it. Furthermore, Batch-2 PF spheres with additional PEGDA did not degrade when suspended in trypsin solution overnight while spheres made of Seliktar's PF degraded in trypsin solution within 5 minutes. Batch-2 PF's resistance to enzymatic degradation was the most notable difference between the two batches of PF used for encapsulation.

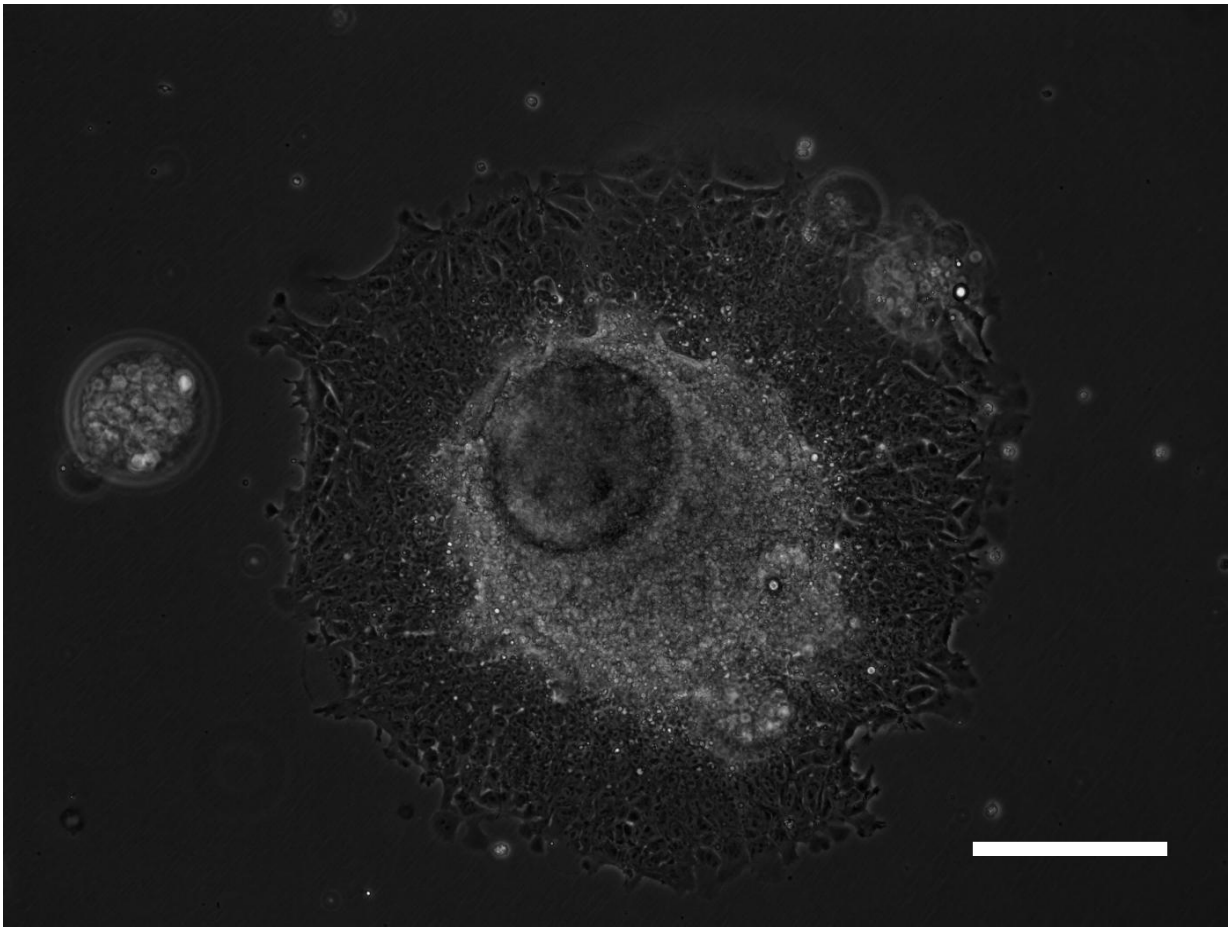

Figure 32: Encapsulated EBs attached to culture dish. An attached EB on Day 14 of differentiation. Cells encapsulated in Seliktar's PF enzymatically degraded microspheres within 2 weeks of differentiation and attached to the culture dish. This representative image was taken from cells encapsulated at 60 million cells/mL Seliktar's PF. The formation of different tissue types was observed in attached EBs, where fibroblasts and endothelial cells formed on the outer edges of the attached colony, while the inner colony mass exhibited a dense tissue structure. Scale bar = 200μm.

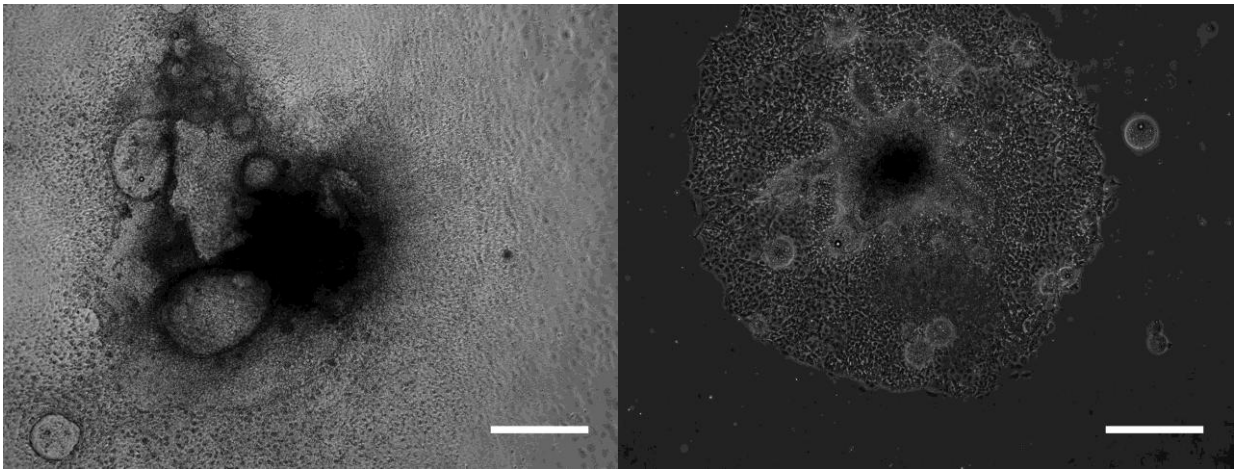

Figure 33: Large attached EBs formed. Large attached EBs which degraded their microsphere boundary and attached to the dish are shown in large scale. The original encapsulation condition used 60 million cells/mL Seliktar's PF. Left) An attached EB with other microspheres embedded within the attached colony. Cystic structures are present in this attached colony. This image was taken on Day 14 of differentiation. Right) An attached EB with on Day 16 of differentiation. Scale bars = 500μm.

3.10 *EB formation success rate*

mESC that were encapsulated in PF microspheres successfully formed EBs at a very low rate. Each time an encapsulation was performed, three emulsions (referred to as trials) were made using the conditions to be tested. Typically, mESCs suspended within the microsphere hydrogel matrix would exhibit positive signs of proliferation through the first several days of differentiation. After 3 days of differentiation, however, growth of colonies would halt and would not continue with further cell culture. When colony growth was robust and would persist past Day 3, the differentiation trial would be deemed to be successful and observation of the trial would continue until colony proliferation halted or until EB-microspheres ceased to spontaneously contract. Encapsulation trials using the optimized emulsion process are summarized in Table 3.

Material, Cell density [millions/mL PF]	# of trials	Number of trials yielding EBs past day 3	Number of trials yielding spontaneously contracting EBs	EB type with contract	Contract initiation day
PFS, 5	3	0	0	-	-
PFS, 15	3	0	0	-	-
PFS, 30	3	0	0	-	-
PFS, 45	9	1 *	1	Attached	11
PFS, 60	39	2 **	2	Mostly attached, some encapsulat-ed	14
PFS + 2% PEGDA, 60	6	0***	0	-	-
PF2 + 2% PEGDA, 5	3	0	0	-	-
PF2 + 2% PEGDA, 15	3	2	2	Encapsulat-ed	12
PF2 + 2% PEGDA, 45	3	2	2	Encapsulat-ed	11
PF2 + 2% PEGDA, 60	3	2	1	Encapsulat-ed	11

Table 3: Summary of optimized encapsulation trials. All encapsulation trials using the optimized emulsion method for cell encapsulation and differentiation are summarized. "PFS" refers to Seliktar's PF, while PF2 refers to Batch-2 PF. Rigorous repetition was carried out using PFS at an encapsulation density of 60 million cells/mL PF. Note that successful EB development within microspheres experienced relatively high success rate during early attempts, but the majority of later attempts were unsuccessful. *Last 6 consecutive trials yielded poor growth. **Last 36 consecutive trials yielded poor growth. ***All trials performed after likely contamination event.

Although success rates were low in the conditions that were repeated more than three times, it should be noted that almost all of those encapsulation trials performed (except for the first three trials performed using 45 and 60 million cells/mL PFS) were done so with cells that

had likely developed a loss of pluripotency and with encapsulated cells that were differentiated in an incubator that was likely malfunctioning and contaminated. However, further experiments not reported within this thesis showed that success rates were over 50% when using pluripotent cells and a properly functioning incubator.

3.11 *Response to epinephrine*

In order to assess for the presence of cardiac tissue that was not driven to spontaneously contract due to the lack of pacemaker cells within encapsulated EBs, attached-EBs or EB-microspheres were exposed to epinephrine, also known as adrenaline, to promote contraction. Three separate dishes originating from 2 encapsulation trials using 60 million cells/mL in Seliktar's PF were used for the attached study. An average of 43.3 attached colonies were counted in each dish. The epinephrine was administered to these dishes on Day 16 of differentiation, two days following the first observation of spontaneous contraction of the attached colonies. EBs which had attached to the culture dish showed a marked increase in contraction activity when exposed to media supplemented with epinephrine, as shown in Figure 34. The contracting EB's sustained their increased contraction 24 hours post treatment, although the percentage of contracting EBs decreased when compared to the percentage of contracting EBs 2 hours following the dosage. Such a result may indicate the presence of cardiomyocytes in the attached EBs while also showing a deficiency in pacemaking nodal cells which drive spontaneous contraction.

Similarly, a separate epinephrine dosing experiment was carried out on fully encapsulated (rather than attached) EB-microspheres formed using an encapsulation density of 15 million cells/mL of Batch-2 PF with a supplement of 2% (w/v) PEGDA. Epinephrine stock solution was administered to the media of three separate trials containing EB-microspheres on Day 28 of

differentiation. Note that spontaneously contracting EB-microspheres were first observed in these dishes on day 12 of differentiation. One of the three trials did not contain spontaneously contracting EBs prior to or after administering the drug, and thus the data was not included in Figure 35. To quantify the number of contracting EBs, the culture dishes containing the trials were swirled to cause all EBs to aggregate at the center of the dish. The effects of the epinephrine on the percentage of contracting EBs and contraction frequency are shown in Figure 35. Epinephrine increased the spontaneous contractile activity of encapsulated EBs.

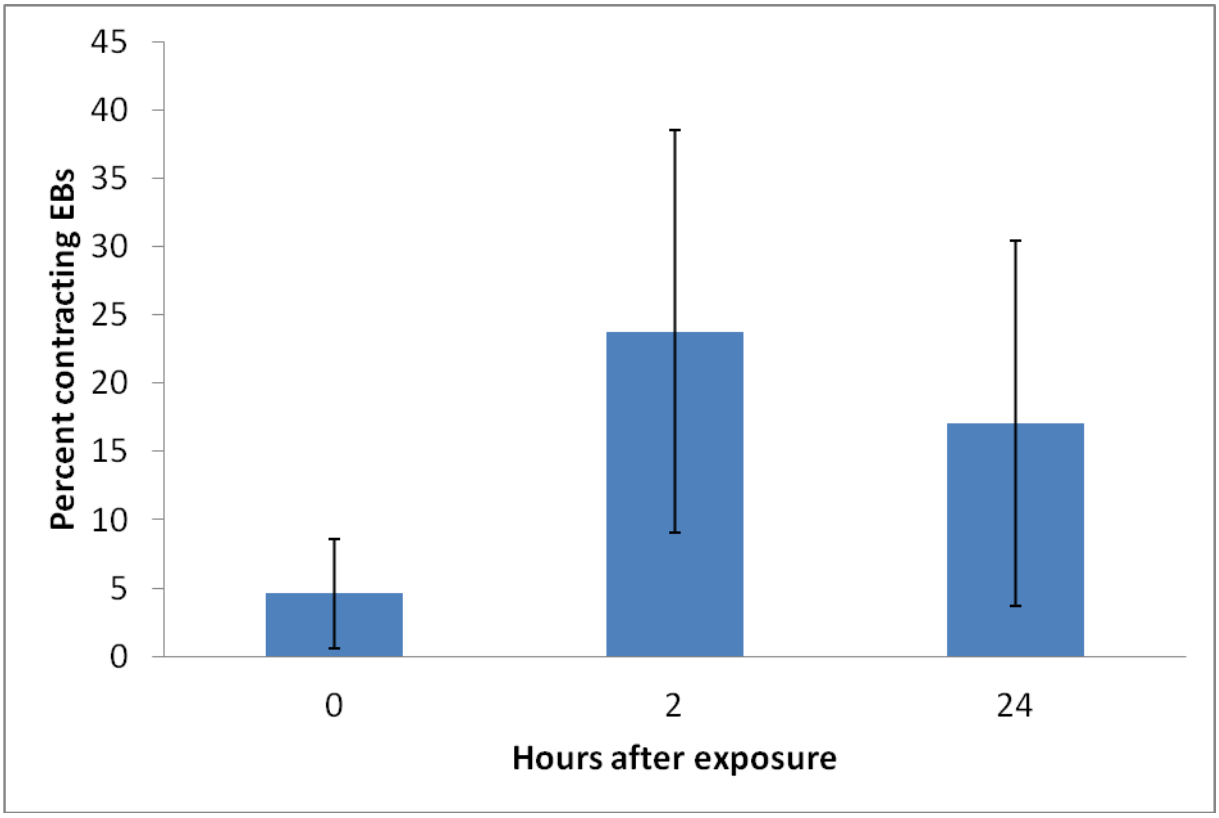

Figure 34: Attached EBs responded to epinephrine. The percentage of contracting attached EB-microspheres increased upon exposure to epinephrine, and the effect was sustained 24 hours post exposure. Error bars reflect standard deviation of percent of contracting EBs in each of 3 dishes. There were 80, 40, and 10 dishes in each respective dish. Note that attached EBs were derived from mESCs encapsulated at a density of 60 million cells/mL of Seliktar's PF, and the epinephrine dosage was administered on Day 16 of differentiation.

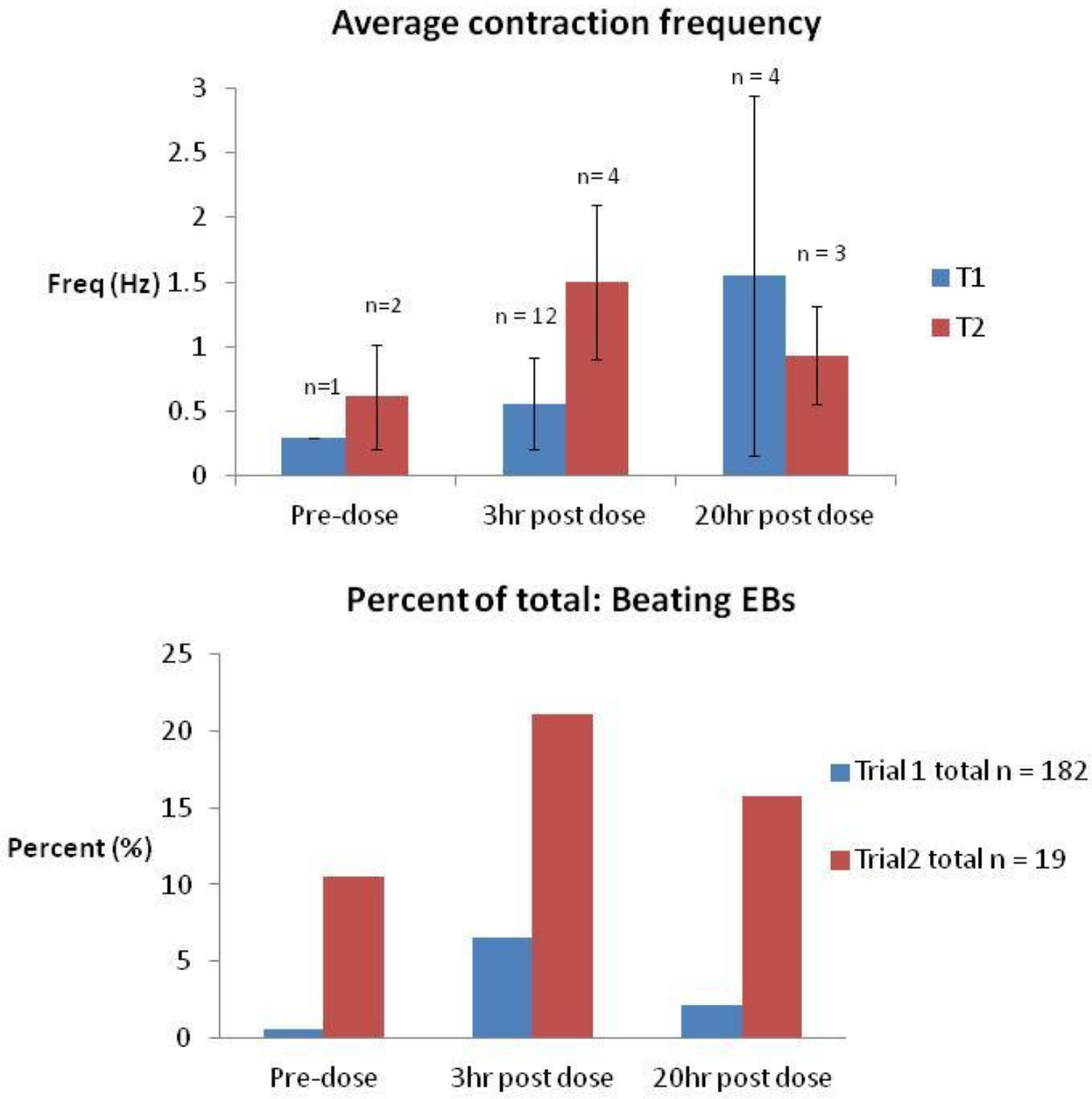

Figure 35: Encapsulated EBs in suspension responded to epinephrine. EB-microspheres with an initial encapsulation density of 15 million cells/mL Batch-2 PF with supplemented 2% PEGDA (w/v) were administered with epinephrine on Day 28 of differentiation. Data was taken from two separate trials containing spontaneously contracting EB-microspheres. Note that encapsulated EBs were still in suspension and were derived from mESCs encapsulated in Batch-2 PF.

3.12 *Gene expression*

To confirm that encapsulated cells were differentiating, expression of pluripotency marker Oct3/4 and early mesoderm marker Nkx2.5 were measured using GAPDH as a control. Measurements were taken using a qPCR instrument (BioRad). All measurements were run in triplicate from two samples: Day 0 un-differentiated mESCs and Day 3 PF microsphere encapsulated mESCs. The $\Delta\Delta C_t$ method was used to assess for fold-increase of gene expression. Results showed that Oct3/4 was downregulated by a factor of 232 from Day 0 to Day 3, and Nkx2.5 showed a 79 fold increase. GAPDH, a housekeeping gene, was used as the control gene used to normalize between both samples.

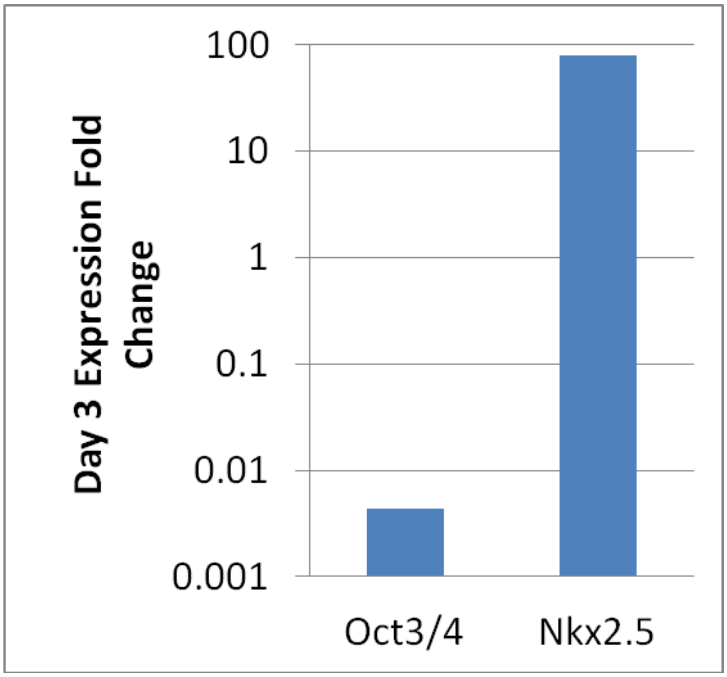

Figure 36: Gene expression of encapsulated cells indicated differentiation. Gene expression from one triplicate run comparing expression of Oct3/4 and Nkx2.5 from day 3 encapsulated cells. Expression fold change is in comparison to day 0 undifferentiated mESCs. Control gene was GAPDH. Error bars and statistical analysis are absent due to the sampling from one sample from each of two time points.

3.13 *Immunohistochemistry*

Undifferentiated mESCs affixed to gelatin-coated microscope slides were stained for the pluripotency marker Oct4 and nuclear stain DAPI. Figure 37 shows that the mESCs were all Oct4 positive, indicating that they were pluripotent.

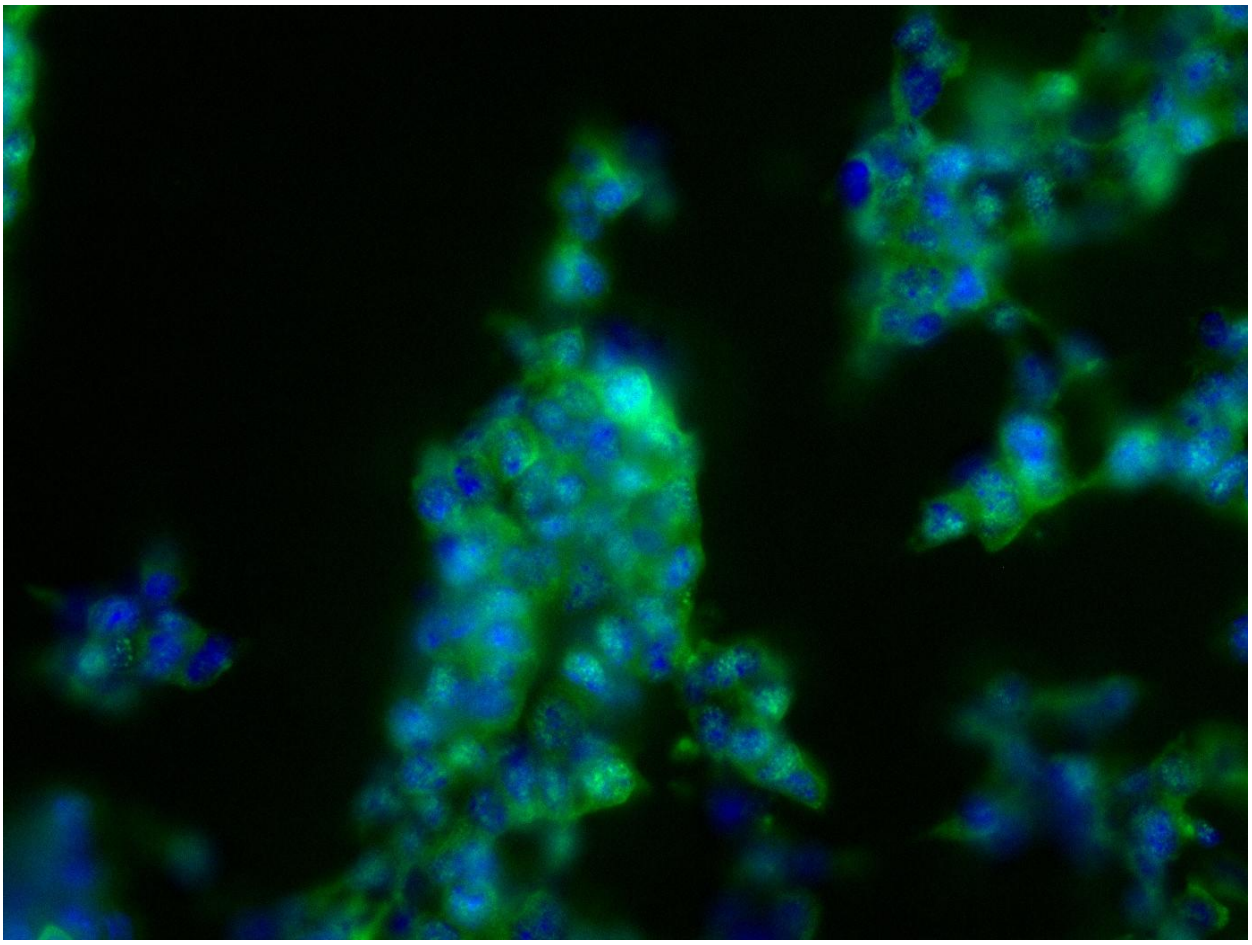

Figure 37: Immunhistochemistry verified mESC pluripotency. A fluorescent image of mESCs stained with pluripotency marker Oct4 (green) and nuclear stain DAPI (blue) indicated that the cells were pluripotent due to the global localization of nuclei and Oct4 stain. mESCs were cultured in media supplemented with LIF immediately prior to immunohistochemical processing.

IV. Discussion and Conclusions

Hydrogel microsphere encapsulation of stem cells allowed for their proliferation and for the formation of embryoid bodies, which lead to their differentiation into different tissue types. To the best of my knowledge, this thesis reports the first use of a PEG-based hydrogel for the encapsulation of stem cells as a vehicle for long-term *in vitro* differentiation. The emulsion based method for processing microspheres is highly scalable in that it produces thousands of cell-laden microspheres in less than one minute. Compared to other methods of microsphere formation, the emulsion method's greatest advantage is its scalability and low cost. However by using this method, viability of microsphere encapsulated cells was poor. The losses accrued by the viability caveat may be made up for, nevertheless, simply due to the scalability of the method. Microspheres with low cell viability will not yield growing EBs and thus can be separated from microspheres containing successfully growing colonies by size exclusion.

Currently, many researchers of cell encapsulation use sophisticated extrusion encapsulation systems, typically with an encapsulator or a microfluidic chip. For example, microspheres with extremely homogeneous size distribution have been created using bead generators with either electrostatic[39,61] or laminar jet break-up through vibration[62], which in turn yielded cell aggregates of consistent sizes depending on cell encapsulation density[61]. Microfluidic chips have also been designed to generate microspheres and have yielded spheres with consistent diameters with under 10% coefficient of variation (CV) for small spheres (between 73 and 148μm) and a CV of under 5% for larger spheres (D > 200 μm)[63,64]. The production rate of microspheres using these systems varied from 14-20mL/min[62], correlating to 36,000 to 50,000 beads produced per minute. Such methods also yielded high cell viability[61, 62], which is comparable to the high viability seen in an emulsion-based system[59]. Although the

emulsion processing method for producing PF microspheres is very similar to the method used by Franco *et al.*[59], the PF microspheres resulted in lower cell viability. Seliktar *et al.* reported high viability of cardiomyocytes within their PF constructs[65], demonstrating the material's biocompatibility. Although viability was directly not quantified, preliminary experiments with PF constructs resulted in a high percentage of colony formation (refer to Figures 14 and 15), so the lower viability seen in the PF microspheres may then be attributed to the combination of the processing method and the material. The exposure to oil, acetophenone, and vortexing and subsequent washing and centrifugation steps may have all contributed to the lower viability of microsphere-encapsulated mESCs. However the PF construct studies were valuable to show that the emulsion processing method was the primary cause for the lower viability. Additionally, the encapsulation of mESCs in the PF constructs first verified that the material would support the proliferation and differentiation of the cells.

The size distributions of microspheres were analyzed for different cell-encapsulation densities, and it was found that increasing cell density did not increase mean microsphere diameter until the density was increased to 60 million cells/mL precursor solution. Because this was the highest encapsulation density explored, it would be possible that the microsphere size would continue to increase by further increasing encapsulation density above 60 million cells/mL. It is possible that at some cell concentration between 45 and 60 million cells/mL, the cells reach a "saturation" concentration within the PF biomaterial, meaning that the cells cannot be packed any more densely. The result could be a continual expansion in the particle size of microspheres generated using encapsulation densities above 60 million cells/mL of precursor. Because microspheres produced in this study resulted in mean diameters typically no larger 100 microns, the use of extremely high cell encapsulation densities could result in much larger

microspheres. This is desirable since it has been shown by Zandstra *et al.*[53] that ESC aggregates with an initial size of 200 μm differentiated preferentially into endoderm, while larger aggregates of 1200 μm resulted in tissues with higher mesoderm fraction. Since cardiac tissue arises from mesoderm, a future goal using the PF microsphere system would be to test cell encapsulated microspheres that are much larger than those produced in this study. Although the PF microsphere system described here is substantially different from the aggregate-size control study by Zandstra *et al*., it is hypothesized that larger microspheres used for pluripotent cell encapsulation could result in higher yields of cardiomyocytes based on the work of Zandstra *et al.*

Future production of PF microspheres could be optimized by developing a non-emulsion based method for sphere generation, such as by using an encapsulator described by Cellesi *et al.*[63] or by employing a microfluidic device. Viability could be increased by averting cell exposure to oil, vortexing, and repeated centrifugation, which are all necessary using the described emulsion-based method. The size distribution using the emulsion based system was subject to variation since standard deviations of diameter were consistently about one-third the mean diameter value. This large variation in diameter is similar to the size distribution reported by Franco *et al.*[59]. The encapsulation and differentiation of mESCs within the microspheres proved to have advantages over conventional EB differentiation protocols. Particularly, EBs cultured without a hydrogel carrier material typically will aggregate with neighboring EBs due to inter-EB cellular adhesions. The resultant aggregated EBs introduce greater heterogeneity into differentiation systems. Encapsulation of the colonies using the developed PF microsphere system averted this possibility of EB aggregation in solution, allowing for better control over differentiation. EBs formed within Seliktar's PF would remodel their microsphere matrices and

"escape" them around day 10 of differentiation, leading to attachment to the culture vessel. Such a result could be better controlled by a variety or combination of methods. Coating the culture vessel with poly-heme, a material coating for culture systems which resists cell adhesion, would be one possible solution. Translation of the culture system from a static system to a stirred bioreactor could also mitigate the propensity of encapsulated colonies to attach to the culture vessel. Additionally, it was found that the incorporation of un-conjugated PEGDA to the PF precursor polymer resulted in microspheres which resisted enzymatic degradation and attachment to the culture vessel. A novel method could be developed to provide delicate control over the degradation rate of the microsphere so that the enzymatic release of colonies from the microsphere carriers could be controlled temporally. PEG is an excellent material for designing such an engineered scaffold due to its high modification potential.

EB formation was observed within PF microspheres, but the microspheres were not particularly efficient in generating EBs of uniform size. Heterogeneity was also still an issue in this system, since the stem cells were suspended as single cells within a matrix, which prohibited their aggregation. Furthermore, dead cells could not be removed from the matrix and may have impeded the outward growth of viable colonies. Because the cells were singly suspended, most EBs were descended from a single cell, which was evident in many of the images showing multiple EBs competing for space within a single microsphere. Multiple EBs were reported in similar experiments where stem cells were encapsulated within an alginate matrix[39], but a study using collagen microspheres saw the formation of single colonies of human mesenchymal stem cells (hMSC)[66]. A notable result from the study conducted by Chan *et al.* was that the hMSC-laden collagen microspheres shrank after being placed in culture media[66], which may have enhanced the ability of the hMSCs to aggregate and form a single colony. The single colony

formation may also be attributed to the type of cell used (MSC rather an ESC). Despite issues with heterogeneity, the PF microsphere system is the first microsphere encapsulation system to yield spontaneously contracting cardiac material. To further coax uniform ESC aggregation within a microsphere, it could be ideal to use a microsphere with a polymer outer shell and a liquid core, similar to the beads generated using a double nozzle extrusion device[62]. However, the use of a liquid core does not allow for much cell-matrix interaction, as the cells encapsulated within a liquid-core bead are essentially cultured in an isolated suspension. The ability to apply mechanical stimulus from the scaffold to the cells is also lost by using a liquid-core system.

The incorporation of fibrinogen into the microsphere material has demonstrated the versatility of PEG-based hydrogels in that the "blank slate" nature of PEG allows for bio-functionalization of the hydrogel via conjugation of a biological ECM component, fibrinogen. Differentiation of mESCs was possible using PF as the microsphere material because the encapsulated cells had a substrate to which they could tether. Furthermore, the presence of enzymatic degradation sites within fibrinogen allowed cells to remodel and degrade the hydrogel matrix to allow for the growth of new tissue. Further experiments may explore the incorporation of other bio-functional motifs within the microsphere material, and combinations of such co-polymers may further diversify the types of signals presented to encapsulated cells. Tissue neo-vascularization is one crucial requirement for engineered heart tissues[8], so the incorporation of factors such as VEGF could lead to the development of healthy engineered heart tissue with improved vascularization. Furthermore, as a differentiation vehicle for cardiogenesis, cardiac inducing factors such as BMPs and TGF-β could be tethered to or entrapped within the hydrogel matrix to increase cardiomyocyte yield. These factors (specifically including TGF-β, BMP-2,

BMP-4 and Activin-A) affect the TGF-β superfamily and have been demonstrated to improve cardiac yield or cardiac expression from human ESCs[7].

Initial analysis of gene expression in day 3 microsphere-encapsulated EBs showed that the encapsulated stem cells were differentiating due to the downregulation of Oct3/4 and the upregulation of Nkx2.5. However, further characterization must be performed in order to more clearly understand gene expression of encapsulated stem cells. A major challenge in assessing gene expression of encapsulated cells in this system at early differentiation time points is deriving sufficient quantities of RNA due to the low quantity of viable encapsulated cells. Further work is then also necessary to develop techniques to acquire sufficient quantities of RNA from encapsulated cells to produce sufficient data to statistically analyze.

In addition to the results presented by preliminary gene expression data, immunohistochemistry of encapsulated cells at different differentiation time points is necessary to understand the temporal development and localization of differentiating tissues within the PF microspheres. Confocal microscopy would be a useful tool to aid in three-dimensional mapping of the architecture of different tissue types at early time points in differentiation. As the three-dimensional structure of the encapsulated EBs increases in size, 2-D cross sections of colonies could be taken by embedding the colonies in paraffin and sectioning them to understand the layer-by-layer organization of tissues within the encapsulated tissue. At later times of differentiation, such information would be useful to analyze any heterogeneous differentiation occurring within the microsphere.

PEG-fibrinogen microspheres have untapped potential as differentiation vehicles for encapsulated stem cells. This bio-active hydrogel biomaterial has been shown to support the proliferation and differentiation of mESCs into functional cardiac tissue. The tunable nature of

PEGDA was demonstrated to have an effect on the enzymatic degradability of the hydrogel dependent on the presence of conjugated or un-conjugated PEGDA to fibrinogen. Because of the difference in susceptibility to enzymatic degradation between Seliktar's PF and Batch-2 PF, differentiated encapsulated EBs resulted in either attached or unattached cardiac tissue. Thus, the tissues derived from this scalable differentiation system could be clinically applied in two separate methods. If the differentiated tissue was engineered to attach to the culture vessel, cardiac cell sheets could be derived, and these sheets could be grafted into infarcted myocardium, or be used as a drug testing platform. The great advantage to using microspheres for encapsulation is that the microspheres could be injected into the heart. Injection is advantageous because it is less invasive than opening the chest cavity to implant tissue such as cell sheets. Cell-laden microspheres could be injected using a needle with the appropriate gauge size to allow for their unhindered passage through the needle. Furthermore, the microsphere biomaterial could be designed to specifically attach to the infarcted myocardium or other target tissue type, further increasing the integration efficacy of the cell therapy.

The necessity of a stiff matrix or substrate to derive cardiomyocytes from encapsulated mESCs within the biomaterial was shown by initial encapsulation trials with PF constructs. Additional work is needed to better characterize the effects of mechanical stimuli on cell proliferation and differentiation. Low cell viability is a serious drawback using the aforementioned method, and it may be necessary to develop a gentler processing method for encapsulation that does not sacrifice scalability. Furthermore, future work related to this study aims to characterize gene expression via quantitative PCR and immunohistochemistry, which necessitates the development of efficient protocols for collecting such data. However, the results from this study are novel and exciting because they describe the first system of pluripotent cell

encapsulation with a PEG-based biomaterial which also allowed for the proliferation and differentiation of the stem cells to form spontaneously contracting tissue. Overall, this study exhibits the potential of PF-microspheres as a highly scalable system for the derivation of cardiac tissue from a pluripotent cell source. The emulsion processing method is quick, relatively cheap, and highly scalable, making it a promising method for deriving large batches of tissues for research and clinical purposes.

V. Reference list

[1] Nardo PD, Forte G, Ahluwalia A, Minieri M. *Cardiac Progenitor Cells: Potency and Control.* 2010. J. Cell. Physiol. 224: 590–600.

[2] Chen QZ, Harding SE, Ali NN, Lyon AR, Boccaccin AR. *Biomaterials in cardiac tissue engineering: Ten Years of research survey*. 2008. Materials Science and Engineering R 59:1–37.

[3]Wang F, Guan J. *Cellular cardiomyoplasty and cardiac tissue engineering for myocardial therapy.* 2010. Advanced Drug Delivery Reviews 62: 784–797.

[4] http://www.cdc.gov/nchs/fastats/heart.htm. January 5, 2012

[5] Taylor DO, Edwards LB, Boucek MM, Trulock EP, Aurora P, Christie J, Dobbels F, Rahmel AO, Keck BM, Hertz MI. *Registry of the International Society for Heart and Lung Transplantation: twenty-fourth official adult heart transplant report--2007.* 2007. J Heart Lung Transplant. 26(8):769.

[6]J Wei, KK Cheng, DY Tung, CY Chang, WM Wan, YC Chuang. *Successful Use of Phoenix-7 Total Artificial Heart.* 1998. Transplantation Proceedings 30:3403-4

[7] Kehat I, Kenyagin-Karsenti D, Snir M, Segev H, Amit M, Gepstein A, Livne E, Binah O, Itskovitz-Eldor J, Gepstein L. *Human embryonic stem cells can differentiate into myocytes with structural and functional properties of cardiomyocytes.* 2001. J Clin Invest. 108(3):407–414.

[8] Kocher AA, Schuster MD, Szabolcs MJ, Takuma S, Burkhoff D, Wang J, Homma S, Edwards NM, Itescu S. *Neovascularization of ischemic myocardium by human bonemarrow–derived angioblasts prevents cardiomyocyte apoptosis, reduces remodeling and improves cardiac function*. 2001. Nature 7(4): 430-436.

[9] Segers VFM, Lee RT. *Stem-cell therapy for cardiac disease*. 2008. Nature 451: 937-942

[10] Borchardt T, Braun T. *Cardiovascular regeneration in non-mammalian model systems: what are the differences between newts and man?* 2007. Thromb. Haemost. 98: 311–318.

[11] Lepilina A, Coon AN, Kikuchi K, Holdway JE, Roberts RW, Burns CG, Poss KD. *A dynamic epicardial injury response supports progenitor cell activity during zebrafish heart regeneration.* 2006. Cell 127: 607–619.

[12] Rubart M, Field LJ. *Cardiac regeneration: repopulating the heart.* 2006. Annu. Rev. Physiol. 68: 29–49.

[13] Laflamme MA, Murry CE. *Regenerating the heart.* 2005. Nature Biotechnol. 23: 845–856.

[14] Cleland JG, Coletta AP, Abdellah AT, Nasir M, Hobson N, Freemantle N, Clark AL. *Clinical trials update from the American Heart Association 2006: OAT, SALT 1 and 2, MAGIC, ABCD, PABA-CHF, IMPROVE-CHF, and percutaneous mitral annuloplasty.* 2007. Eur. J. Heart Fail. 9, 92–97.

[15] Leri A, Kajstura J, Anversa P. *Cardiac stem cells and mechanisms of myocardial regeneration.* 2005. Physiol. Rev. 85: 1373–1416.

[16] Segers VFM, Lee RT. *Stem-cell therapy for cardiac disease*. 2008. Nature 451: 937-942.

[17] Young P P, Vaughan DE, Hatzopoulos AK. *Biologic properties of endothelial progenitor cells and their potential for cell therapy.* 2007. Prog. Cardiovasc. Dis. 49, 421–429.

[18] Narmoneva DA, Vukmirovic R, Davis ME, Kamm RD, Lee RT. *Endothelial cells promote cardiac myocyte survival and spatial reorganization: implications for cardiac regeneration.* 2004. Circulation 110, 962–968.

[19] Caplan AI, Dennis JE. *Mesenchymal stem cells as trophic mediators.* 2006. J. Cell. Biochem. 98, 1076–1084.

[20] Miyahara Y, Nagaya N, Kataoka M, Yanagaw B, Tanaka K, Hao H, Ishino K, Ishida H, Shimizu T, Kangawa K, Sano S, Okano T, Kitamura S, Mori H. *Monolayered mesenchymal stem cells repair scarred myocardium after myocardial infarction.* 2006. Nature Med. 12, 459–465.

[21] Amado LC, Saliaris AP, Schuleri KH, St. John M, Xie JS, Cattaneo S, Durand DJ, Fitton T, Kuang JQ, Stewart G, Lehrke S, Baumgartner WW, Martin BJ, Heldman AW, Hare JM. *Cardiac repair with intramyocardial injection of allogeneic mesenchymal stem cells after myocardial infarction*. 2005. Proc. Natl Acad. Sci. USA 102, 11474–11479.

[22] Thompson J, Itskovitz-Eldor J, Shapiro SS, Waknitz MA, Swiergiel JJ, Marshall VS, Jones JM. *Embryonic Stem Cell Lines Derived from Human Blastocysts*. 1998. Science 282: 1145-1147.

[23] Reubinoff B, Pera MF, Fong CY, Trounson A, Bongso A. *Embryonic stem cell lines from human blastocysts: somatic differentiation in vitro.* 1999. Nature Biotechnology 18: 399-404.

[24] Breitbach M, Bostani T, Roell W, Xia Y, Dewald O, Nygren JM, Fries JWU, Tiemann K, Bohlen H, Hescheler J, Welz A, Bloch W, Jacobsen SEW, Fleischmann BK. *Potential risks of bone marrow cell transplantation into infarcted hearts.* 2007. Blood 110: 1362–1369.

[25] Nussbaum J, Minami E, Laflamme MA, Virag JAI, Ware CB, Masino A, Muskheli V, Pabon L, Reinecke H, Murry CE. *Transplantation of undifferentiated murine embryonic stem cells in the heart: teratoma formation and immune response.* 2007. FASEB J. 21: 1345–1357.

[26] Huber I, Itzhaki I, Caspi O, Arbel G, Tzukerman M, Gepstein A, Manhal H, Yankelson L, Kehat Izhak, Gepstein L. *Identification and selection of cardiomyocytes during human embryonic stem cell differentiation.* 2007. FASEB J. 21: 2551–2563.

[27] Kehat I, Kenyagin-Karsenti D, Snir M, Segev H, Amit M, Gepstein A, Livne E, Binah O, Itskovitz-Eldor J, Gepstein L. *Human embryonic stem cells can differentiate into myocytes with structural and functional properties of cardiomyocytes.* 2001. J. Clin. Invest. 108: 407–14.

[28] Kehat I, Khimovich L, Caspi O, Gepstein A, Shofti R, Arbel G, Huber I, Satin J, Itskovitz-Eldor J, Gepstein L. *Electromechanical integration of cardiomyocytes derived from human embryonic stem cells.* 2004. Nat. Biotechnol. 22: 1282–9.

[29] Mummery C, Ward D, van den Brink CE, Bird SD, Doevendans PA, Opthof T, De La Riviere AB, Tertoolen L, Van Der Heyden M, Pera M. *Cardiomyocyte differentiation of mouse and human embryonic stem cells.* 2002. J. Anat. 200: 233–42.

[30] Yang L, Soonpaa MH, Adler ED, Roepke TK, Kattman SJ, Kennedy M, Henckaerts E, Bonham K, Abbott GW, Linden RM, field LJ, Keller GM. *Human cardiovascular progenitor cells develop from a KDR+ embryonic-stem-cell-derived population.* 2008. Nature 453: 524–8.

[31] Zwi L, Caspi O, Arbel G, Huber I, Gepstein A, Park IH, Gepstein L. *Cardiomyocyte differentiation of human induced pluripotent stem cells.* 2009. Circulation 120: 1513–23.

[32] Zhang J, Wilson GF, Soerens AG, Koonce CH, Yu J, Palecek SP, Thomson JA, Kamp TJ. *Functional cardiomyocytes derived from human induced pluripotent stem cells.* 2009. Circ. Res. 104: e30–41.

[33] Moretti A, Bellin M, Jung CB, Thies TM, Takashima Y, Bernshausen A, Schiemann M, Fischer S, Moosmang S, Smith AG, Lam JT, Laugwitz KL. *Mouse and human induced pluripotent stem cells as a source for multipotent Isl1+ cardiovascular progenitors.* 2010. *FASEB J.* 24: 700–11.

[34] Okita K, Ichisaka T, Yamanaka S. *Generation of germline-competent induced pluripotent stem cells.* 2007. Nature 48**:** 313-18.

[35] Pang PP, Yang N, Vierbuchen T, Ostermeier A, Fuentes DR, Yang TQ, Citri A, Sebastiano V, Marro S, Sudhof TC, Wernig M. *Induction of human neuronal cells by defined transcription factors.* 2011. Nature 476 (7359): 220-223.

[36] Drury J, Mooney D. *Hydrogels for tissue engineering: scaffold design variables and applications.* 2003. Biomaterials 24: 4337–4351.

[37] Cellesi F, Tirelli N, Hubbell JA. *Materials for Cell Encapsulation via a New Tandem Approach Combining Reverse Thermal Gelation and Covalent Crosslinking.* 2002. Macromol. Chem. Phys. 203, 1466–1472.

[38]Leung A, Nielsen LK, Trau M, Timmins NE. *Tissue transplantation by stealth—Coherent alginate microcapsules for immunoisolation.* 2010. Biochemical Engineering Journal 48: 337–347.

[39] Magyar JP, Nemir M, Ehler E, Suter N, Perriard JC, Eppenberger HM. *Mass production of embryoid bodies in microbeads.* 2001. Annals of the New York Academy of Sciences: Bioartificial Organs Iii: Tissue Sourcing, Immunoisolation, and Clinical Trials 944:135-143.

[40] Rowley JA, Madlambayan G, Mooney DJ. *Alginate hydrogels as synthetic extracellular matrix materials.* 1999. Biomaterials 20: 45-53.

[41] Lee CH, Singla A, Lee Y. *Biomedical applications of collagen.* 2001. Int J Pharm 221:1–22.

[42] Zimmerman WH, Melnychenko I, Eschenhagen T. *Engineered heart tissue for regeneration of diseased hearts*. 2004. Biomaterials 25: 1639-1647.

[43] Fairbanks BD, Schwartz MP, Bowman CN, Anseth KS. *Photoinitiated polymerization of PEG-diacrylate with lithium phenyl-2,4,6-trimethylbenzoylphosphinate: polymerization rate and cytocompatibility*. 2009. Biomaterials 30:6702-6707.

[44] Aimetti AA, Machen AJ, Anseth KS. *Poly(ethylene glycol) hydrogels formed by thiol-ene photopolymerization for enzyme-responsive protein delivery.* 2009. Biomaterials 30: 6048-6054.

[45] Olabisi RM, Lazard ZW, Franco CL, Hall MA, Kwon SK, Sevick-Muraca EM, Hipp JA, Davis AR, Olmsted-Davis EA, West JL. *Hydrogel Microsphere Encapsulation of a Cell-Based Gene Therapy System Increases Cell Survival of Injected Cells, Transgene Expression, and Bone Volume in a Model of Heterotopic Ossification.* 2010. Tissue Engineering Part A 16 (12): 3727-36.

[46] Gonen-Wadmany M, Oss-Ronen L, Seliktar D. *Protein-polymer conjugates for forming photopolymerizable biomimetic hydrogels for tissue engineering.* 2007. Biomaterials 28: 3876-3886.

[47] Seliktar D, Zisch AH, Lutolf MP,Wrana JL, Hubbell JA. *MMP-2 sensitive, VEGFbearing bioactive hydrogels for promotion of vascular healing.* 2004. J Biomed Mater Res A 68:704e16.

[48] Polizzotti BD, Fairbanks BD, Anseth KS. *Three-dimensional biochemical patterning of Click-based composite hydrogels via thiol-ene photopolymerization.* 2008. Biomacromolecules 9:1084e7.

[49] Zhu JM. *Bioactive modification of poly(ethylene glycol) hydrogels for tissue engineering*. 2010. Biomaterials 31: 4639-4656.

[50] Seliktar D, Zisch, AH, Lutolf MP, Wrana JL, Hubbell JA. *MMP-2 sensitive, VEGF-bearing bioactive hydrogels for promotion of vascular healing.* 2004. Journal of Biomedical Materials Research Part A 68A:704-716.

[51] Lutolf MP, Lauer-Fields JL, Schmoekel HG, Metters AT, Weber FE, Fields GB, Hubbell JA. *Synthetic matrix metalloproteinase-sensitive hydrogels for the conduction of tissue regeneration: engineering cell-invasion characteristics.* 2003. PNAS 100 (9): 5413-5418.

[52] Habib M, Caspi O, Gepstein L. *Human embryonic stem cells for cardiomyogenesis*. 2008. Journal of Molecular and Cellular Cardiology 45 462–474

[53] Lee LH, Peerani R, Ungrin M, Joshi C, Kumacheva E, Zandstra PW. *Micropatterning of human embryonic stem cells dissects the mesoderm and endoderm lineages.* 2009. Stem Cell Research 2:155-162.

[54] Peerani R, Rao B. M, Bauwens C, Yin T, Wood GA, Nagy A, Kumacheva E, Zandstra PW. *Niche-mediated control of human embryonic stem cell self-renewal and differentiation.* 2007. Embo Journal 26: 4744-4755.

[55] Bauwens CL, Peerani R, Niebruegge S, Woodhouse KA, Kumacheva E, Husain M, Zandstra PW. *Control of human embryonic stem cell colony and aggregate size heterogeneity influences differentiation trajectories.* 2008. Stem Cells 26:2300-2310.

[56] Carpenedo RL, Bratt-Leal AM, Marklein RA, Seaman SA, Bowen NJ, McDonald JF, McDevitt TC. *Homogeneous and organized differentiation within embryoid bodies induced by microsphere-mediated delivery of small molecules.* 2009. Biomaterials 30: 2507-2515.

[57] Carpenedo RL, Seaman SA, McDevitt TC. *Microsphere size effects on embryoid body incorporation and embryonic stem cell differentiation.* 2010. Journal of Biomedical Materials Research Part A 94A:466-475.

[58] Kurosawa H. *Methods for Inducing Embryoid Body Formation: In Vitro Differentiation System of Embryonic Stem Cells*. 2007. Journal of Bioscience and Bioengineering: 103, No. 5, 389–398.

[59] Franco CL, Price J, West JL. *Development and optimization of a dual-photoinitiator, emulsion-based technique for rapid generation of cell-laden hydrogel microspheres.* 2011. Acta Biomaterialia. 7: 3267–3276.

[60] Williams R, Peisajovich SG, Miller OJ, Magdassi S, Tawfik DS, Griffiths AD. *Amplification of complex gene libraries by emulsion PCR.* 2006. Nature Methods 3, No. 7, 545-550.

[61] Maguire T, Novik E, Schloss R, Yarmush M. *Alginate-PLL Microencapsulation: Effect on the Differentiation of Embryonic Stem Cells Into Hepatocytes.* 2005. Biotechnology and Bioengineering 93(3): 581-591.

[62] Cellesi F, Weber W, Fussenegger M, Hubbell JA, Tirelli N. *Towards a Fully Synthetic Substitute of Alginate: Optimization of a Thermal Gelation/Chemical Cross-Linking Scheme (''Tandem'' Gelation) for the Production of Beads and Liquid-Core Capsules.* 2004. Biotechnology and Bioengineering 88(6): 740-749.

[63] Huang SB, Wu MH, Lee GB. *Microfluidic device utilizing pneumatic micro-vibrators to generate alginate microbeads for microencapsulation of cells.* 2010. Sensor and Actuators B 147: 755-764.

[64] Wu MH, Pan WC. *Development of microfluidic alginate microbead generator tunable by pulsed airflow injection for the microencapsulation of cells.* 2010. Microfluid Nanofluid 8:823-835.

[65] Shapira-Schweitzer K, Seliktar D. *Matrix stiffness affects spontaneous contraction of cardiomyocytes cultured within a PEGylated fibrinogen biomaterial.* 2007. Acta Biomateriala 3:33-41.

[66] Chan BP, Hui TY, Yeung CW, Li J, Mo I, Chan GCF. *Self-assembled collagen–human mesenchymal stem cell microspheres for regenerative medicine.* 2007. Biomaterials 28: 4652-4666.

VI. Appendix

6.1 Tetronic and Pluronic physical gelation

A) Tetronic pellets were dissolved in PBS at 10% (w/v):

It was difficult to fully dissolve Tetronic even at this low concentration at room temperature, but was slightly easier to handle if the solution was placed in the refrigerator. 10% Tetronic was combined with 10% PEGDA solution at the following volume:volume ratios of 10% Tetronic solution:10% PEGDA solution:

1:0; 1:1; 2:1; 1:2; 0:1

All gels were placed in the cell culture incubator for 1 hour and 24 hours and it was found that no physical gelling resulted.

B) 10% Tetronic solution in PBS (w/v) was combined with 10% PEGDA solution at the same ratios described above in Section 6.1.A.

Additionally, 5 µL acetophenone stock solution was added per mL of polymer solution.

Solutions were exposed to 365 nm UV light source for 5 minutes at room temperature.

Photo-crosslinked gels were observed for all gels containing any PEGDA, since gels consisting of only Tetronic did not crosslink and did not physically gel.

Additionally a swelling study was performed by combining Tetronic and PEGDA at varied concentrations and adding acetophenone at the aforementioned concentration. Gels were photo-crosslinked with 365 nm light source for 5 minutes and subsequently weighed and swelled. The results are shown in Figure 6.1.B.

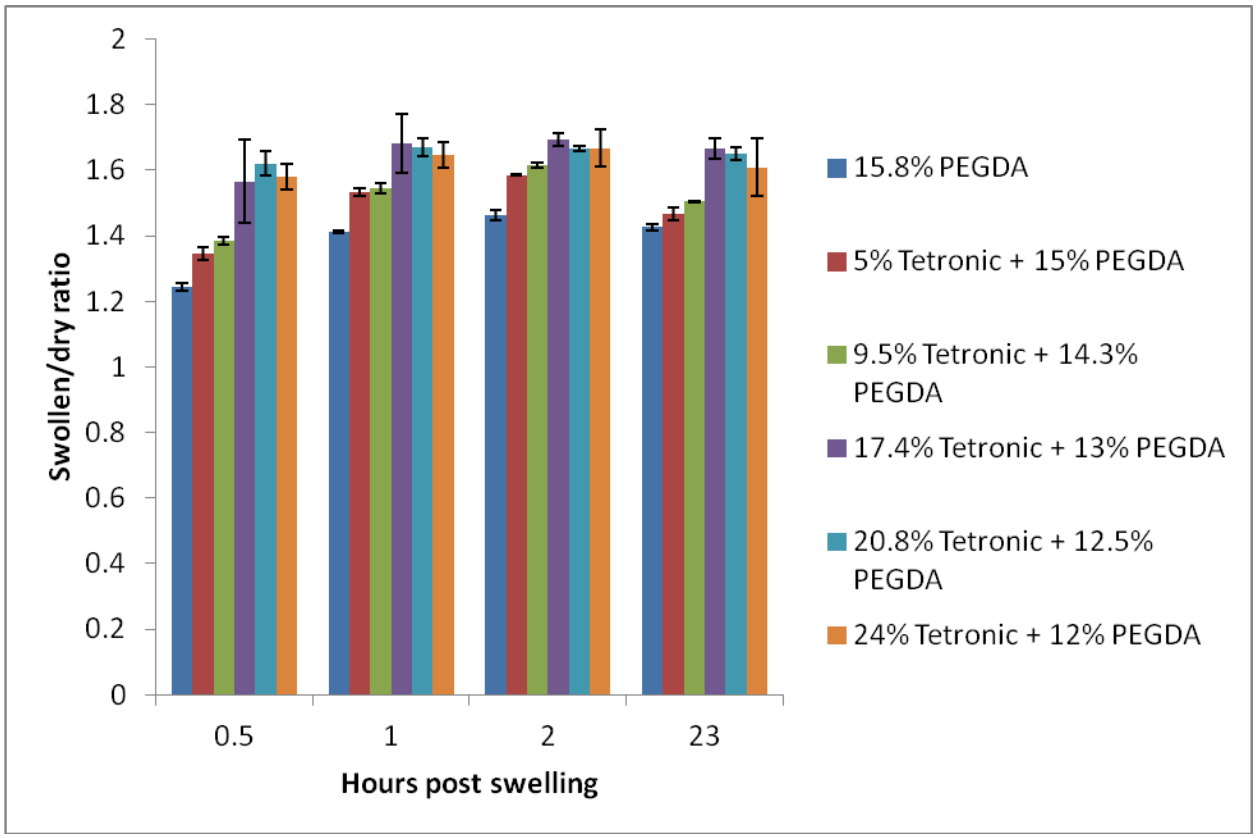

Figure 6.1.B. Tetronic/PEGDA gels swelling ratios

C) 30% Tetronic solution was prepared in PBS. It would not dissolve at this concentration at room temperature. The partially-dissolved solution was placed in the refrigerator for a week and was still not fully dissolved. A 25% Tetronic solution was prepared in PBS and was dissolved in a cold room with stirring. Full dissolution was achieved by moving the mixture with stir plate and stir bar to a cold room. The resultant solution was highly viscous, like molasses, even in the cold room where it had to be handled as a liquid. Thermal gelation was investigated again with the 25% Tetronic stock solution. 25% Tetronic solution was combined with PEGDA solution at varied concentrations and were assessed for reverse physical gelation. The results are summarized in Table 6.1.C

Tetronic % (w/v)	PEGDA % (w/v)	Physical gellation when moved from cold to RT?
25	0	Yes
0	20%	No
20	4	Partial
16.3	6.6	Partial
8.3	13.3	No
5	16	No

Table 6.1.C

D) Tetronic dropping experiments

Polymer mixtures of Tetronic combined with PEGDA were made at the following concentrations:

25% Tetronic + 4% PEGDA

20% Tetronic + 6.66% PEGDA

5 µL acetophenone photoinitiator solution was added per mL of polymer solution. A 150 mL glass beaker was filled with 40 mL 10% (w/v) Pluronic F127 in PBS with a stir bar. The 150 mL beaker was then placed in a water bath consisting of a 250 mL glass beaker filled with 150mL water. The nested beakers were then placed on a hot plate with stirrer and the water bath was heated to 37°C. 2.5 µL drops of each Tetronic/PEGDA solution were dropped into the Pluronic bath and exposed to UV light. However, the Tetronic/PEGDA polymer would break up upon impact with the bath, thus not forming spheres. It was found later that the addition of both Tween 80 and n-hexane to the bath were necessary to allow spheres to form upon impacting the bath (refer to Materials and Methods).

Additionally, Tetronic solutions were extruded using a syringe attached to a 20 gauge needle at room temperature. Polymer solution was attempted to be extruded over the hardening bath. However, at room temperature, the Tetronic pre-polymer would physically gel and be too viscous to extrude from the syringe needle. A high-powered homogenizer was touched to the

needle tip to attempt to break up the extruded polymer into smaller spheres. However, this only resulted in un-controlled spraying of the polymer upon reaching the needle opening, rather than having the polymer cleanly breaking up into droplets and dropping into the bath.

E) Pluronic F127 physical gel

Pluronic stock solutions of 20%, 30% were created by dissolving Pluronic F127 pellets in PBS in the cold room under stirring. Pluronic F127 solutions were more viscous than Tetronic solutions of the same weight/volume concentrations. Furthermore, Pluronic could not be fully dissolved at 40% concentration, while Tetronic could be dissolved at 40% concentration. It was impossible to combine the two polymers at reliable volumetric ratios because they were both highly viscous even in the cold room. The high viscosity resulted in the polymer sticking to the inside of pipette tips and centrifuge tubes, making it impossible to measure volumes.

6.2 Emulsion formulations

A) Many different emulsion formulations were investigated to produce dispersed and crosslinked polymer microspheres with sphere diameters on the order of about 100 microns. Initial tests explored long vortex and UV crosslinking times with a photoinitiator in only the aqueous phase. These typically resulted in poor polymerization and dispersion. The second batteries of tests incorporated photoinitiator into both aqueous and oil phases, resulting in crosslinking but spheres were also clumped and poorly dispersed. Additionally, the addition of TEA into the emulsions yielded more consistent crosslinking. Note that Eosin Y was investigated as a hydrophilic photoinitiator for incorporation into the aqueous phase, but this resulted in pink polymer and this effect interfered with live/dead fluorescent staining. The next sets of emulsions investigated the incorporation of surfactants, and it was found that Griffith's

surfactant and Pluronic F127 were very good at dispersing spheres. In fact, they formed spheres that were too small for this application, and this was evident by "milky" or "cloudy" emulsions.

Aqueous compo-sition	**Photo-initiator**	**Oil composition**	**Aqueous/ Oil ratio**	**Vortex time/UV time**	**Light/ Tube**	**Result**
30% (w/v) Tetronic + 150 mg PEGDA/mL Tetronic solution	Acetophenone (5 µL/mL polymer)	Mygliol oil	1:5	30s:30s	365 nm/ 15 mL	Insufficient cross-linking
" "	" "	' '	3:20	30s:30s	" "	" "
" "	" "	' '	1:5	2min:2min	" "	" "
" "	" "	' '	1:10	1min:1min	" "	" "
" "	" "	" "	1:5	4min:4min	" "	" "
" "	" "	" "	1:50	2min:2min	" "	" "
" "	" "	" "	1:5	5min:5min	" "	" "
" "	Acetophenone (5 µL/mL polymer) (And 7.5 µL/mL oil)	" "	1:5	3min:3min	" "	Partially crosslinked and dispersed
" "	" "	" "	" "	3.5min:3.5 min	" "	Clumped and crosslinked
30% (w/v) PEGDA in Serum-free mESC media	Acetophenone (9 µL/mL polymer) (And 3.75 µL/mL oil)	" "	1:5	4min:4min	" "	No crosslinking or dispersion
" "	Acetophenone (18 µL/mL polymer)	" "	1:4	5min:5min	" "	" "

Aqueous compo-sition	Photo-initiator	Oil composition	Aqueous/ Oil ratio	Vortex time/UV time	Light/ Tube	Result
“ ”	Acetophenone (5 µL/mL polymer) (And 7.5 µL/mL oil)	“ ”	1:5	5min:5min	“ ”	“ ”
30% (w/v) Tetronic + 150 mg PEGDA/mL Tetronic solution	Acetophenone (7.5 µL/mL polymer) (And 10 µL/mL oil)	“ ”	1:5	4.5min:4.5 min	“ ”	Crosslinked “blob” but does not produce spheres
“ ”	“ ”	“ ”	“ ”	5min:5min	365 nm/1.5 mL micro	Fully crosslinked sphere clumps
“ ”	“ ”	“ ”	“ ”	3.5min:3.5 min	“ ”	“ ”
“ ”	“ ”	“ ”	“ ”	2min:3mn	“ ”	“ ”
10% (w/v) PEGDA in HBS	(4 µL EosinY /mL polymer) (3 µL acetophenone/ mL oil)		1:5	2sec:40sec	365 nm/ 15 mL	Partial polymerization, no spheres, polymer is pink
“ ”	“ ”	“ ”	“ ”	10sec:40sec	“ ”	Clumpy partial polymerization, polymer is pink
“ ”	“ ”	“ ”	1:10	“ ”	“ ”	No polymerization
“ ”	(5 µL EosinY /mL polymer + 1.5 µL TEA/mL polymer) (5 µL acetophenone/ mL + 1.5 µL TEA/mL oil)	“ ”	“ ”	“ ”	“ ”	More dispersed, crosslinked

Aqueous compo-sition	Photo-initiator	Oil composition	Aqueous/ Oil ratio	Vortex time/UV time	Light/ Tube	Result
Batch-1 PF	(20 µL EosinY /mL polymer + 5 µL TEA/mL polymer) (5 µL acetophenone/ mL + 1.5 µL TEA/mL oil)	“ ”	“ ”	1min:1min	Metal halide/ 1.5 mL micro	Yellow crosslinked, clumped spheres
“ ”	“ ”	“ ”	“ ”	45sec:45sec	“ ”	“ ”
“ ”	(25 µL Irgacure 2959 /mL polymer + 15 µL TEA/mL polymer) (5 µL acetophenone/ mL + 1.5 µL TEA/mL oil)	“ ”	“ ”	2min:2min	“ ”	Clear crosslinked, less clumped spheres
“ ”	(25 µL Irgacure 2959 /mL polymer + 25 µL TEA/mL polymer) (5 µL acetophenone/ mL + 1.5 µL TEA/mL oil)	“ ”	“ ”	1min:1min	“ ”	Clear, not fully crosslinked, clumped spheres
“ ”	“ ”	“ ”	“ ”	“ ”	“ ”	More dispersed than previous trial

Aqueous compo-sition	Photo-initiator	Oil composition	Aqueous/ Oil ratio	Vortex time/UV time	Light/ Tube	Result
“ ”	(25 µL Irgacure 2959 /mL polymer + 25 µL TEA/mL polymer) (5 µL acetophenone/ mL + 1.5 µL TEA/mL Griffth’s surfactant)	“ ”	“ ”	40s:40s	“ ”	Ultra-fine, “milky” emulsion
15% (w/v) PEGDA in PBS + 0.1% (w/v) Pluronic F127	(25 µL Irgacure 2959 /mL polymer + 15 µL TEA/mL polymer) (5 µL acetophenone/ mL + 1.5 µL TEA/mL	Sterile mineral oil	1:5	2sec:40sec	“ ”	Clumped
“ ”	“ ”	“ ”	1:10	“ ”	“ ”	“ ”
“ ”	“ ”	“ ”	1:5	“ ”	Metal halide/ Round bottom Glass tube	Some clumped, some well dispersed spheres
“ ”	“ ”	“ ”	1:10	“ ”	“ ”	Well-dispersed!
Batch-1 PF	(25 µL Irgacure 2959 /mL polymer + 15 µL TEA/mL polymer) (5 µL acetophenone/ mL + 1.5 µL TEA/mL	“ ”	“ ”	“ ”	“ ”	Clumped spheres, but form smaller clumps than when using 1.5mL microfuge tube

Aqueous compo-sition	Photo-initiator	Oil composition	Aqueous/ Oil ratio	Vortex time/UV time	Light/ Tube	Result
Batch-1 PF + 0.1% Pluronic F127	“ ”	“ ”	“ ”	“ ”	“ ”	Extremely well dispersed, cloudy crosslinked emulsion
“ ”	“ ”	“ ”	1:5	“ ”	“ ”	“ ”
Batch-1 PF + 0.1% Pluronic F68	“ ”	“ ”	“ ”	“ ”	“ ”	Micro-spheres form in layers: clumped, and very well dispersed spheres.

Note that in the final condition investigated, where Pluronic surfactant was switched from F127 to F68, dispersed spheres with a diameter in the range of 100 microns was finally obtained. Note that using F127 resulted in spheres with very small diameter, perhaps because the F127 surfactant is more effective than F68 in lowering surface tension to the point that spheres are too small. Also note that dispersed spheres were only obtained when using a glass round-bottom tube for the vortex and crosslinking.

B. Griffiths' surfactant

Griffiths' surfactant was investigated for its surfactant efficacy. It was diluted from its original form in Mygliol mineral oil 1:100. 10% PEGDA was dropped into Mygliol oil containing no initial surfactant. The oil was placed in a beaker with stir bar on a stir plate. N-hexane was dropped onto the surface of the oil phase. When PEGDA was initially dropped into the oil bath,

it simply coalesced into one glob. Then, 150 µL Griffiths' surfactant was dropped into the oil bath. With subsequent additions of the surfactant mixture into the oil bath, the PEGDA polymer began to disperse. However, when the stir bar was stopped, the PEGDA would coalesce again, indicating that the dispersion was dependent on mechanical stirring. This was verified by turning the stirrer on again, and the PEGDA phase began to separate into relatively large phases at low stirring rate, and separated into smaller particles with increased stirring rate.